

**ADVANCES IN CLINICAL,
NEUROPATHOLOGIC, AND GENETIC
FEATURES OF CORTICOBASAL
DEGENERATION**

A THESIS
SUBMITTED TO THE FACULTY OF
MAYO CLINIC COLLEGE OF MEDICINE
Mayo Graduate School

BY
Naomi Kouri

IN PARTIAL FULFILLMENT OF THE REQUIREMENTS
FOR THE DEGREE OF
DOCTOR OF PHILOSOPHY IN BIOMEDICAL SCIENCES
NEUROBIOLOGY OF DISEASE

APRIL 2014

UMI Number: 3702551

All rights reserved

INFORMATION TO ALL USERS

The quality of this reproduction is dependent upon the quality of the copy submitted.

In the unlikely event that the author did not send a complete manuscript and there are missing pages, these will be noted. Also, if material had to be removed, a note will indicate the deletion.



UMI 3702551

Published by ProQuest LLC (2015). Copyright in the Dissertation held by the Au

Microform Edition © ProQuest LLC.

All rights reserved. This work is protected against
unauthorized copying under Title 17, United States Code



ProQuest LLC.
789 East Eisenhower
Parkway
P.O. Box 1346

© Naomi Kouri, April 2014

ACKNOWLEDGEMENTS

These studies were made possible because I was awarded a Mayo Graduate School fellowship from the Mayo Clinic College of Medicine. This supported me financially during my tenure in the doctor of philosophy in biomedical sciences program and directed me on a new path of scientific endeavors.

My enjoyment for writing has helped me in science. My father has written two novels that I cannot read because they are in Japanese, but I hope to understand them some day. Growing up, my mother played viola in the symphony, and when she practiced at home she would warm up with Johann Sebastian Bach cello suites (transcribed for viola of course). Over the past five years, I learned that my best writing happens when I listen to Bach cello suites: Rostropovich for elegant, exciting, and awake writing and Yo-Yo Ma for calm, clear, deep thoughts writing. These beautiful sounds keep my brain moving forward that would otherwise make several long pauses along the way, or get stuck in loops - I'm not sure which. Thank you Momma (Judy Kouri), Papa (Harukazu Kouri), and Johann (Sebastian Bach). My family is everything to me and instead of listing everyone, I provide here a pedigree with their names. Not biologically related but close as can be, are Cynthia Prosser and Robert Scott Runnion, Scottie and Freddie Kapel, Inga Layton, Gus Gonzalez, and Mariet and Curt Younkin.

I have been ever so fortunate to work with the exceptional scientist at Mayo Clinic. Dr. Dennis Dickson is a person I cannot thank enough and appreciate him as a human being, SMA Team Tau. His dedication to teaching and mentoring has surpassed and continues to surpass my hopes of being able to work in an intellectually stimulating environment. Dr. Dickson has a gift for teaching, and I thank him for this (plus, he's kind of a big deal!). Drs. Rosa Rademakers, Nilufer Taner, and Owen Ross have taught me how to understand genetics, and I will continue to enjoy our scientific discussions and collaborations. Dr. Allan Bieber kept me on track the whole way through graduate school. Dr. Bieber, I am forever grateful for your help and kindness. Thank you to the individuals who played a role in my transitions from ceramics to chemistry to neuroscience. Drs. Lillian Miller, Stuart Chalk, Michael Lufaso, Kunisi Venkatasubban, Terrone Rosenberry, and Nilufer Taner. Thank you to Drs. Keith Josephs and Neill Graff-Radford, I have learned so much about the art of neurology from the two of you, and I very much appreciate your dedication to teaching.

For my uncle Cecil Fesler who taught we what hard work can bring you.

Publications resulting from this dissertation

1. **Kouri N**, Whitwell JL, Josephs KA, Rademakers R, Dickson DW. Corticobasal degeneration: a pathologically distinct 4R tauopathy. *Nat Rev Neurol* 7: 263-272 (2011)
2. **Kouri N**, Murray ME, Hassan A, Rademakers R, Uitti RJ, Boeve BF, Graff-Radford NR, Wszolek ZK, Litvan I, Josephs KA, Dickson DW. Neuropathological features of corticobasal degeneration presenting as corticobasal syndrome or Richardson syndrome. *Brain : a journal of neurology* 134: 3264-3275 (2011)
3. Dickson DW, **Kouri N**, Murray ME, Josephs KA. Neuropathology of frontotemporal lobar degeneration-tau (FTLD-tau). *J Mol Neurosci* 45: 384-389 (2011)
4. **Kouri N**, Oshima K, Takahashi M, Murray ME, Ahmed Z, Parisi JE, Yen SH, Dickson DW. Corticobasal degeneration with olivopontocerebellar atrophy and TDP-43 pathology: an unusual clinicopathologic variant of CBD. *Acta Neuropathologica* 125: 741-752 (2013)
5. **Kouri N**, Carlomagno Y, Baker M, Liesinger AM, Caselli RJ, Wszolek ZK, Petrucelli L, Boeve BF, Parisi JE, Josephs KA, Uitti RJ, Ross OA, Graff-Radford NR, Deture MA, Dickson DW, Rademakers R. Novel mutation in *MAPT* exon 13 (p.N410H) causes corticobasal degeneration. *Acta Neuropathologica*: Epub 2013/10/15 (2013)

ABSTRACT

This is a dissertation on the neurodegenerative tauopathy corticobasal degeneration (CBD). Because CBD is a rare disorder and has <50% antemortem diagnostic accuracy, we sought to learn as much as possible from our invaluable resource, having the largest, single neuropathologically-confirmed CBD cohort in the world. This is a culmination of several different projects, all focused on neuropathologic, genetic, and clinical features of CBD, with the overall intent being to help patients who will suffer from this devastating disorder. Each study/chapter had a specific hypothesis, aimed to elucidate various unanswered questions about CBD. Essentially, the only possible approach to further our understanding of CBD is what we have done here: use patient tissue and DNA samples who have donated their brains to research.

Richardson syndrome is one of the most common clinical presentations of CBD

Clinicopathologic assessment of CBD patients presenting with Richardson syndrome (CBD-RS) (*i.e.* patients misdiagnosed as progressive supranuclear palsy), identified neuropathologic and clinical signs and symptoms that were able to differentiate CBD-RS from PSP patients. Digital microscopy and image analysis were used to quantify tau pathology in multiple brain regions and found CBD-CBS (corticobasal syndrome) cases had greater peri-Rolandic tau burden and CBD-RS had greater hindbrain and limbic tau pathology. CBD-RS patients exhibited a frontal/dysexecutive syndrome and urinary incontinence more often than PSP patients. We also describe an unusual variant of CBD with olivopontocerebellar atrophy, of which two of the patients presented with Richardson syndrome and had greater hindbrain tau pathology than CBD-CBS, and interestingly had significant TDP-43 (protein inclusions found in FTLD and ALS) pathology in affected regions. Regarding TDP-43 pathology in CBD, we found that >25% of cases have TDP-43 immunoreactive neuronal and glial cytoplasmic inclusions and threads, and the greatest burden was in the basal ganglia. With these studies we were able to show that Richardson syndrome is one of the most common clinical presentations of CBD.

Identification of a novel *MAPT* mutation (p.N410H) in a CBD case that is neuropathologically indistinguishable from sporadic CBD

We screened our autopsy-confirmed CBD cohort for *MAPT* mutations and identified a novel mutation in *MAPT* exon 13 (p.N410H) in a case that is neuropathologically indistinguishable from sporadic CBD. This is not only the first *MAPT* mutation identified to cause CBD, but it is also the first mutation to cause CBD. Functional studies with this mutation showed that there was decreased ability for mutant tau to promote microtubule assembly and exhibited a marked increase in filament formation in vitro. In this study we also identified two rare variants in the 3' untranslated regulatory region of *MAPT* that associate with CBD, and one of these variants also associated with PSP.

CBD and PSP have shared and unique genetic risk factors

Our last study as part of my dissertation, is the first ever CBD genome-wide association study. We performed a discovery stage, replication stage, and meta-analysis in 152 CBD cases versus 3,111 control individuals (discovery), with 67 CBD cases versus 457 controls (replication). This identified two genome-wide significant associations with CBD at *MAPT* and *KIF13B/DUSP4*. Using a candidate gene approach, we tested for CBD association with the top progressive supranuclear palsy GWAS SNPs. This identified strong associations at *MOBP* and *MAPT* H1c haplotype. Another novel genetic association for CBD patients was identified at *SOS1*. Expression/SNP associations were tested from ~400 brain samples of cerebellum and temporal cortex and found significant associations at *MAPT*, *MOBP*, and *SOS1*. The genome-wide significant association at *KIF13B/DUSP4* with CBD will require additional studies to determine which gene is responsible for the association signal. In summary, these findings show for the first time, that CBD and PSP share common genetic variation, other than *MAPT*, at *MOBP* which confers disease risk. Together, warranting future studies to understand the mechanism by which *MOBP* contributes to the CBD and PSP disease processes.

CONTENTS

CHAPTER 1

Introduction: Corticobasal degeneration is a pathologically distinct 4R tauopathy with a range of clinical presentations.....	1
1.1. Overview.....	1
1.2. Background.....	2
1.3. Tauopathies and <i>MAPT</i>	3
1.4. Genetics of CBD.....	3
1.5. Clinical syndromes associated with CBD.....	4
1.5.1. Corticobasal syndrome.....	5
1.5.2. Richardson syndrome.....	6
1.5.3. Behavioral variant frontotemporal dementia.....	7
1.5.4. Primary progressive aphasia.....	9
1.5.5. Posterior cortical atrophy syndrome.....	9
1.6. Diagnosis of corticobasal degeneration.....	10
1.7. Classifying the 4R tauopathies.....	10
1.7.1. Clinical presentations.....	11
1.7.2. Neuropathologic features.....	11
1.7.3. Biochemical features.....	13
1.7.4. Mechanisms of tau-mediated disease.....	13
1.8. Tau-directed therapeutics.....	14
1.9. Identification of biomarkers.....	15
1.10. Conclusions.....	18
1.11. References.....	19

CHAPTER 2

Neuropathologic features of corticobasal degeneration presenting as corticobasal syndrome or Richardson syndrome.....	28
2.1. Abstract.....	28

2.2.	Introduction	29
2.3.	Materials and methods.....	30
2.3.1.	Subject selection	30
2.3.2.	Clinical classification.....	30
2.3.3.	Tissue sampling and pathologic assessment	32
2.3.4.	Tau biochemistry	36
2.3.5.	Statistical analyses	37
2.4.	Results.....	37
2.4.1.	Demographic and initial presentation	37
2.4.2.	Clinical features of CBD and PSP	39
2.4.3.	Neuropathologic findings	41
2.4.3.1.	Neuronal loss in subthalamic nucleus and substantia nigra	41
2.4.3.2.	Atrophy of the corpus callosum	42
2.4.3.3.	Distribution and severity of tau immunoreactivity	42
2.4.3.4.	Tau biochemistry	46
2.5.	Discussion	46
2.5.1.	Corticobasal degeneration – pathologic basis for clinical heterogeneity	48
2.5.2.	Richardson syndrome – pathological heterogeneity.....	49
2.6.	Conclusion	50
2.7.	References	51

CHAPTER 3

	Corticobasal degeneration with olivopontocerebellar atrophy and TDP-43 pathology: an unusual clinicopathologic variant of CBD	55
3.1.	Abstract.....	55
3.2.	Introduction	55
3.3.	Materials and methods.....	56
3.3.1.	Case selection	56
3.3.2.	Tissue sampling and pathologic assessment	57
3.3.3.	Immunohistochemistry.....	57

3.3.4. Genetic analysis	58
3.3.5. Tau biochemistry	58
3.4. Results	59
3.4.1. Clinical features	60
3.4.2. Neuropathologic features	62
3.4.2.1. Macroscopic.....	62
3.4.2.2. CBD pathology.....	64
3.4.2.3. TDP-43 immunohistochemistry.....	66
3.4.2.4. Olivopontocerebellar system	68
3.4.3. Comparison of CBD-OPCA to MSA, typical CBD and PSP	69
3.4.3.1. Neuronal loss.....	69
3.4.3.2. Tau immunohistochemistry image analysis	71
3.4.3.3. Tau biochemistry	72
3.5. Discussion	73
3.5.1. CBD-OPCA is one of several clinical variants of CBD.....	74
3.5.2. CBD-OPCA is an uncommon variant of CBD	75
3.6. References	78

CHAPTER 4

Novel mutation in <i>MAPT</i> exon 13 (p.N410H) causes corticobasal degeneration	81
4.1. Abstract.....	81
4.2. Introduction	81
4.3. Materials and methods.....	84
4.3.1. Subjects and samples	84
4.3.2. DNA sequencing	84
4.3.3. Genotyping analysis	84
4.3.4. Tissue sampling and neuropathologic assessment	85
4.3.5. Recombinant tau purification	85
4.3.6. Microtubule Assembly	86

4.3.7. Tau filament formation.....	86
4.3.8. Western blot	87
4.3.9. Tau Quantitative Real-Time PCR	87
4.3.10. Statistical analysis	87
4.4. Results.....	88
4.4.1. Sequencing and association studies of MAPT in CBD	88
4.4.2. p.N410H MAPT mutation in pathologically-confirmed CBD	91
4.4.2.1. Clinical history.....	91
4.4.2.2. Neuropathology	92
4.4.2.3. <i>In vivo</i> characterization of p.N410H mutant tau in patient brain samples	98
4.4.2.4. p.N410H tau has impaired ability to promote microtubule assembly.....	99
4.4.2.5. p.N410H induces tau filament formation.....	100
4.5. Discussion	102
4.6. References	Error! Bookmark not defined.

CHAPTER 5

Genome-wide association study identifies microtubule-associated protein tau (<i>MAPT</i>) and myelin-associated oligodendrocytic basic protein (<i>MOBP</i>) as shared genetic risk factors for corticobasal degeneration and progressive supranuclear palsy.....	109
5.1. Abstract.....	109
5.2. Introduction	110
5.3. Methods and Materials.....	110
5.3.1. Samples	110
5.3.2. Quality control	113
5.3.3. Population substructure.....	113
5.3.4. Association analysis	116
5.3.5. Whole genome transcript levels – DASL	116
5.4. Results.....	117
5.4.1. Discovery stage	117
5.4.2. Replication stage.....	122

5.4.3. <i>MOBP</i> locus	123
5.4.4. Brain expression quantitative trait loci	124
5.5. Discussion	125
5.6. References	129

CHAPTER 6

Conclusions	132
6.1. Richardson syndrome is a common clinical presentation of CBD	132
6.2. <i>MAPT</i> mutation identified in a CBD case	135
6.3. CBD and PSP have shared and unique genetic risk factors	136
6.4. Future directions	138
6.4.1. Mechanism of p.N410H <i>MAPT</i> mutation	138
6.4.2. Complex genetics of CBD	139
6.5. References	141

LIST OF FIGURES

Figure 1.1	The distinct histological lesions of CBD and PSP visualized with tau immunohistochemistry.....	12
Figure 1.2	Patterns of gray matter loss in groups of patients with autopsy-confirmed CBD but different clinical syndromes.....	17
Figure 2.1	Digital image analysis with ImageScope software.....	35
Figure 2.2	Illustration of the technique used to measure corpus callosum thickness..	36
Figure 2.3	Semi-quantitative assessment of neuronal loss in the substantia nigra and subthalamic nucleus	41
Figure 2.4	Anterior corpus callosum measurements differentiate CBD and PSP.....	42
Figure 2.5	Tau immunohistochemistry in representative brain regions.	44
Figure 2.6	Regional distribution of tau immunoreactivity as assessed by image analysis in CBD-CBS, CBD-RS and PSP-RS.....	45
Figure 2.7	Immunoblot analysis of the sarkosyl-insoluble fraction from frontal cortex homogenates of CBD-CBS, CBD-RS and PSP-RS.....	46
Figure 3.1	Brain magnetic resonance imaging (MRI) from Case 3.....	62
Figure 3.2	CBD-OPCA macroscopic features.....	63
Figure 3.3	Tau and TDP-43 immunohistochemistry in CBD-OPCA.....	66
Figure 3.4	CBD-OPCA olivopontocerebellar system pathology.....	69
Figure 3.5	Neuronal loss in CBD-OPCA, CBD, MSA, PSP, and normal controls.....	70
Figure 3.6	Image analysis tau burden in CBD-OPCA and CBD.	72
Figure 3.7	Biochemical analysis of tau in CBD-OPCA, CBD, and PSP.....	73
Figure 4.1	MAPT locus within the large 900 kb inversion on chromosome 17q21.31 .	83
Figure 4.2	Novel MAPT p.N410H mutation in exon 13	89
Figure 4.3	p.N410H macroscopic features	92
Figure 4.4	Neuropathology of a CBD case with p.N410H MAPT mutation	94
Figure 4.5	TDP-43 pathology burden in CBD-OPCA, CBD, and p.N410H	98
Figure 4.6	Tau biochemical analysis in sporadic CBD and p.N410H mutation carrier.	99
Figure 4.7	Microtubule assembly and tau filament formation	100
Figure 4.8	Thioflavin-S fluorescence measurements of tau filament assembly.....	101
Figure 5.1	Multidimensional scaling plots for CBD and controls.....	114
Figure 5.2	Quantile-quantile plots in CBD genome-wide scan	115
Figure 5.3	CBD genome-wide association results	119
Figure 5.4	Quantile-quantile plots in CBD genome-wide scan excluding all SNPs at 17q21.31 locus.	120
Figure 5.5	Regional association plot (LocusZoom) of the H1c haplotype-tagging SNP rs242557.....	123
Figure 5.6	Linkage disequilibrium structure at the <i>MOBP</i> locus	124

LIST OF TABLES

Table 1.1	Clinical heterogeneity of pathologically confirmed CBD	5
Table 2.1	Clinical signs and symptoms of autopsy-proven CBD cases presenting with corticobasal syndrome or Richardson syndrome ^a	32
Table 2.2	Side of brain evaluated and clinical asymmetry	33
Table 2.3	Two way analysis of variance adjusting for side of brain evaluated	33
Table 2.4	Demographics and final clinical diagnosis	38
Table 2.5	Initial clinical presenting signs and symptoms	39
Table 2.6	Symptoms/signs in pathologically confirmed corticobasal degeneration and progressive supranuclear palsy	40
Table 3.1	Summary of demographics, clinical, and neuropathology of CBD-OPCA ...	60
Table 3.2	Tau pathology in Case 1	64
Table 3.3	Tau pathology in Case 2	65
Table 3.4	Tau pathology in Case 3	65
Table 3.5	TDP-43-positive neuronal cytoplasmic inclusions.....	67
Table 3.6	TDP-43-positive glial inclusions	67
Table 3.7	TDP-43-positive threads	68
Table 3.8	Summary of cases and controls used for quantitative neuronal counts.....	70
Table 4.1	Cohort description.....	89
Table 4.2	Description of variants in the 3'UTR of <i>MAPT</i> and logistic regression results for association test with CBD and PSP.....	90
Table 4.3	Genotype counts and frequencies for MAPT 3'UTR variants in CBD, PSP, Control Series 1, and Control Series 2.	91
Table 4.4	Semiquantitative assessment of tau and TDP-43 pathology in p.N410H case	96
Table 4.5	TDP-43 pathology severity and distribution separated by inclusion type in four sporadic CBD cases.....	97
Table 5.1	Description of samples.....	111
Table 5.2	Discovery Stage power (%) to detect associations of SNPs and CBD status with 150 cases, 3000 controls for given odds ratios for different minor allele frequencies.....	112
Table 5.3	Replication Stage power (%) to detect associations of SNPs and CBD status with 60 cases, 700 controls for given odds ratios for different minor allele frequencies.	112
Table 5.4	Neuropathologic diagnoses for DASL transcriptome analysis samples.....	117
Table 5.5	Results from discovery stage, replication stage, and meta-analysis	118
Table 5.6	Results for CBD association with top PSP GWAS SNPs	119
Table 5.7	Twelve additional SNPs at Chr. 17q21 with genome-wide significant associations with CBD	121

Table 5.8 Comparison of minor allele frequencies (MAF) of SNPs with significant association with CBD based on CBD cases and controls and older controls from publicly available datasets from dbGaP.....	122
Table 5.9 Association results for SNPs predicted to be in regulatory regions at <i>MOBP</i> with CBD.....	124
Table 5.10 CBD GWAS SNP/transcript associations in cerebellum and temporal cortex	125

Chapter 1

Introduction: Corticobasal degeneration is a pathologically distinct 4R tauopathy with a range of clinical presentations

1.1. Overview

Corticobasal degeneration (CBD) is a rare, progressive neurodegenerative disorder with onset in the 5th to 7th decade of life. It is associated with heterogeneous motor, sensory, behavioral and cognitive symptoms, which make its diagnosis difficult in a living patient. The etiology of CBD is unknown; however, neuropathologic and genetic evidence supports a pathogenetic role for microtubule-associated protein tau. CBD pathology is characterized by circumscribed cortical atrophy with spongiosis and ballooned neurons; the distribution of these changes dictates the patient's clinical presentation. Neuronal and glial tau pathology is extensive in gray and white matter of the cortex, basal ganglia, diencephalon and rostral brainstem. Abnormal tau accumulation within astrocytes forms pathognomonic astrocytic plaques. The classic clinical presentation, termed corticobasal syndrome (CBS), comprises asymmetric progressive rigidity and apraxia with limb dystonia and myoclonus. CBS also occurs in conjunction with other diseases, including Alzheimer disease and progressive supranuclear palsy. Moreover, the pathology of CBD is associated with clinical presentations other than CBS, including Richardson syndrome, behavioral variant frontotemporal dementia, primary progressive aphasia and posterior cortical syndrome. Progress in the development of therapeutic agents for CBD and recent efforts to develop biomarkers that can distinguish tauopathies from tau-unrelated degenerative disorders are briefly described. The latter will become increasingly important for designing future pharmacological trials in this rare neurodegenerative tauopathy.

1.2. Background

CBD is a rare, progressive neurodegenerative 4-repeat (4R) tauopathy associated with a wide variety of motor, sensory, behavioral and cognitive symptoms that can also occur in other conditions. This clinical heterogeneity and lack of specific features make CBD difficult to diagnose prior to the patient's death.¹ Owing to the wide spectrum of clinical presentations of CBD, neuropathologic examination is required for a definitive diagnosis. Little is known about the epidemiology of CBD, and the available studies offer only crude estimates of its incidence. CBD has an estimated prevalence of 4.9–7.3 cases per 100,000 individuals² and an annual incidence rate of 0.02 cases per 100,000 individuals on the basis of an Eastern European and Asian population study.³ Disease onset is typically in the 5th to 7th decades of life, with an average disease duration of 7 years. No sex bias has been observed. The pathogenesis of CBD is unknown, and no effective therapy is currently available to treat this disease or even to slow its progression.

CBD was originally described as a movement disorder, but over the past few decades, as more clinical and pathological studies have been performed, the disease is now considered a disorder of both movement and cognition. CBD was first reported in 1968 by Rebeiz *et al.*, who described clinical and neuropathologic features of three patients in whom the disorder was termed corticodentatonigral degeneration with neuronal achromasia.⁴ Gibb and Marsden coined the term CBD in 1989,⁵ and this pathology has also been referred to as corticobasal ganglionic degeneration by some authors.⁶⁻⁸ The initial descriptions of CBD emphasized progressive movement abnormalities, which began as a unilateral slowing of voluntary movements with concurrent involuntary movements that eventually became generalized but remained asymmetric. In their paper, Rebeiz *et al.* noted, "...[the patients'] intellect was relatively preserved until the end."⁴ However, their well-documented report describes cognitive as well as behavioral dysfunction in all three patients. On neuropathologic examination, the researchers found distinct features common among the three patients, which included frontoparietal atrophy with neuronal loss, gliosis, 'achromatic' or ballooned neurons, and pigment loss in the substantia nigra.

The classic clinical movement disorder described by Rebeiz *et al.* in 1968 is now referred to as corticobasal syndrome (CBS), and its cardinal features are progressive asymmetric rigidity and apraxia with additional signs of cortical and basal ganglia involvement, such as aphasia and dystonia.^{5,8} Although CBS has some predictive value for finding CBD pathology, autopsy studies demonstrate considerable heterogeneity in

the pathology of patients who present with CBS.⁹ Over the years, clinical and pathological studies have highlighted several focal cortical syndromes associated with CBD pathology and, therefore, defining widely accepted clinical diagnostic criteria for research purposes is nearly impossible.^{7, 10-12} Tau pathology is also found in other neurodegenerative disorders, such as Alzheimer disease (AD)¹³ and progressive supranuclear palsy (PSP), and as tau-directed therapies undergo clinical trials, determining the correct underlying pathology in patients with CBS has become of more than merely academic interest.

1.3. Tauopathies and *MAPT*

Microtubule-associated protein tau, encoded by the *MAPT* gene, is required for microtubule assembly and stability, and is highly expressed in neuronal axons.¹⁴⁻¹⁶ When tau pathology is considered to be the main contributing factor to neurodegeneration, the disorder is classified as a tauopathy. The phosphorylation status of tau regulates its function and in tauopathies, tau is aberrantly phosphorylated and has an abnormal conformation that favors aggregation and inclusion formation.¹³ The human *MAPT* gene is located on chromosome 17q21.3 and alternative splicing of exons 2, 3, and 10 produces six tau protein isoforms in the adult CNS.^{17, 18} Tauopathies are characterized by their distinct biochemical protein isoform profiles, with regard to the presence of either three or four repeats (3R or 4R, respectively) in the tau microtubule-binding domain. In Alzheimer disease, tau neurofibrillary tangles are composed of both 3R and 4R isoforms,¹⁷ CBD and PSP have predominantly 4R tau pathology,¹⁹ and Pick's disease has predominantly 3R tau pathology.²⁰

1.4. Genetics of CBD

Mutations in *MAPT* disrupt tau alternative splicing and/or the protein properties of tau to interact with microtubules. The result of *MAPT* mutations show an increase in tau aggregation properties and lead to frontotemporal dementia with parkinsonism (FTDP-17), unequivocally demonstrating that tau dysfunction is sufficient to cause neurodegeneration.²¹⁻²³ Over 40 pathogenic *MAPT* mutations have been identified in more than 100 families affected by FTDP-17.²⁴ Patients with *MAPT* mutations can exhibit clinical and pathological features associated with corticobasal degeneration,²⁵⁻²⁷ yet we have reported the only CBD case that meets neuropathologic diagnostic criteria harboring tau mutation (p.N410H; **Chapter 4**).²⁸ Whole-exome sequencing in a family

with pathologically-confirmed CBD was recently reported, however there was no display of tau immunohistochemistry for the CBD case, so it is not clear if the case did in fact have CBD.²⁹

Genetic analyses of *MAPT* identified common inversion at chromosome 17q21.3 encompassing *MAPT*.³⁰ Prior to the discovery of *MAPT* mutations, Conrad, *et al.* reported an association of risk of PSP with a dinucleotide repeat located in intron 9 of *MAPT*.³¹ Subsequently, multiple polymorphisms were identified to be in complete linkage disequilibrium and this led to the definition of two major haplotypes on chromosome 17q21, termed H1 and H2.³² As a result of these studies and others, it was then clear that there is an increased risk to develop PSP and CBD for individuals carrying the H1 haplotype.³³⁻⁴⁰ From the recently completed PSP genome-wide association study it is clear that H1 tau haplotype confers risk for developing PSP ($P = 1.5 \times 10^{-116}$, OR = 5.5).⁴¹

1.5. Clinical syndromes associated with CBD

The clinical syndrome in patients with neurodegenerative diseases is a representation of the topography of the lesions but not necessarily the nature of the underlying pathology. Since CBD is a disease with prominent focal cortical atrophy and variable subcortical pathology, patients with CBD can exhibit a range of distinct clinical syndromes, including CBS, Richardson syndrome (the most common clinical presentation of PSP), primary progressive aphasia, frontotemporal dementia (FTD), and posterior cortical atrophy (PCA) (**Table 1.1**).^{6, 42-50} Although diagnostically far from perfect, clinical features can help to distinguish CBD from its so-called mimickers in some patients.

Reference	Sex F:M	Age at onset/ disease duration ^a	Common features at onset (% of patients)					Clinical diagnosis ^b (% of patients)				
			Limb apraxia	Memory impairment	Behavioral changes	Gait disturbance	Speech disorder	CBS	AD or PD	FTD	RS	
Schneider <i>et al.</i> (1997) ⁴⁶	10:1	67/7.9	64	18	9	9	9	64	27	0	0	
Litvan <i>et al.</i> (2000) ⁵¹	14:13	64/7.0	37	33	33	26	22	22	30	7	4	
Murray <i>et al.</i> (2007) ⁴⁴	8:7	61/5.4	33	33	40	27	40	40	13	33	13	
Ling <i>et al.</i> (2010) ⁴⁵	9:10	66/6.0	26	37	26	63	16	26	10	5	42	
Totals	41:31	65/6.6	38	32	29	33	22	33	21	11	15	

^aAge at onset and disease duration in years. ^bThe total does not equal 100% because some series had final diagnoses other than the diseases listed here. AD, Alzheimer disease; CBD, corticobasal degeneration; CBS, corticobasal syndrome; FTD, frontotemporal dementia; NA, not available; PD, Parkinson disease; RS, Richardson syndrome.

1.5.1. Corticobasal syndrome

CBS, the classic motor presentation of CBD as first described by Rebeiz and co-workers,⁴ accounts for <50% of autopsy-confirmed cases. Core features of CBS include levodopa-unresponsive parkinsonism, asymmetric akinesia, and rigidity, accompanied by other cortical and basal ganglia dysfunction, such as limb and oculomotor apraxia, cortical sensory deficits, dystonic posturing of a limb, myoclonus, and alien limb phenomenon.^{10, 52} These cortical signs and symptoms are attributed to a predominant frontal and parietal involvement. Patients can present with either motor or cognitive complaints or with a combination of the two. In a combined series of 27 individuals with CBD confirmed by autopsy, the most frequent features at onset of the disease were limb clumsiness in 37% of the patients, followed by memory loss and behavioral changes in another 33%.^{47, 51, 53} A separate longitudinal study of 15 individuals with CBD reported an exclusively cognitive change presentation in about half of the patients; another 20% had a motor abnormality presentation, and the remaining 30% had both motor and cognitive complaints.⁴⁴ Owing to the remarkably low sensitivity and positive predictive

value of these features for diagnosing CBD, studies of the neuropsychiatric features of patients with a clinical diagnosis of CBD should be interpreted with caution.

The accuracy of clinical diagnosis of CBD may, however, improve with disease progression. In a review of 27 autopsy-confirmed CBD patients by Litvan and co-workers, 22% of the patients had CBS as the initial diagnosis, increasing to 41% before death.⁵¹ Similarly, in a study of 13 autopsy-confirmed cases of CBD, 35% had CBS as an initial diagnosis, increasing to 54% prior to death.⁵⁴ Being able to predict CBD pathology as early in the disease course as possible is of great importance owing to the growing number of tau-directed therapies currently being developed.

The CBD mimickers, which resemble CBS but have different underlying pathologies, include AD, PSP and frontotemporal lobar degeneration with TDP-43 pathology (FTLD–TDP, sporadic and familial), among others.^{9, 12, 47, 55-57} Whitwell *et al.* reported that although a region of atrophy was common to all pathologies that result in CBS, CBS caused by FTLD-TDP was associated with notable frontotemporal gray matter atrophy; CBS caused by AD was associated with prominent temporoparietal atrophy; and in CBS caused by CBD or PSP gray matter atrophy was focused in the premotor cortex with additional involvement of superior posterior frontal cortex.⁵⁸

1.5.2. Richardson syndrome

CBD and PSP are indeed distinct clinical and pathological entities, but their overlapping features have become increasingly apparent. Richardson syndrome is the typical presentation of PSP,^{43, 59} characterized by postural instability leading to falls soon after disease onset, vertical supranuclear gaze palsy, dysarthria, dysphagia, and subcortical cognitive disturbances.⁶⁰ The occurrence of PSP presenting as CBS has been attributed to either greater cortical tau pathology than is observed in typical PSP⁶¹ or an asymmetrical tau burden.⁶² A study from 2010 assessed differences in cortical atrophy by MRI in patients with CBS and showed that different patterns of atrophy are associated with specific histopathologic abnormalities.⁵⁸ When patients with CBD present with bilateral motor disturbances and early frontal lobe dementia, they are frequently misdiagnosed as having PSP since both disorders involve levodopa-unresponsive parkinsonism and can share several other clinical features.^{63, 64} Asymmetry of clinical signs and symptoms may have been overemphasized in the early CBD literature, as several studies of autopsy-confirmed cases have reported the occurrence of symmetric motor disturbances.^{45, 65, 66}

Subtle differences in eye movement abnormalities may be able to differentiate CBD from PSP. Patients with CBD can develop eye movement abnormalities similar to those seen in PSP patients. Decreased vertical saccadic velocities preceding vertical supranuclear gaze palsy are typically seen in patients with PSP, whereas increased saccadic latencies with preserved velocity are seen in patients with CBD, and the horizontal and vertical planes are similarly affected.⁶⁷⁻⁶⁹ Ling *et al.* described clinical features of patients with CBD presenting with Richardson syndrome and confirmed that differences in these eye movement abnormalities were diagnostically helpful in differentiating CBD from PSP.⁴⁵

Postural instability and falls occurring within the first year of symptom onset are indicative of PSP.⁷⁰ By contrast, the current literature shows that if patients with CBD do experience falls, they usually occur late in the disease course; when the patient has asymmetric motor disturbances, falls tend to incline towards the affected side of the body. Few studies have compared the neuropsychiatric profiles of patients with CBD and PSP. In a clinical series, Cummings and Litvan used the Neuropsychiatric Inventory to assess behavioral symptoms in patients with dementia and found that depression and irritability were notably more frequent in patients with CBD than in those with PSP. The latter, by contrast, exhibited an increased frequency of apathy.⁷¹

Patients with pathologically confirmed CBD and PSP show differing patterns of brain atrophy on MRI.⁷² When grouped according to their presenting feature (extrapyramidal versus cognitive impairment), patients with CBD who had an extrapyramidal presentation had greater cortical atrophy and less brainstem atrophy compared to patients with PSP who had an extrapyramidal presentation. Among patients who presented with cognitive impairment, those with CBD had substantially greater atrophy of cortical and subcortical gray matter, and less atrophy of subcortical white matter, than those who had PSP.⁷² Future neuroimaging studies are warranted and may help differentiate underlying CBD from PSP pathology in patients presenting with RS.

1.5.3. Behavioral variant frontotemporal dementia

Patients who present with behavioral variant FTD (bvFTD) exhibit marked behavioral and personality changes, including apathy, disinhibition, perseveration, executive dysfunction, obsessive–compulsive behaviors, and dramatically impaired insight.⁷³ In approximately 50% of such patients, the underlying pathology is tau-positive (PSP, CBD,

or Pick's disease). The other 50% have tau-negative FTLD with ubiquitin immunoreactive inclusions (FTLD-U), which in the majority of cases are TDP-43-positive.^{74, 75} Although imaging signatures have been identified for specific pathologies, in one large study of patients with bvFTD no specific signature pattern of atrophy could distinguish tau-positive from tau-negative patients.^{76, 77} Josephs *et al.* found that bvFTD was the syndrome least predictive of underlying pathology.⁷⁷ In spite of this finding, some studies have identified clinical and neuropsychiatric features that could help to distinguish tau-positive from tau-negative bvFTD. Hodges *et al.* found that patients with tau-positive bvFTD were substantially older at the time of diagnosis (mean 61.7 years) than the tau-negative cases (mean 53.7 years).⁷⁴ Forman *et al.* found that the presence of both a behavioral disorder and aphasia at disease onset was more predictive of FTLD-U than were AD or other tauopathies.⁷⁵ Grossman *et al.* found that tau-positive FTLD was associated with visual perceptual and spatial difficulties, whereas tau-negative FTLD was linked to language and executive dysfunction.⁷⁸ In another clinicopathologic study, Hu *et al.* found that poor planning and judgment was associated with tau pathology, whereas impaired personal conduct and an absence of dysexecutive symptoms were predictive of FTLD-U pathology.⁵⁶ These observations suggest that longitudinal evaluations of neuropsychologic features may be useful in antemortem differentiation between tau-positive and tau-negative pathology.

The nearly equal distribution of tau-positive and tau-negative underlying pathologies in bvFTD syndrome highlights the considerable overlap in clinical features of CBD, PSP, and FTLD. Indeed, some are in favor of grouping these three conditions under the single designation of FTD–Pick complex.⁴⁸ Kertesz *et al.* have shown that bvFTD followed by the late development of progressive aphasia is usually caused by tau-negative FTLD.⁵⁴ In another distinct syndrome progression, which is highly predictive of tau-positive pathology, patients present with a movement disorder (such as CBS) or the movement disorder develops after primary progressive aphasia. The differential diagnosis, however, is complicated because some patients with CBD develop only minimal CBS features late in the disease course, but present with notable features of bvFTD.⁶³ The bvFTD CBD phenotype requires additional clinicopathologic studies to further our understanding of bvFTD as a clinical presentation of CBD.

1.5.4. Primary progressive aphasia

Primary progressive aphasia is a focal dementia disorder where the dominant deficit is progressive language impairment.⁷⁹ A distinct form of primary progressive aphasia—termed progressive nonfluent aphasia—is most often associated with tau-positive pathology, including CBD, PSP and Pick disease.^{49, 76, 80} The other forms of primary progressive aphasia, semantic dementia and logopenic progressive aphasia, are more often associated with FTLD–TDP and AD pathology, respectively.⁸¹ The characteristics of progressive nonfluent aphasia include errors in language production with agrammatism and grammatical simplification.⁷³ Speech production is typically strained or halting, with speech-sound errors occurring as a result of coexisting motor speech problems, referred to as apraxia of speech.

Clinicopathologic studies in patients with progressive nonfluent aphasia have highlighted the difficulty of obtaining an accurate antemortem diagnosis, yet apraxia of speech, with or without progressive nonfluent aphasia, is often observed in patients with a tauopathy, but not in those with FTLD–TDP.⁴⁹ As with the other primary progressive aphasia subtypes, several different pathologies have been reported to occur at varying frequencies in patients with progressive nonfluent aphasia. Some researchers have suggested that quantitative studies of neuropsychologic features can be useful to predict the underlying pathology in patients with progressive language deterioration. Josephs *et al.* suggested that one could differentiate between patients with CBD and PSP since apraxia of speech without nonfluent aphasia was more frequent in the patients with PSP, whereas those with CBD tended to have both apraxia of speech and nonfluent aphasia. In three combined series of 93 pathologically confirmed individuals, 80% of patients with progressive nonfluent aphasia had tau-positive pathology, suggesting this can be used as a distinguishing feature in predicting underlying tau or TDP-43 pathology.^{74, 76, 82}

1.5.5. Posterior cortical atrophy syndrome

Patients with posterior cortical atrophy (PCA) exhibit disturbances in visual perception with features of Balint syndrome, Gerstmann syndrome, visual agnosia, and/or alexia due to predominantly affected occipitoparietal cortices.⁸³ PCA is most often associated with neuropathology of AD or Creutzfeldt–Jakob disease,⁸⁴ although posterior cortical atrophy syndrome has been described in patients with pathologically confirmed CBD.⁸⁴⁻⁸⁶ Two patients with CBD who had PCA syndrome carried the brunt of the tau pathology in

the posterior parietal cortex and Brodmann areas 17 and 18.⁸⁵ Although this is an uncommon clinical presentation of CBD, CBD-PCA is recognized as a CBD variant.

1.6. Diagnosis of corticobasal degeneration

Several features can help to distinguish corticobasal degeneration from its clinical mimickers.

Progressive supranuclear palsy

- Postural instability with falls occurring within the 1st year of disease onset
- Vertical (especially downward) supranuclear gaze palsy
- Usually symmetric parkinsonism, although cases of asymmetric parkinsonism associated with progressive supranuclear palsy have been described
- Absent cortical features, such as myoclonus and apraxia

Parkinson disease

- Marked and sustained benefit from dopaminergic therapy
- Resting tremor

Dementia with Lewy bodies

- Visual hallucinations (not drug-related)
- Rapid eye movement sleep behavior disorder
- Fluctuating cognition

Multiple system atrophy

- Pronounced dysautonomia
- Cerebellar ataxia
- Disruption of rapid eye movement sleep behavior

Alzheimer disease

- Initial prominent short-term memory impairment

Creutzfeldt–Jakob disease

- Rapid disease progression with a disease course <1 year

1.7. Classifying the 4R tauopathies

When they were originally described, CBD and PSP were considered distinct clinical and pathological disorders,^{4, 60} and they have remained distinct nosological entities over the years. However, there is a consensus that CBD and PSP could represent a disease spectrum, since they have overlapping clinical, pathological, genetic, and biochemical

features. Both disorders involve an accumulation of the abnormal 4R tau isoform in neurons and glial cells (oligodendroglia and astrocytes). They also share a similar genetic basis, with a higher frequency of the *MAPT* H1 haplotype than is found in healthy controls. These characteristics of CBD and PSP support grouping them as the 4R tauopathies. This approach could prove useful in the design of tau-directed therapeutic clinical trials. Whether CBD and PSP share the same disease mechanism remains unknown; nevertheless, diagnostic accuracy is substantially improved when CBD and PSP are grouped as a single entity.

1.7.1. Clinical presentations

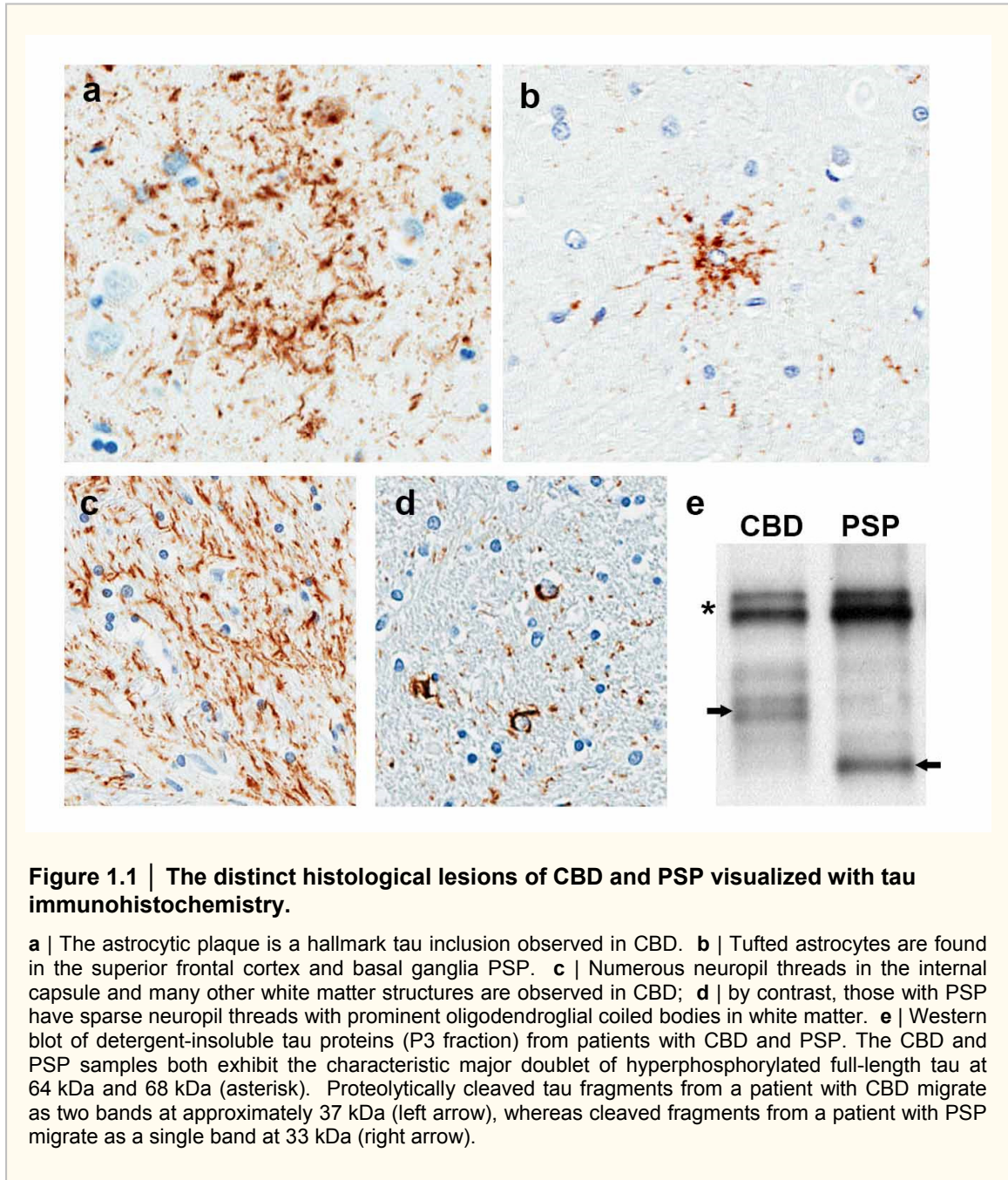
In the archetypal presentations of CBD and PSP (CBS and Richardson syndrome, respectively), the two disorders have distinct clinical features; however, the differential diagnosis is often complicated and misdiagnosis is not infrequent, even at autopsy. Some studies suggest PSP has a slightly later age of onset than CBD, but few meaningful differences in any clinical or demographic feature have been demonstrated.

1.7.2. Neuropathologic features

Neuropathologic diagnostic criteria for CBD have been refined and validated on the basis of tau immunohistochemical analysis, with an emphasis on tau-positive neuropil threads in gray and white matter of the cortex, basal ganglia, diencephalon and rostral brainstem (**Figure 1.1**).⁸⁶ In contrast to the original description by Rebeiz *et al.*, these updated criteria place reduced emphasis on the ballooned neuron because this finding can lack diagnostic specificity.⁸⁷

The main difficulty in neuropathologic diagnosis arises in patients with atypical CBD who have greater than usual brainstem and cerebellar pathology,⁶⁵ and in patients with PSP who have greater than usual cortical pathology.^{61, 88} In the majority of individuals, the distribution of tau pathology differs according to whether they have CBD or PSP: tau pathology in patients with CBD occurs predominantly in both gray and white matter of forebrain structures, whereas in those with PSP tau pathology occurs predominantly in hindbrain structures and tau pathology burden in white matter is not as severe as found in CBD.⁸⁹ However, exceptions to these general rules exist in patients with atypical presentations of both disorders. The strongest argument for separating these two diseases comprises their distinct pathological and biochemical features. For

example, the astrocytic lesions associated with CBD and PSP are distinct and rarely (if ever) coexist.⁹⁰ The pathognomonic astrocytic lesion in CBD is the astrocytic plaque,^{90, 91} whereas tufted astrocytes are characteristic of PSP (**Figure 1.1**).⁹²



1.7.3. Biochemical features

Although CBD and PSP are both 4R tauopathies, biochemical studies show differences in tau protein profiles associated with the two disorders. In particular, the tau protein cleavage fragments differ in patients with CBD and PSP. Detergent-insoluble, lower molecular weight tau fragments from patients with CBD migrate as two bands (a doublet of around 37 kDa), whereas those from PSP patients migrate as a single band at 33 kDa (**Figure 1.1**).^{93, 94} It is possible that these differences in proteolytic processing of tau may be related to the differences in glial lesions that occur in patients with CBD and PSP. Whether differences also exist between these biochemical profiles in various brain regions remains to be determined. Except for differences in the size of tau cleavage fragments, the biochemical properties of tau are similar in the brains of patients with CBD and PSP. The disease relevance of tau proteolytic fragments is currently unknown. It remains a possibility that tau aggregation occurs and subsequently the tau fragments are generated. Or another possibility is that tau is cleaved first and then the proteolytic fragments induce nucleation of tau into insoluble aggregates.

1.7.4. Mechanisms of tau-mediated disease

Under pathological conditions, tau becomes hyperphosphorylated, reducing its binding affinity for microtubules. This change leads to a loss of proper microtubule functioning and/or a toxic gain of function, as dissociated tau has a greater propensity for multimerization and aggregation than microtubule-bound tau. The cellular dysfunction that causes tau to become hyperphosphorylated in sporadic tauopathies is currently unknown; however, some evidence supports a role for microglia in sporadic tauopathies,^{95, 96} and a molecular biology study published in 2010 described a mechanism through which microglial signaling enhances tau hyperphosphorylation in neurons in the setting of neuroinflammation.⁹⁷ Further work is needed, however, to determine whether this mechanism, which provides a drug target upstream of tau hyperphosphorylation, will lead to the development of new strategies for the treatment of tauopathies.

Although an extensive amount of research has gone into elucidating the mechanism of tau-mediated neurodegeneration, many gaps remain in our current knowledge. Two studies have localized initial tau dysfunction to the synapse, which is the region where cell–cell communication occurs. Ittner *et al.* showed that tau has a role

in targeting fyn kinase to postsynaptic compartments and modulates *N*-methyl-D-aspartate (NMDA) receptors, resulting in excitotoxic downstream signaling.⁹⁸ Hoover *et al.* also showed that tau accumulates in dendritic spines, causing a disruption in synaptic function by reducing the levels of α -amino-3-hydroxy-5-methyl-4-isoxazolepropionic acid (AMPA) and NMDA receptors.⁹⁹ These studies have advanced our understanding of the pathophysiological processes underlying tauopathies that could provide new strategies for the development of tau-directed therapeutics.

1.8. Tau-directed therapeutics

Interest in the development of tau-directed therapeutics is growing. Several different approaches to reducing tau-mediated neurodegeneration focus on compensating for the loss of tau function using microtubule-stabilizing agents, reducing hyperphosphorylation of tau through the inhibition of protein kinases, inhibiting the toxic aggregation of tau fibrils using agents that block protein–protein interactions, and enhancing intracellular tau degradation by targeting proteins involved in the ubiquitin–proteasome system. Three compounds progressed to human clinical testing: methylene blue, lithium chloride, and an octapeptide (Asn–Ala–Pro–Val–Ser–Ile–Pro–Gln) known as NAP.¹⁰⁰ Methylene blue was the first drug to demonstrate inhibition of tau aggregation and to alter the structure of paired-helical filaments that make up neurofibrillary tangles in the brains of patients with AD.¹⁰¹ Methylene blue has already been approved by the FDA for several conditions and is currently undergoing phase III clinical testing in patients with AD, suggesting that patients with other forms of neurodegenerative tauopathy could also benefit from methylene blue treatment.

Lithium chloride is an inhibitor of glycogen synthase kinase 3 β (GSK3 β), one of several kinases that phosphorylate tau.^{102, 103} GSK3 β has been extensively studied as a therapeutic target in AD animal models. Treatment with lithium chloride consistently results in an attenuation of tau hyperphosphorylation and pathology in animal models of tauopathies.¹⁰⁴⁻¹⁰⁸ Transgenic animals that harbor human *MAPT* mutations recapitulate key features of the neuropathology seen in human tauopathies, and these models are being used as a tool for preclinical drug discovery.¹⁰⁹

Microtubule-stabilizing compounds, including the anticancer drug paclitaxel, showed improved microtubule density, accelerated axonal transport, and increased motor function in a mouse model of tauopathy.¹¹⁰ These benefits were accompanied by intolerable adverse effects, however, because paclitaxel does not readily cross the

blood–brain barrier and, therefore, high doses were required to observe any therapeutic effect. Efforts to explore other microtubule- stabilizing agents with improved blood–brain barrier permeability led to discovery of the neuroprotective octapeptide NAP, which has shown promise as a therapy for tauopathies by reducing the levels of hyperphosphorylated tau.¹¹¹⁻¹¹³ Treatment with another microtubule-stabilizing compound, epothilone D, was reported in 2010 to increase microtubule density and reduce cognitive deficits in an animal model of tauopathy.¹¹⁴ Neither NAP nor epothilone D were efficacious in phase 1 clinical trials, and have since been discontinued. Enhancing the cellular machinery responsible for degrading pathological tau species using inhibitors of heat-shock protein 90 reduces levels of hyperphosphorylated tau *in vitro* and *in vivo*.^{115, 116} High-throughput drug library screens have been performed to identify novel molecules capable of inhibiting tau fibrillization. None of these molecules has yet been tested in animal models, but this methodology shows promise for future identification of therapeutic compounds for tauopathy patients.¹¹⁷

1.9. Identification of biomarkers

Development of imaging and cerebrospinal fluid (CSF) biomarkers for CBD and related tauopathies is still in the early stages; however, such markers have the potential to improve CBD diagnostic accuracy. Tau levels in CSF have been studied quite extensively in patients with AD and, since 1997, these levels have been monitored in clinical series of patients with PSP and CBD.¹¹⁸⁻¹²⁰ Some studies have shown an increase in total tau levels in patients with CBD compared with controls,^{119, 121} whereas others found no notable difference in CSF tau levels in patients with CBD compared with both healthy controls and patients with PSP.^{122, 123} Although these initial studies have preliminarily assessed total tau and phosphorylated tau levels, biochemical evidence in CBD and PSP brain tissue suggests that evaluating levels of tau proteolytic fragment species could be useful in differentiating these neurodegenerative tauopathies.^{120, 124, 125}

Levels of other CSF proteins, including amyloid- β_{42} , neurofilament light chain, and neurofilament heavy chain, have been reported to be different in patients with PSP compared to healthy control individuals and patients with other parkinsonian disorders.^{122, 126, 127} Future biomarker diagnostic studies could use unbiased proteomic methods in brain tissue and CSF to explore the differences in expression of proteins between individuals with CBD and PSP. Again, the requirement for autopsy

confirmation in CBD slows our progress in understanding the CBD disease mechanism, here as an example, delaying the studies required to identify diagnostic biomarkers.

Studies have identified distinctive patterns of brain atrophy on neuroimaging in patients with autopsy-confirmed CBD and PSP,⁷² showing that CBD patients have a characteristic pattern of posterior frontal atrophy regardless of the clinical syndrome (**Figure 1.2**). This pattern of brain atrophy could prove to be a useful biomarker of CBD pathology. Differences in atrophy patterns elsewhere in the brain seem to reflect clinical differences: for example, marked prefrontal atrophy is observed in patients with CBD related to bvFTD, and substantial atrophy in posterior regions of the brain is observed in those with CBD related to posterior cortical atrophy. If CBD and PSP can be differentiated in living patients by use of inexpensive and relatively noninvasive methods, our knowledge of the epidemiology and pathogenesis of CBD will increase exponentially, as opposed to having to rely on a neuropathologic diagnosis to identify those with CBD.

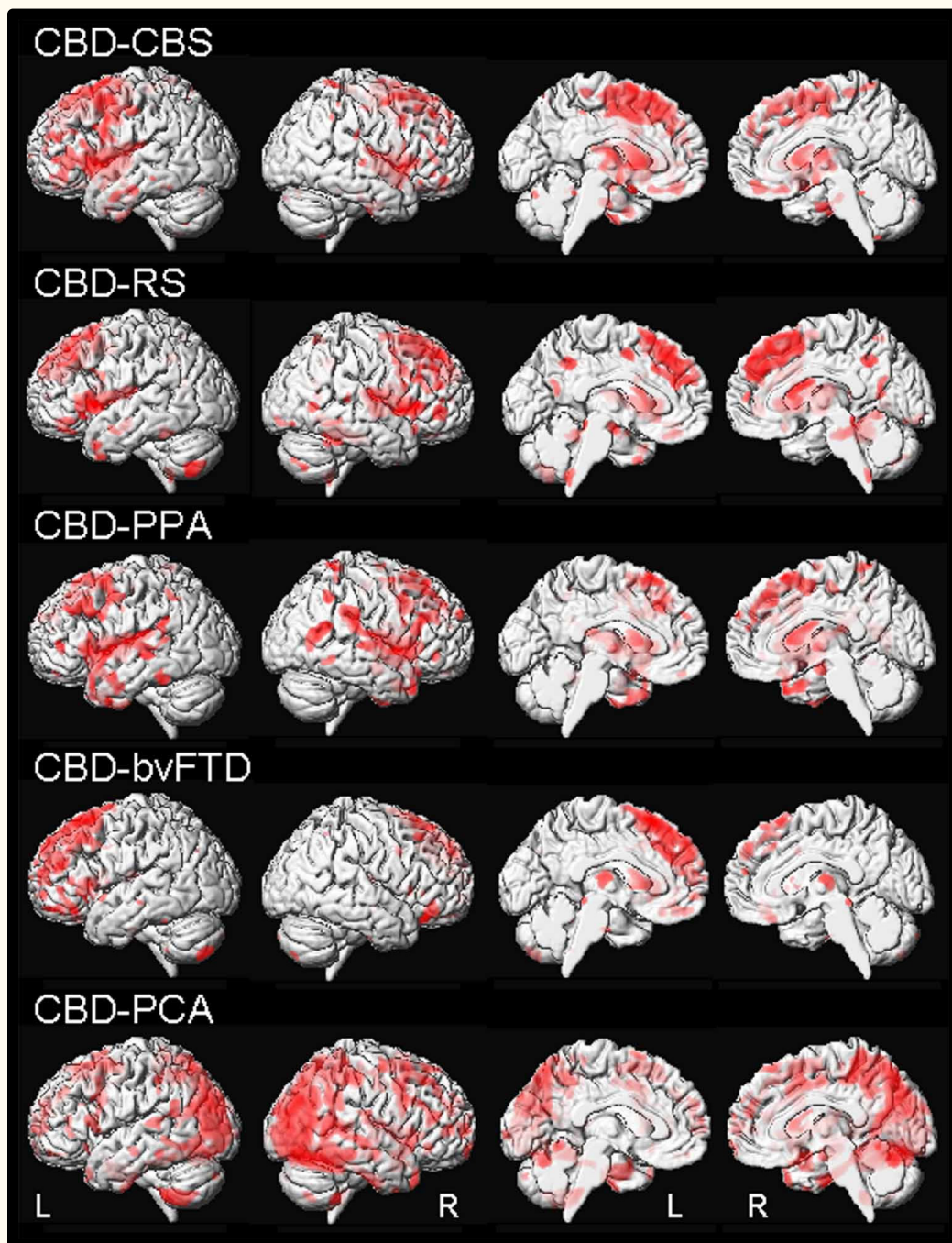


Figure 1.2 | Patterns of gray matter loss in groups of patients with autopsy-confirmed CBD but different clinical syndromes.

The results were generated using voxel-based morphometry and are shown on three-dimensional surface and medial renders of the brain. All clinical groups show gray matter loss as indicated by red coloration in the posterior lateral and medial frontal lobe, suggesting that this is a signature pattern of CBD pathology; however, patterns of gray matter loss that differ between groups extend into other regions of the brain. These differences are thought to cause the various clinical syndromes associated with CBD.

1.10. Conclusions

This dissertation focuses on the clinical heterogeneity associated with CBD pathology to emphasize the requirement for autopsy confirmation in CBD genetic studies. This CBD clinical conundrum is addressed in chapters 2 and 3 and these data show the advantages of using quantitative neuropathology to illustrate the topographic distribution of tau pathology as it relates to clinical presentations of CBD patients. The quantitative neuropathology methodology used in these studies confirm that CBD can be a pathologic substrate of Richardson syndrome. Importantly, the studies herein show that the frequency of CBD misdiagnosed as PSP is significantly more common than previously described.

A paucity of genetic studies in CBD is a direct result of this marked antemortem diagnostic inaccuracy. In the second part of this dissertation, CBD genetic studies were made feasible due to the availability of the largest, single neuropathologically confirmed CBD cohort. A systematic sequence analysis of *MAPT* in CBD is described in chapter 4 and genome-wide association study of CBD compared to control individuals is presented in chapter 5. The complex and highly variable clinical presentation of CBD is the prevailing difficulty in identifying and accurately diagnosing this disorder in living patients.

Efforts are currently being made to improve the accuracy of diagnosis using imaging and CSF biomarkers. Although considerable progress has been made in delineating the clinical picture of CBD, these studies are inherently limited because they can only be performed retrospectively owing to the necessity of obtaining an autopsy-confirmed diagnosis. The first completed genome-wide association study for PSP is a key endeavor that will help to elucidate the genetic basis of this 4R tauopathy and may give us insight into CBD genetic risk factors as well.⁴¹ These genomic data will provide important insight into novel pathways and the fundamental biology involved in the pathogenesis of tauopathies, which might lead to new pharmacological strategies for the treatment of patients with this devastating condition.

1.11. References

1. Litvan, I, Agid, Y, Goetz, C, Jankovic, J, Wenning, GK, Brandel, JP, Lai, EC, Verny, M, Ray-Chaudhuri, K, McKee, A, Jellinger, K, Pearce, RK & Bartko, JJ. Accuracy of the clinical diagnosis of corticobasal degeneration: a clinicopathologic study. *Neurology* 48, 119-25 (1997).
2. Togasaki, DM & Tanner, CM. Epidemiologic aspects. in *Corticobasal degeneration* (eds. Litvan, I., Goetz, C.G. & Lang, A.E.) 53-59 (Lippincott, Williams & Wilkins, Philadelphia, 2000).
3. Winter, Y, Bezdolnyy, Y, Katunina, E, Avakjan, G, Reese, JP, Klotsche, J, Oertel, WH, Dodel, R & Gusev, E. Incidence of Parkinson's disease and atypical parkinsonism: Russian population-based study. *Mov Disord* 25, 349-56 (2010).
4. Rebeiz, JJ, Kolodny, EH & Richardson, EP, Jr. Corticodentatonigral degeneration with neuronal achromasia. *Arch Neurol* 18, 20-33 (1968).
5. Gibb, WR, Luthert, PJ & Marsden, CD. Corticobasal degeneration. *Brain* 112 (Pt 5), 1171-92 (1989).
6. Bergeron, C, Pollanen, MS, Weyer, L, Black, SE & Lang, AE. Unusual clinical presentations of cortical-basal ganglionic degeneration. *Ann Neurol* 40, 893-900 (1996).
7. Watts, RL & Mirra, SS. Corticobasal ganglionic degeneration. in *Movement disorders* (eds. Marsden, C.D. & Fahn, S.) 282-299 (Butterworth, London, 1994).
8. Riley, DL, A. Corticobasal ganglionic degeneration (CBGD): further observations in six additional cases. *Neurology* 38, 360 (1988).
9. Boeve, BF, Maraganore, DM, Parisi, JE, Ahlskog, JE, Graff-Radford, N, Caselli, RJ, Dickson, DW, Kokmen, E & Petersen, RC. Pathologic heterogeneity in clinically diagnosed corticobasal degeneration. *Neurology* 53, 795-800 (1999).
10. Riley, DE, Lang, AE, Lewis, A, Resch, L, Ashby, P, Hornykiewicz, O & Black, S. Cortical-basal ganglionic degeneration. *Neurology* 40, 1203-12 (1990).
11. Bak, TH & Hodges, JR. Corticobasal degeneration: clinical aspects. *Handbook of clinical neurology* 89, 509-21 (2008).
12. Lang, AE, Bergeron, C, Pollanen, MS & Ashby, P. Parietal Pick's disease mimicking cortical-basal ganglionic degeneration. *Neurology* 44, 1436-40 (1994).
13. Grundke-Iqbal, I, Iqbal, K, Quinlan, M, Tung, YC, Zaidi, MS & Wisniewski, HM. Microtubule-associated protein tau. A component of Alzheimer paired helical filaments. *J Biol Chem* 261, 6084-9 (1986).
14. Binder, LI, Frankfurter, A & Rebhun, LI. The distribution of tau in the mammalian central nervous system. *J Cell Biol* 101, 1371-8 (1985).
15. LoPresti, P, Szuchet, S, Papasozomenos, SC, Zinkowski, RP & Binder, LI. Functional implications for the microtubule-associated protein tau: localization in oligodendrocytes. *Proc Natl Acad Sci U S A* 92, 10369-73 (1995).
16. Witman, GB, Cleveland, DW, Weingarten, MD & Kirschner, MW. Tubulin requires tau for growth onto microtubule initiating sites. *Proc Natl Acad Sci U S A* 73, 4070-4 (1976).
17. Goedert, M, Spillantini, MG, Jakes, R, Rutherford, D & Crowther, RA. Multiple isoforms of human microtubule-associated protein tau: sequences and localization in neurofibrillary tangles of Alzheimer's disease. *Neuron* 3, 519-26 (1989).

18. Andreadis, A, Brown, WM & Kosik, KS. Structure and novel exons of the human tau gene. *Biochemistry* 31, 10626-33 (1992).
19. Sergeant, N, Watzel, A & Delacourte, A. Neurofibrillary degeneration in progressive supranuclear palsy and corticobasal degeneration: tau pathologies with exclusively "exon 10" isoforms. *Journal of neurochemistry* 72, 1243-9 (1999).
20. Delacourte, A, Sergeant, N, Watzel, A, Gauvreau, D & Robitaille, Y. Vulnerable neuronal subsets in Alzheimer's and Pick's disease are distinguished by their tau isoform distribution and phosphorylation. *Ann Neurol* 43, 193-204 (1998).
21. Hutton, M, Lendon, CL, Rizzu, P, Baker, M, Froelich, S, Houlden, H, Pickering-Brown, S, Chakraverty, S, Isaacs, A, Grover, A, Hackett, J, Adamson, J, Lincoln, S, Dickson, D, Davies, P, Petersen, RC, Stevens, M, de Graaff, E, Wauters, E, van Baren, J, Hillebrand, M, Joosse, M, Kwon, JM, Nowotny, P, Che, LK, Norton, J, Morris, JC, Reed, LA, Trojanowski, J, Basun, H, Lannfelt, L, Neystat, M, Fahn, S, Dark, F, Tannenberg, T, Dodd, PR, Hayward, N, Kwok, JB, Schofield, PR, Andreadis, A, Snowden, J, Craufurd, D, Neary, D, Owen, F, Oostra, BA, Hardy, J, Goate, A, van Swieten, J, Mann, D, Lynch, T & Heutink, P. Association of missense and 5'-splice-site mutations in tau with the inherited dementia FTDP-17. *Nature* 393, 702-5 (1998).
22. Poorkaj, P, Bird, TD, Wijsman, E, Nemens, E, Garruto, RM, Anderson, L, Andreadis, A, Wiederholt, WC, Raskind, M & Schellenberg, GD. Tau is a candidate gene for chromosome 17 frontotemporal dementia. *Annals of neurology* 43, 815-25 (1998).
23. Spillantini, MG, Murrell, JR, Goedert, M, Farlow, MR, Klug, A & Ghetti, B. Mutation in the tau gene in familial multiple system tauopathy with presenile dementia. *Proc Natl Acad Sci U S A* 95, 7737-41 (1998).
24. Spillantini, MG & Goedert, M. Tau pathology and neurodegeneration. *Lancet neurology* 12, 609-22 (2013).
25. Bugiani, O, Murrell, JR, Giaccone, G, Hasegawa, M, Ghigo, G, Tabaton, M, Morbin, M, Primavera, A, Carella, F, Solaro, C, Grisoli, M, Savoirdo, M, Spillantini, MG, Tagliavini, F, Goedert, M & Ghetti, B. Frontotemporal dementia and corticobasal degeneration in a family with a P301S mutation in tau. *J Neuropathol Exp Neurol* 58, 667-77 (1999).
26. Spillantini, MG, Yoshida, H, Rizzini, C, Lantos, PL, Khan, N, Rossor, MN, Goedert, M & Brown, J. A novel tau mutation (N296N) in familial dementia with swollen achromatic neurons and corticobasal inclusion bodies. *Ann Neurol* 48, 939-43 (2000).
27. Rossi, G, Marelli, C, Farina, L, Laura, M, Maria Basile, A, Ciano, C, Tagliavini, F & Pareyson, D. The G389R mutation in the MAPT gene presenting as sporadic corticobasal syndrome. *Mov Disord* 23, 892-5 (2008).
28. Kouri, N, Carlomagno, Y, Baker, M, Liesinger, AM, Caselli, RJ, Wszolek, ZK, Petrucelli, L, Boeve, BF, Parisi, JE, Josephs, KA, Uitti, RJ, Ross, OA, Graff-Radford, NR, DeTure, MA, Dickson, DW & Rademakers, R. Novel mutation in MAPT exon 13 (p.N410H) causes corticobasal degeneration. *Acta Neuropathologica* 127, 271-282 (2014).
29. Fekete, R, Bainbridge, M, Baizabal-Carvallo, JF, Rivera, A, Miller, B, Du, P, Kholodovych, V, Powell, S & Ondo, W. Exome sequencing in familial corticobasal degeneration. *Parkinsonism & related disorders* 19, 1049-52 (2013).
30. Stefansson, H, Helgason, A, Thorleifsson, G, Steinthorsdottir, V, Masson, G, Barnard, J, Baker, A, Jonasdottir, A, Ingason, A, Gudnadottir, VG, Desnica, N, Hicks, A, Gylfason, A, Gudbjartsson, DF, Jonsdottir, GM, Sainz, J, Agnarsson, K, Birgisdottir, B, Ghosh, S, Olafsdottir, A, Cazier, JB, Kristjansson, K, Frigge, ML, Thorgeirsson, TE, Gulcher, JR, Kong, A & Stefansson, K. A common inversion under selection in Europeans. *Nat Genet* 37, 129-37 (2005).

31. Conrad, C, Andreadis, A, Trojanowski, JQ, Dickson, DW, Kang, D, Chen, X, Wiederholt, W, Hansen, L, Masliah, E, Thal, LJ, Katzman, R, Xia, Y & Saitoh, T. Genetic evidence for the involvement of tau in progressive supranuclear palsy. *Ann Neurol* 41, 277-81 (1997).
32. Baker, M, Litvan, I, Houlden, H, Adamson, J, Dickson, D, Perez-Tur, J, Hardy, J, Lynch, T, Bigio, E & Hutton, M. Association of an extended haplotype in the tau gene with progressive supranuclear palsy. *Human molecular genetics* 8, 711-5 (1999).
33. Ezquerra, M, Pastor, P, Valldeoriola, F, Molinuevo, JL, Blesa, R, Tolosa, E & Oliva, R. Identification of a novel polymorphism in the promoter region of the tau gene highly associated to progressive supranuclear palsy in humans. *Neurosci Lett* 275, 183-6 (1999).
34. Hoenicka, J, Perez, M, Perez-Tur, J, Barabash, A, Godoy, M, Vidal, L, Astarloa, R, Avila, J, Nygaard, T & de Yébenes, JG. The tau gene A0 allele and progressive supranuclear palsy. *Neurology* 53, 1219-25 (1999).
35. Higgins, JJ, Golbe, LI, De Biase, A, Jankovic, J, Factor, SA & Adler, RL. An extended 5'-tau susceptibility haplotype in progressive supranuclear palsy. *Neurology* 55, 1364-7 (2000).
36. Houlden, H, Baker, M, Morris, HR, MacDonald, N, Pickering-Brown, S, Adamson, J, Lees, AJ, Rossor, MN, Quinn, NP, Kertesz, A, Khan, MN, Hardy, J, Lantos, PL, St George-Hyslop, P, Munoz, DG, Mann, D, Lang, AE, Bergeron, C, Bigio, EH, Litvan, I, Bhatia, KP, Dickson, D, Wood, NW & Hutton, M. Corticobasal degeneration and progressive supranuclear palsy share a common tau haplotype. *Neurology* 56, 1702-6 (2001).
37. Pastor, P, Ezquerra, M, Tolosa, E, Munoz, E, Marti, MJ, Valldeoriola, F, Molinuevo, JL, Calopa, M & Oliva, R. Further extension of the H1 haplotype associated with progressive supranuclear palsy. *Movement disorders : official journal of the Movement Disorder Society* 17, 550-6 (2002).
38. Pastor, P, Ezquerra, M, Perez, JC, Chakraverty, S, Norton, J, Racette, BA, McKeel, D, Perlmutter, JS, Tolosa, E & Goate, AM. Novel haplotypes in 17q21 are associated with progressive supranuclear palsy. *Ann Neurol* 56, 249-58 (2004).
39. Rademakers, R, Melquist, S, Cruts, M, Theuns, J, Del-Favero, J, Poorkaj, P, Baker, M, Sleegers, K, Crook, R, De Pooter, T, Bel Kacem, S, Adamson, J, Van den Bossche, D, Van den Broeck, M, Gass, J, Corsmit, E, De Rijk, P, Thomas, N, Engelborghs, S, Heckman, M, Litvan, I, Crook, J, De Deyn, PP, Dickson, D, Schellenberg, GD, Van Broeckhoven, C & Hutton, ML. High-density SNP haplotyping suggests altered regulation of tau gene expression in progressive supranuclear palsy. *Hum Mol Genet* 14, 3281-92 (2005).
40. Pittman, AM, Myers, AJ, Abou-Sleiman, P, Fung, HC, Kaleem, M, Marlowe, L, Duckworth, J, Leung, D, Williams, D, Kilford, L, Thomas, N, Morris, CM, Dickson, D, Wood, NW, Hardy, J, Lees, AJ & de Silva, R. Linkage disequilibrium fine mapping and haplotype association analysis of the tau gene in progressive supranuclear palsy and corticobasal degeneration. *Journal of medical genetics* 42, 837-46 (2005).
41. Hoglinger, GU, Melhem, NM, Dickson, DW, Sleiman, PM, Wang, LS, Klei, L, Rademakers, R, de Silva, R, Litvan, I, Riley, DE, van Swieten, JC, Heutink, P, Wszolek, ZK, Uitti, RJ, Vandrovцова, J, Hurtig, HI, Gross, RG, Maetzler, W, Goldwurm, S, Tolosa, E, Borroni, B, Pastor, P, Cantwell, LB, Han, MR, Dillman, A, van der Brug, MP, Gibbs, JR, Cookson, MR, Hernandez, DG, Singleton, AB, Farrer, MJ, Yu, CE, Golbe, LI, Revesz, T, Hardy, J, Lees, AJ, Devlin, B, Hakonarson, H, Muller, U & Schellenberg, GD. Identification of common variants influencing risk of the tauopathy progressive supranuclear palsy. *Nature genetics* 43, 699-705 (2011).
42. Bergeron, C, Davis, A & Lang, AE. Corticobasal ganglionic degeneration and progressive supranuclear palsy presenting with cognitive decline. *Brain Pathol* 8, 355-65 (1998).

43. Williams, DR, de Silva, R, Paviour, DC, Pittman, A, Watt, HC, Kilford, L, Holton, JL, Revesz, T & Lees, AJ. Characteristics of two distinct clinical phenotypes in pathologically proven progressive supranuclear palsy: Richardson syndrome and PSP-parkinsonism. *Brain* 128, 1247-58 (2005).
44. Murray, R, Neumann, M, Forman, MS, Farmer, J, Massimo, L, Rice, A, Miller, BL, Johnson, JK, Clark, CM, Hurtig, HI, Gorno-Tempini, ML, Lee, VM, Trojanowski, JQ & Grossman, M. Cognitive and motor assessment in autopsy-proven corticobasal degeneration. *Neurology* 68, 1274-83 (2007).
45. Ling, H, O'Sullivan, SS, Holton, JL, Revesz, T, Massey, LA, Williams, DR, Paviour, DC & Lees, AJ. Does corticobasal degeneration exist? A clinicopathological re-evaluation. *Brain* 133, 2045-57 (2010).
46. Schneider, JA, Watts, RL, Gearing, M, Brewer, RP & Mirra, SS. Corticobasal degeneration: neuropathologic and clinical heterogeneity. *Neurology* 48, 959-69 (1997).
47. Grimes, DA, Lang, AE & Bergeron, CB. Dementia as the most common presentation of cortical-basal ganglionic degeneration. *Neurology* 53, 1969-74 (1999).
48. Kertesz, A, Martinez-Lage, P, Davidson, W & Munoz, DG. The corticobasal degeneration syndrome overlaps progressive aphasia and frontotemporal dementia. *Neurology* 55, 1368-75 (2000).
49. Josephs, KA, Duffy, JR, Strand, EA, Whitwell, JL, Layton, KF, Parisi, JE, Hauser, MF, Witte, RJ, Boeve, BF, Knopman, DS, Dickson, DW, Jack, CR, Jr. & Petersen, RC. Clinicopathological and imaging correlates of progressive aphasia and apraxia of speech. *Brain* 129, 1385-98 (2006).
50. Raggi, A, Marcone, A, Iannaccone, S, Ginex, V, Perani, D & Cappa, SF. The clinical overlap between the corticobasal degeneration syndrome and other diseases of the frontotemporal spectrum: three case reports. *Behavioural neurology* 18, 159-64 (2007).
51. Litvan, I, Grimes, DA & Lang, AE. Phenotypes and prognosis: clinicopathologic studies of corticobasal degeneration. *Adv Neurol* 82, 183-96 (2000).
52. Gibb, WR, Luthert, PJ & Marsden, CD. Clinical and pathological features of corticobasal degeneration. *Adv Neurol* 53, 51-4 (1990).
53. Wenning, GK, Litvan, I, Jankovic, J, Granata, R, Mangone, CA, McKee, A, Poewe, W, Jellinger, K, Ray Chaudhuri, K, D'Olhaberriague, L & Pearce, RK. Natural history and survival of 14 patients with corticobasal degeneration confirmed at postmortem examination. *J Neurol Neurosurg Psychiatry* 64, 184-9 (1998).
54. Kertesz, A, McMonagle, P, Blair, M, Davidson, W & Munoz, DG. The evolution and pathology of frontotemporal dementia. *Brain* 128, 1996-2005 (2005).
55. Horoupian, DS & Wasserstein, PH. Alzheimer's disease pathology in motor cortex in dementia with Lewy bodies clinically mimicking corticobasal degeneration. *Acta Neuropathol* 98, 317-22 (1999).
56. Hu, WT, Rippon, GW, Boeve, BF, Knopman, DS, Petersen, RC, Parisi, JE & Josephs, KA. Alzheimer's disease and corticobasal degeneration presenting as corticobasal syndrome. *Mov Disord* 24, 1375-9 (2009).
57. Benussi, L, Ghidoni, R, Pegoiani, E, Moretti, DV, Zanetti, O & Binetti, G. Progranulin Leu271LeufsX10 is one of the most common FTL and CBS associated mutations worldwide. *Neurobiol Dis* 33, 379-85 (2009).
58. Whitwell, JL, Jack, CR, Jr., Boeve, BF, Parisi, JE, Ahlskog, JE, Drubach, DA, Senjem, ML, Knopman, DS, Petersen, RC, Dickson, DW & Josephs, KA. Imaging correlates of pathology in corticobasal syndrome. *Neurology* 75, 1879-87 (2010).

59. Williams, DR, Lees, AJ, Wherrett, JR & Steele, JC. J. Clifford Richardson and 50 years of progressive supranuclear palsy. *Neurology* 70, 566-73 (2008).
60. Steele, JC, Richardson, JC & Olszewski, J. Progressive Supranuclear Palsy. A Heterogeneous Degeneration Involving the Brain Stem, Basal Ganglia and Cerebellum with Vertical Gaze and Pseudobulbar Palsy, Nuchal Dystonia and Dementia. *Arch Neurol* 10, 333-59 (1964).
61. Tsuboi, Y, Josephs, KA, Boeve, BF, Litvan, I, Caselli, RJ, Caviness, JN, Uitti, RJ, Bott, AD & Dickson, DW. Increased tau burden in the cortices of progressive supranuclear palsy presenting with corticobasal syndrome. *Mov Disord* 20, 982-8 (2005).
62. Oide, T, Ohara, S, Yazawa, M, Inoue, K, Itoh, N, Tokuda, T & Ikeda, S. Progressive supranuclear palsy with asymmetric tau pathology presenting with unilateral limb dystonia. *Acta Neuropathol* 104, 209-14 (2002).
63. Litvan, I, Grimes, DA, Lang, AE, Jankovic, J, McKee, A, Verny, M, Jellinger, K, Chaudhuri, KR & Pearce, RK. Clinical features differentiating patients with postmortem confirmed progressive supranuclear palsy and corticobasal degeneration. *J Neurol* 246 Suppl 2, II1-5 (1999).
64. Dickson, DW. Neuropathologic differentiation of progressive supranuclear palsy and corticobasal degeneration. *J Neurol* 246 Suppl 2, II6-15 (1999).
65. Shiozawa, M, Fukutani, Y, Sasaki, K, Isaki, K, Hamano, T, Hirayama, M, Imamura, K, Mukai, M, Arai, N & Cairns, NJ. Corticobasal degeneration: an autopsy case clinically diagnosed as progressive supranuclear palsy. *Clin Neuropathol* 19, 192-9 (2000).
66. Hassan, A, Whitwell, JL, Boeve, BF, Jack, CR, Jr., Parisi, JE, Dickson, DW & Josephs, KA. Symmetric corticobasal degeneration (S-CBD). *Parkinsonism Relat Disord* 16, 208-14 (2010).
67. Vidailhet, M, Rivaud, S, Gouider-Khouja, N, Pillon, B, Bonnet, AM, Gaymard, B, Agid, Y & Pierrot-Deseilligny, C. Eye movements in parkinsonian syndromes. *Ann Neurol* 35, 420-6 (1994).
68. Rivaud-Pechoux, S, Vidailhet, M, Gallouedec, G, Litvan, I, Gaymard, B & Pierrot-Deseilligny, C. Longitudinal ocular motor study in corticobasal degeneration and progressive supranuclear palsy. *Neurology* 54, 1029-32 (2000).
69. Zadikoff, C & Lang, AE. Apraxia in movement disorders. *Brain* 128, 1480-97 (2005).
70. Houghton, DJ & Litvan, I. Unraveling progressive supranuclear palsy: from the bedside back to the bench. *Parkinsonism Relat Disord* 13 Suppl 3, S341-6 (2007).
71. Cummings, JL & Litvan, I. Neuropsychiatric aspects of corticobasal degeneration. *Adv Neurol* 82, 147-52 (2000).
72. Josephs, KA, Whitwell, JL, Dickson, DW, Boeve, BF, Knopman, DS, Petersen, RC, Parisi, JE & Jack, CR, Jr. Voxel-based morphometry in autopsy proven PSP and CBD. *Neurobiol Aging* 29, 280-9 (2008).
73. Neary, D, Snowden, JS, Gustafson, L, Passant, U, Stuss, D, Black, S, Freedman, M, Kertesz, A, Robert, PH, Albert, M, Boone, K, Miller, BL, Cummings, J & Benson, DF. Frontotemporal lobar degeneration: a consensus on clinical diagnostic criteria. *Neurology* 51, 1546-54 (1998).
74. Hodges, JR, Davies, RR, Xuereb, JH, Casey, B, Broe, M, Bak, TH, Kril, JJ & Halliday, GM. Clinicopathological correlates in frontotemporal dementia. *Ann Neurol* 56, 399-406 (2004).
75. Forman, MS, Farmer, J, Johnson, JK, Clark, CM, Arnold, SE, Coslett, HB, Chatterjee, A, Hurtig, HI, Karlawish, JH, Rosen, HJ, Van Deerlin, V, Lee, VM, Miller, BL, Trojanowski, JQ

- & Grossman, M. Frontotemporal dementia: clinicopathological correlations. *Ann Neurol* 59, 952-62 (2006).
76. Whitwell, JL, Jack, CR, Jr., Senjem, ML, Parisi, JE, Boeve, BF, Knopman, DS, Dickson, DW, Petersen, RC & Josephs, KA. MRI correlates of protein deposition and disease severity in postmortem frontotemporal lobar degeneration. *Neurodegener Dis* 6, 106-17 (2009).
 77. Josephs, KA, Petersen, RC, Knopman, DS, Boeve, BF, Whitwell, JL, Duffy, JR, Parisi, JE & Dickson, DW. Clinicopathologic analysis of frontotemporal and corticobasal degenerations and PSP. *Neurology* 66, 41-8 (2006).
 78. Grossman, M, Xie, SX, Libon, DJ, Wang, X, Massimo, L, Moore, P, Vesely, L, Berkowitz, R, Chatterjee, A, Coslett, HB, Hurtig, HI, Forman, MS, Lee, VM & Trojanowski, JQ. Longitudinal decline in autopsy-defined frontotemporal lobar degeneration. *Neurology* 70, 2036-45 (2008).
 79. Mesulam, MM. Primary progressive aphasia. *Ann Neurol* 49, 425-32 (2001).
 80. Knibb, JA, Xuereb, JH, Patterson, K & Hodges, JR. Clinical and pathological characterization of progressive aphasia. *Ann Neurol* 59, 156-65 (2006).
 81. Grossman, M. Primary progressive aphasia: clinicopathological correlations. *Nat Rev Neurol* 6, 88-97 (2010).
 82. Josephs, KA, Holton, JL, Rossor, MN, Godbolt, AK, Ozawa, T, Strand, K, Khan, N, Al-Sarraj, S & Revesz, T. Frontotemporal lobar degeneration and ubiquitin immunohistochemistry. *Neuropathol Appl Neurobiol* 30, 369-73 (2004).
 83. Benson, DF, Davis, RJ & Snyder, BD. Posterior cortical atrophy. *Arch Neurol* 45, 789-93 (1988).
 84. Renner, JA, Burns, JM, Hou, CE, McKeel, DW, Jr., Storandt, M & Morris, JC. Progressive posterior cortical dysfunction: a clinicopathologic series. *Neurology* 63, 1175-80 (2004).
 85. Tang-Wai, DF, Graff-Radford, NR, Boeve, BF, Dickson, DW, Parisi, JE, Crook, R, Caselli, RJ, Knopman, DS & Petersen, RC. Clinical, genetic, and neuropathologic characteristics of posterior cortical atrophy. *Neurology* 63, 1168-74 (2004).
 86. Dickson, DW, Bergeron, C, Chin, SS, Duyckaerts, C, Houroupan, D, Ikeda, K, Jellinger, K, Lantos, PL, Lippa, CF, Mirra, SS, Tabaton, M, Vonsattel, JP, Wakabayashi, K & Litvan, I. Office of Rare Diseases neuropathologic criteria for corticobasal degeneration. *J Neuropathol Exp Neurol* 61, 935-46 (2002).
 87. Fujino, Y, Delucia, MW, Davies, P & Dickson, DW. Ballooned neurones in the limbic lobe are associated with Alzheimer type pathology and lack diagnostic specificity. *Neuropathol Appl Neurobiol* 30, 676-82 (2004).
 88. Josephs, KA, Katsuse, O, Beccano-Kelly, DA, Lin, WL, Uitti, RJ, Fujino, Y, Boeve, BF, Hutton, ML, Baker, MC & Dickson, DW. Atypical progressive supranuclear palsy with corticospinal tract degeneration. *Journal of neuropathology and experimental neurology* 65, 396-405 (2006).
 89. Dickson, DW. Sporadic tauopathies: Pick's disease, corticobasal degeneration, progressive suranuclear palsy and argyrophilic grain disease. in *The Neuropathology of Dementia* (eds. Esiri, M.M., Lee, V.M.-Y. & Trojanowski, J.Q.) 227-256 (Cambridge University Press, Cambridge, 2004).
 90. Komori, T, Arai, N, Oda, M, Nakayama, H, Mori, H, Yagishita, S, Takahashi, T, Amano, N, Murayama, S, Murakami, S, Shibata, N, Kobayashi, M, Sasaki, S & Iwata, M. Astrocytic plaques and tufts of abnormal fibers do not coexist in corticobasal degeneration and progressive supranuclear palsy. *Acta Neuropathol* 96, 401-8 (1998).

91. Feany, MB & Dickson, DW. Widespread cytoskeletal pathology characterizes corticobasal degeneration. *Am J Pathol* 146, 1388-96 (1995).
92. Yamada, T, McGeer, PL & McGeer, EG. Appearance of paired nucleated, Tau-positive glia in patients with progressive supranuclear palsy brain tissue. *Neurosci Lett* 135, 99-102 (1992).
93. Arai, T, Ikeda, K, Akiyama, H, Tsuchiya, K, Yagishita, S & Takamatsu, J. Intracellular processing of aggregated tau differs between corticobasal degeneration and progressive supranuclear palsy. *Neuroreport* 12, 935-8 (2001).
94. Arai, T, Ikeda, K, Akiyama, H, Nonaka, T, Hasegawa, M, Ishiguro, K, Iritani, S, Tsuchiya, K, Iseki, E, Yagishita, S, Oda, T & Mochizuki, A. Identification of amino-terminally cleaved tau fragments that distinguish progressive supranuclear palsy from corticobasal degeneration. *Ann Neurol* 55, 72-9 (2004).
95. Ishizawa, K & Dickson, DW. Microglial activation parallels system degeneration in progressive supranuclear palsy and corticobasal degeneration. *J Neuropathol Exp Neurol* 60, 647-57 (2001).
96. Gerhard, A, Trender-Gerhard, I, Turkheimer, F, Quinn, NP, Bhatia, KP & Brooks, DJ. In vivo imaging of microglial activation with [¹¹C](R)-PK11195 PET in progressive supranuclear palsy. *Mov Disord* 21, 89-93 (2006).
97. Bhaskar, K, Konerth, M, Kokiko-Cochran, ON, Cardona, A, Ransohoff, RM & Lamb, BT. Regulation of tau pathology by the microglial fractalkine receptor. *Neuron* 68, 19-31 (2010).
98. Ittner, LM, Ke, YD, Delerue, F, Bi, M, Gladbach, A, van Eersel, J, Wolfing, H, Chieng, BC, Christie, MJ, Napier, IA, Eckert, A, Staufenbiel, M, Hardeman, E & Gotz, J. Dendritic function of tau mediates amyloid-beta toxicity in Alzheimer's disease mouse models. *Cell* 142, 387-97 (2010).
99. Hoover, BR, Reed, MN, Su, J, Penrod, RD, Kotilinek, LA, Grant, MK, Pitstick, R, Carlson, GA, Lanier, LM, Yuan, LL, Ashe, KH & Liao, D. Tau mislocalization to dendritic spines mediates synaptic dysfunction independently of neurodegeneration. *Neuron* 68, 1067-81 (2010).
100. Brunden, KR, Ballatore, C, Crowe, A, Smith, AB, 3rd, Lee, VM & Trojanowski, JQ. Tau-directed drug discovery for Alzheimer's disease and related tauopathies: a focus on tau assembly inhibitors. *Exp Neurol* 223, 304-10 (2010).
101. Wischik, CM, Edwards, PC, Lai, RY, Roth, M & Harrington, CR. Selective inhibition of Alzheimer disease-like tau aggregation by phenothiazines. *Proc Natl Acad Sci U S A* 93, 11213-8 (1996).
102. Gong, CX, Grundke-Iqbal, I & Iqbal, K. Targeting tau protein in Alzheimer's disease. *Drugs & aging* 27, 351-65 (2010).
103. Mandelkow, EM, Drewes, G, Biernat, J, Gustke, N, Van Lint, J, Vandenheede, JR & Mandelkow, E. Glycogen synthase kinase-3 and the Alzheimer-like state of microtubule-associated protein tau. *FEBS Lett* 314, 315-21 (1992).
104. Perez, M, Hernandez, F, Lim, F, Diaz-Nido, J & Avila, J. Chronic lithium treatment decreases mutant tau protein aggregation in a transgenic mouse model. *J Alzheimers Dis* 5, 301-8 (2003).
105. Noble, W, Planel, E, Zehr, C, Olm, V, Meyerson, J, Suleman, F, Gaynor, K, Wang, L, LaFrancois, J, Feinstein, B, Burns, M, Krishnamurthy, P, Wen, Y, Bhat, R, Lewis, J, Dickson, D & Duff, K. Inhibition of glycogen synthase kinase-3 by lithium correlates with reduced tauopathy and degeneration in vivo. *Proc Natl Acad Sci U S A* 102, 6990-5 (2005).

106. Nakashima, H, Ishihara, T, Suguimoto, P, Yokota, O, Oshima, E, Kugo, A, Terada, S, Hamamura, T, Trojanowski, JQ, Lee, VM & Kuroda, S. Chronic lithium treatment decreases tau lesions by promoting ubiquitination in a mouse model of tauopathies. *Acta Neuropathol* 110, 547-56 (2005).
107. Engel, T, Goni-Oliver, P, Lucas, JJ, Avila, J & Hernandez, F. Chronic lithium administration to FTDP-17 tau and GSK-3beta overexpressing mice prevents tau hyperphosphorylation and neurofibrillary tangle formation, but pre-formed neurofibrillary tangles do not revert. *J Neurochem* 99, 1445-55 (2006).
108. Caccamo, A, Oddo, S, Tran, LX & LaFerla, FM. Lithium reduces tau phosphorylation but not A beta or working memory deficits in a transgenic model with both plaques and tangles. *Am J Pathol* 170, 1669-75 (2007).
109. Lee, VM, Kenyon, TK & Trojanowski, JQ. Transgenic animal models of tauopathies. *Biochim Biophys Acta* 1739, 251-9 (2005).
110. Zhang, B, Maiti, A, Shively, S, Lakhani, F, McDonald-Jones, G, Bruce, J, Lee, EB, Xie, SX, Joyce, S, Li, C, Toleikis, PM, Lee, VM & Trojanowski, JQ. Microtubule-binding drugs offset tau sequestration by stabilizing microtubules and reversing fast axonal transport deficits in a tauopathy model. *Proc Natl Acad Sci U S A* 102, 227-31 (2005).
111. Gozes, I & Divinski, I. The femtomolar-acting NAP interacts with microtubules: Novel aspects of astrocyte protection. *J Alzheimers Dis* 6, S37-41 (2004).
112. Matsuoka, Y, Gray, AJ, Hirata-Fukae, C, Minami, SS, Waterhouse, EG, Mattson, MP, LaFerla, FM, Gozes, I & Aisen, PS. Intranasal NAP administration reduces accumulation of amyloid peptide and tau hyperphosphorylation in a transgenic mouse model of Alzheimer's disease at early pathological stage. *J Mol Neurosci* 31, 165-70 (2007).
113. Matsuoka, Y, Jouroukhin, Y, Gray, AJ, Ma, L, Hirata-Fukae, C, Li, HF, Feng, L, Lecanu, L, Walker, BR, Planel, E, Arancio, O, Gozes, I & Aisen, PS. A neuronal microtubule-interacting agent, NAPVSIPQ, reduces tau pathology and enhances cognitive function in a mouse model of Alzheimer's disease. *J Pharmacol Exp Ther* 325, 146-53 (2008).
114. Brunden, KR, Zhang, B, Carroll, J, Yao, Y, Potuzak, JS, Hogan, AM, Iba, M, James, MJ, Xie, SX, Ballatore, C, Smith, AB, 3rd, Lee, VM & Trojanowski, JQ. Epothilone D improves microtubule density, axonal integrity, and cognition in a transgenic mouse model of tauopathy. *J Neurosci* 30, 13861-6 (2010).
115. Luo, W, Dou, F, Rodina, A, Chip, S, Kim, J, Zhao, Q, Moulick, K, Aguirre, J, Wu, N, Greengard, P & Chiosis, G. Roles of heat-shock protein 90 in maintaining and facilitating the neurodegenerative phenotype in tauopathies. *Proc Natl Acad Sci U S A* 104, 9511-6 (2007).
116. Dickey, CA, Kamal, A, Lundgren, K, Klosak, N, Bailey, RM, Dunmore, J, Ash, P, Shoraka, S, Zlatkovic, J, Eckman, CB, Patterson, C, Dickson, DW, Nahman, NS, Jr., Hutton, M, Burrows, F & Petrucelli, L. The high-affinity HSP90-CHIP complex recognizes and selectively degrades phosphorylated tau client proteins. *J Clin Invest* 117, 648-58 (2007).
117. Pickhardt, M, Gazova, Z, von Bergen, M, Khlistunova, I, Wang, Y, Hascher, A, Mandelkow, EM, Biernat, J & Mandelkow, E. Anthraquinones inhibit tau aggregation and dissolve Alzheimer's paired helical filaments in vitro and in cells. *J Biol Chem* 280, 3628-35 (2005).
118. Urakami, K, Mori, M, Wada, K, Kowa, H, Takeshima, T, Arai, H, Sasaki, H, Kanai, M, Shoji, M, Ikemoto, K, Morimatsu, M, Hikasa, C & Nakashima, K. A comparison of tau protein in cerebrospinal fluid between corticobasal degeneration and progressive supranuclear palsy. *Neurosci Lett* 259, 127-9 (1999).
119. Urakami, K, Wada, K, Arai, H, Sasaki, H, Kanai, M, Shoji, M, Ishizu, H, Kashihara, K, Yamamoto, M, Tsuchiya-Ikemoto, K, Morimatsu, M, Takashima, H, Nakagawa, M,

- Kurokawa, K, Maruyama, H, Kaseda, Y, Nakamura, S, Hasegawa, K, Oono, H, Hikasa, C, Ikeda, K, Yamagata, K, Wakutani, Y, Takeshima, T & Nakashima, K. Diagnostic significance of tau protein in cerebrospinal fluid from patients with corticobasal degeneration or progressive supranuclear palsy. *J Neurol Sci* 183, 95-8 (2001).
120. Borroni, B, Gardoni, F, Parnetti, L, Magno, L, Malinverno, M, Saggese, E, Calabresi, P, Spillantini, MG, Padovani, A & Di Luca, M. Pattern of Tau forms in CSF is altered in progressive supranuclear palsy. *Neurobiol Aging* 30, 34-40 (2009).
 121. Mitani, K, Furiya, Y, Uchihara, T, Ishii, K, Yamanouchi, H, Mizusawa, H & Mori, H. Increased CSF tau protein in corticobasal degeneration. *J Neurol* 245, 44-6 (1998).
 122. Noguchi, M, Yoshita, M, Matsumoto, Y, Ono, K, Iwasa, K & Yamada, M. Decreased beta-amyloid peptide42 in cerebrospinal fluid of patients with progressive supranuclear palsy and corticobasal degeneration. *J Neurol Sci* 237, 61-5 (2005).
 123. Arai, H, Morikawa, Y, Higuchi, M, Matsui, T, Clark, CM, Miura, M, Machida, N, Lee, VM, Trojanowski, JQ & Sasaki, H. Cerebrospinal fluid tau levels in neurodegenerative diseases with distinct tau-related pathology. *Biochem Biophys Res Commun* 236, 262-4 (1997).
 124. Portelius, E, Hansson, SF, Tran, AJ, Zetterberg, H, Grognet, P, Vanmechelen, E, Hoglund, K, Brinkmalm, G, Westman-Brinkmalm, A, Nordhoff, E, Blennow, K & Gobom, J. Characterization of tau in cerebrospinal fluid using mass spectrometry. *J Proteome Res* 7, 2114-20 (2008).
 125. Guillozet-Bongaarts, AL, Glajch, KE, Libson, EG, Cahill, ME, Bigio, E, Berry, RW & Binder, LI. Phosphorylation and cleavage of tau in non-AD tauopathies. *Acta Neuropathol* 113, 513-20 (2007).
 126. Holmberg, B, Rosengren, L, Karlsson, JE & Johnels, B. Increased cerebrospinal fluid levels of neurofilament protein in progressive supranuclear palsy and multiple-system atrophy compared with Parkinson's disease. *Mov Disord* 13, 70-7 (1998).
 127. Brettschneider, J, Petzold, A, Sussmuth, SD, Landwehrmeyer, GB, Ludolph, AC, Kassubek, J & Tumani, H. Neurofilament heavy-chain NfH(SMI35) in cerebrospinal fluid supports the differential diagnosis of Parkinsonian syndromes. *Mov Disord* 21, 2224-7 (2006).

Chapter 2

Neuropathologic features of corticobasal degeneration presenting as corticobasal syndrome or Richardson syndrome

2.1. Abstract

Patients with corticobasal degeneration (CBD) can present with several different clinical syndromes, making antemortem diagnosis a challenge. Corticobasal syndrome (CBS) is the clinical phenotype originally described for CBD, characterized by asymmetric rigidity and apraxia, cortical sensory deficits, dystonia and myoclonus. Some patients do not develop these features, but instead have clinical features consistent with the Richardson syndrome (RS) presentation of progressive supranuclear palsy (PSP), characterized by postural instability, early unexplained falls, vertical supranuclear gaze palsy, symmetric motor disability and dysphagia. The aim of this study was to identify differences in CBD presenting with CBS ($n = 11$) or RS ($n = 15$) with respect to demographic, clinical and neuropathologic features. CBD cases were also compared to patients with pathologically-proven PSP with RS ($n = 15$). CBD cases, regardless of presentation, shared histopathologic and tau biochemical characteristics, but they had differing densities of tau pathology in neuroanatomical regions that correlated with their clinical presentation. In particular, those with CBS presentation (CBD-CBS) had greater tau pathology in the primary motor and somatosensory cortices and putamen, while those with RS (CBD-RS) had greater tau pathology in limbic and hindbrain structures. Compared to PSP, patients with CBD-RS had less neuronal loss in the subthalamic nucleus, but more severe neuronal loss in the medial substantia nigra and greater atrophy of the anterior corpus callosum. Clinically, CBD-RS had more severe cognitive impairment and frontal behavioral dysfunction. The results indicate that RS is a common clinical presentation of cases with CBD pathology. Atrophy of anterior corpus callosum may be a potential neuroimaging marker to differentiate CBD from PSP in patients presenting with RS.

2.2. Introduction

CBD is a progressive neurodegenerative disorder with distinct pathologic features. There is typically focal cortical atrophy affecting parasagittal superior frontoparietal regions with relative sparing of the temporal and occipital lobes. Neuropathologic diagnostic criteria for CBD require tau inclusions in neurons and glia, with astrocytic plaques and extensive thread-like pathology in both white matter and gray matter.¹ Tau-positive globose neurofibrillary tangles or “corticobasal bodies” are common in the substantia nigra and locus coeruleus, while ballooned or achromatic neurons are common in affected cortical regions.

The classic clinical presentation of CBD, CBS, was first described in three cases by Rebeiz and co-workers.² Core features of CBS include levodopa-unresponsive parkinsonism, asymmetric akinesia and rigidity, accompanied by evidence of cortical and basal ganglia dysfunction, such as limb and oculomotor apraxia, cortical sensory deficits, dystonic posturing of a limb, myoclonus, and alien limb phenomenon.^{3, 4} Clinicopathologic studies have highlighted the prominent clinical heterogeneity of CBD pathology, causing frequent antemortem clinical misdiagnosis.⁵ CBS is the clinical presentation in <50% of CBD cases,⁶ with other presentations including progressive nonfluent aphasia,^{7, 8} severe cognitive dysfunction and dementia,⁹⁻¹¹ executive dysfunction with behavioral disturbances resembling frontotemporal dementia,¹²⁻¹⁴ and a clinical syndrome indistinguishable from the RS presentation of PSP.^{7, 15, 16} Due to the rarity of CBD coupled with the required autopsy confirmation, the relative frequency of these various clinical presentations in CBD is unknown.

PSP and CBD have overlapping tau pathology,¹⁷ and both are characterized by accumulation of insoluble tau enriched in the four-repeat (4R tau) isoforms.¹⁸ CBD typically has greater cortical involvement, whereas PSP has greater hindbrain tau pathology.¹⁹ The most distinguishing histopathologic feature of CBD and PSP is the different astrocytic lesions – astrocytic plaques in CBD and tufted astrocytes in PSP.^{20, 21} There is also evidence to suggest that tau protein profiles may differ between CBD and PSP with respect to lower molecular weight tau proteolytic cleavage fragments.²²

In this study, we compared demographic, clinical, and neuropathologic features in CBD presenting as one of two different clinical syndromes – CBS or RS. For comparison purposes, we included similar studies in PSP patients clinically presenting with RS. For each case we assessed anatomical distribution of tau pathology with state-of-the-art digital imaging methods, semiquantitative neuronal loss in key basal ganglia

nuclei, and anterior corpus callosum width in an effort to account for the distinct clinical presentations of CBS and RS in CBD and to identify clinical and pathological features that may be useful in differentiating CBD and PSP pathology in patients with RS.

2.3. Materials and methods

2.3.1. Subject selection

Patients with a neuropathologic diagnosis of CBD were identified from the neuropathology files of the Mayo Clinic Jacksonville brain bank between 1999 and 2009.¹ From 108 autopsy-confirmed CBD cases, 41 had clinical features consistent with RS²³ and 21 had clinical features consistent with CBS,⁶ with the remainder having a range of other clinical presentations. A subset of CBS ($n = 11$) and RS ($n = 15$) patients were selected for further study based upon the quality and completeness of the medical records. A subset of neuropathologically typical PSP ($n = 15$) with RS clinical presentation were selected as a comparison group from over 600 autopsy-confirmed PSP patients in the CurePSP/Society for PSP Brain Bank.²⁴ PSP-RS cases were selected based on the quality and completeness of the medical records, and they were matched to the 26 CBD patients for demographic features, including age of onset and sex. Of the final 41 patients, 34% were followed at Mayo Clinic and 66% were referral cases to the CurePSP/Society for PSP Brain Bank. There was no significant difference ($X^2 = 4.0$; $P = 0.41$) in the proportion of patients referred to the PSP Brain Bank compared to other referral sources for the three study groups. Most patients (56%) were evaluated by a movement disorder specialist, with the remaining followed by a behavioral neurologist (12%) or a general practice neurologist (32%). There was no significant difference in the proportion of patients followed by specialists compared to general practice neurologists for the three groups (*i.e.* CBD-CBS, CBD-RS, and PSP-RS) ($X^2 = 3.7$; $P = 0.45$). Forty one patients were Caucasian and one was African-American.

2.3.2. Clinical classification

The demographics and clinical information abstracted from medical records included age of onset, age of death, sex and race, as well as symptoms and signs arising during the course of the disease. Initial symptoms reported by the subject or caregiver and evidence of signs reported in the first neurologic examination were recorded for each patient. The following clinical features were recorded as present or absent: history of

falls, handwriting difficulty, depression, cognitive and memory impairment, urinary incontinence, dysphagia and dysarthria. Information about neurologic findings included: bradykinesia, tremor, postural instability, rigidity (appendicular and axial), limb apraxia, dystonia (limb, cervical, and blepharospasm), myoclonus, alien limb phenomenon, pyramidal signs, frontal release signs, cortical sensory loss, vertical supranuclear gaze palsy and aphasia. Behavioral and cognitive measures included: impairments in learning and memory, impairments in executive abilities, perseveration, and personality disorder of either abulic/apathetic or disinhibited types. Given the retrospective nature of this study, if a symptom or sign was not specifically mentioned in the medical records, it was so noted and not considered to be absent. Disease duration was defined as the difference between the age at onset of the first sign or symptom and the age at death.

CBS and RS clinical features adapted from the latest clinical diagnostic criteria for CBD are shown in **Table 2.1**.³⁶ The present study was performed prior to the 2013 CBD clinical criteria, and therefore CBD cases were not categorized as probable or possible CBS. Instead we used the generally accepted criteria for CBS, including presence of progressive asymmetric rigidity and apraxia, accompanied by signs of cortical or basal ganglia dysfunction, such as, cortical sensory loss, myoclonus and dystonia.^{6, 25} Because patients in this study were not part of a prospective study with standardized collection of clinical data and since medical records from a variety of clinical sources were reviewed retrospectively, we used RS criteria as proposed by Williams *et al.*,²³ rather than more stringent National Institute of Neurological Disorders and Stroke – Society for Progressive Supranuclear Palsy (NINDS-SPSP) research criteria for clinically probable PSP.²⁶ Cases with RS as operationalized by Williams and colleagues had ‘gradual onset of postural instability and falls within the first 2 years of disease, along with vertical supranuclear gaze palsy, a frontal dysexecutive syndrome, and rigidity and bradykinesia that is unresponsive to levodopa’.²³ For analysis purposes, we also considered the number of patients in each group who also met NINDS-SPSP research criteria for clinically probable PSP.

Table 2.1 | Clinical signs and symptoms of autopsy-proven CBD cases presenting with corticobasal syndrome or Richardson syndrome^a

Clinical phenotype	Features
Probably corticobasal syndrome	<p><u>Asymmetric presentation – two of:</u></p> <ul style="list-style-type: none"> a) limb rigidity or akinesia b) limb dystonia c) limb myoclonus <p><u>Plus two of:</u></p> <ul style="list-style-type: none"> d) orobuccal or limb apraxia e) cortical sensory deficit f) alien limb phenomena (more than simple levitation)
Possible corticobasal syndrome	<p><u>May be symmetric – one of:</u></p> <ul style="list-style-type: none"> a) limb rigidity or akinesia b) limb dystonia c) limb myoclonus <p><u>Plus one of:</u></p> <ul style="list-style-type: none"> d) orobuccal or limb apraxia e) cortical sensory deficit f) alien limb phenomena (more than simple levitation)
Richardson syndrome	<p><u>Three of:</u></p> <ul style="list-style-type: none"> a) axial or symmetric limb rigidity or akinesia b) postural instability or falls c) urinary incontinence d) behavioral changes e) supranuclear vertical gaze palsy or decreased velocity of vertical saccades

^aAdapted from the most recent CBD clinical diagnostic criteria²⁶

2.3.3. Tissue sampling and pathologic assessment

Neuropathologic assessment and diagnosis was made according to research criteria for PSP and CBD.^{1, 24} In all cases neuropathologic evaluation was on right or left hemibrains, the other side is frozen for biochemical studies. Given that most of the brains included in this study were from referral sources, it was unfeasible to control which hemibrain was evaluated for each case. Nevertheless, we recorded the side evaluated for neuropathologic studies with respect to the clinical signs and took this into consideration with respect to analysis of tau burden (**Table 2.2**). Two way analysis of variance adjusting for side of the brain neuropathologically evaluated, identified a

significant effect of side detected for parietal lobe gray and white matter (**Table 2.3**). Unexpectedly, the opposite effect was noted for burden of tau in the putamen. In all cases, primary and association cortices, basal ganglia, diencephalon, brainstem and cerebellum were evaluated with tau immunohistochemistry as previously described.²⁷ Thioflavin S fluorescent microscopy was used to assess Alzheimer-type pathology,²⁸ and hematoxylin and eosin stained sections were used to evaluate neuronal loss and gliosis. Cases were also assessed for the presence or absence of argyrophilic grain disease (AGD) with tau immunohistochemistry.²⁹

Table 2.2 Side of brain evaluated and clinical asymmetry						
	Side of brain evaluated		Side of greater clinical involvement			"Correct" side of brain evaluated
	Right	Left	Right	Left	Symmetrical	
CBD-CBS	1	10	6	5	0	5
CBD-RS	3	12	2	0	13	15
PSP-RS	3	12	1	2	12	13

Table 2.3 Two way analysis of variance adjusting for side of brain evaluated				
	CBD-CBS (contralateral)	CBD-CBS (ipsilateral)	CBD-RS	P-value for side*
Somatosensory – gray matter	17 (12, 23)	3.2 (2.6, 6.6)	1.3 (0.44, 2.3)	P<0.001
Somatosensory – white matter	15 (12, 20)	5.5 (3.4, 10)	1.1 (0.44, 2.6)	P<0.001
Putamen	12 (8.5, 17)	27 (21, 29)	9.9 (3.6, 14)	P=0.004

Of the regions that showed significant differences for tau burden between CBD-CBS and CBD-RS, only somatosensory cortex and putamen showed a significant effect for side of brain evaluated with a two way analysis of variance adjusting for side (ipsilateral or contralateral to side of greatest clinical involvement). Values are median (25th , 75th %-tile); *multiple comparison method: Holm-Sidak method.

For tau immunohistochemistry, sections were processed using a DAKO Autostainer (Universal Staining System Carpinteria, CA) using 3, 3'-diaminobenzidine (DAB) as the chromogen and a phospho-tau antibody (CP13, mouse IgG1, 1:1000, kind gift of Dr. Peter Davies, Albert Einstein College of Medicine, Bronx, NY, USA). After immunostaining, the sections were counterstained with hematoxylin.

Stained sections were scanned on the Aperio ScanScope XT slide scanner and converted to high-resolution digital images (**Figure 2.1**). Regions of interest were chosen based on their known involvement in CBD and PSP.³⁰ Additional regions throughout the brain were also examined in order to fully assess the distribution and severity of tau pathology. A total of 25 regions of interest were analyzed in all 41 cases using ImageScope software. The regions of interest included: gray and white matter of the primary motor and somatosensory, superior frontal and inferior temporal cortices, CA2 hippocampal subfield, dentate gyrus, amygdala, putamen, globus pallidus, anterior and ventrolateral thalamic nuclei, subthalamic nucleus (STN), substantia nigra (SN), red nucleus, superior colliculus, cerebral peduncle, pontine nuclei, tegmentum of the medulla, inferior olivary nucleus, corpus callosum, and cerebellar white matter.

Digital image analysis with Aperio ImageScope has the advantage of quantifying histologic features with a continuous variable that displays a dynamic range of values. Additionally, this methodology effectively limits interrater variability because an entire anatomical region of interest is sampled rather than smaller, select microscopic fields that can vary from observer to observer. Regions of interest were outlined, and immunostained pixels were counted with a color deconvolution algorithm. The algorithm was specifically designed to detect chromogen-positive structures and expressed as the number of positive pixels to the total pixels for the entire region of interest as a percent tau burden. Investigators were blinded to clinical status during image analysis procedures.

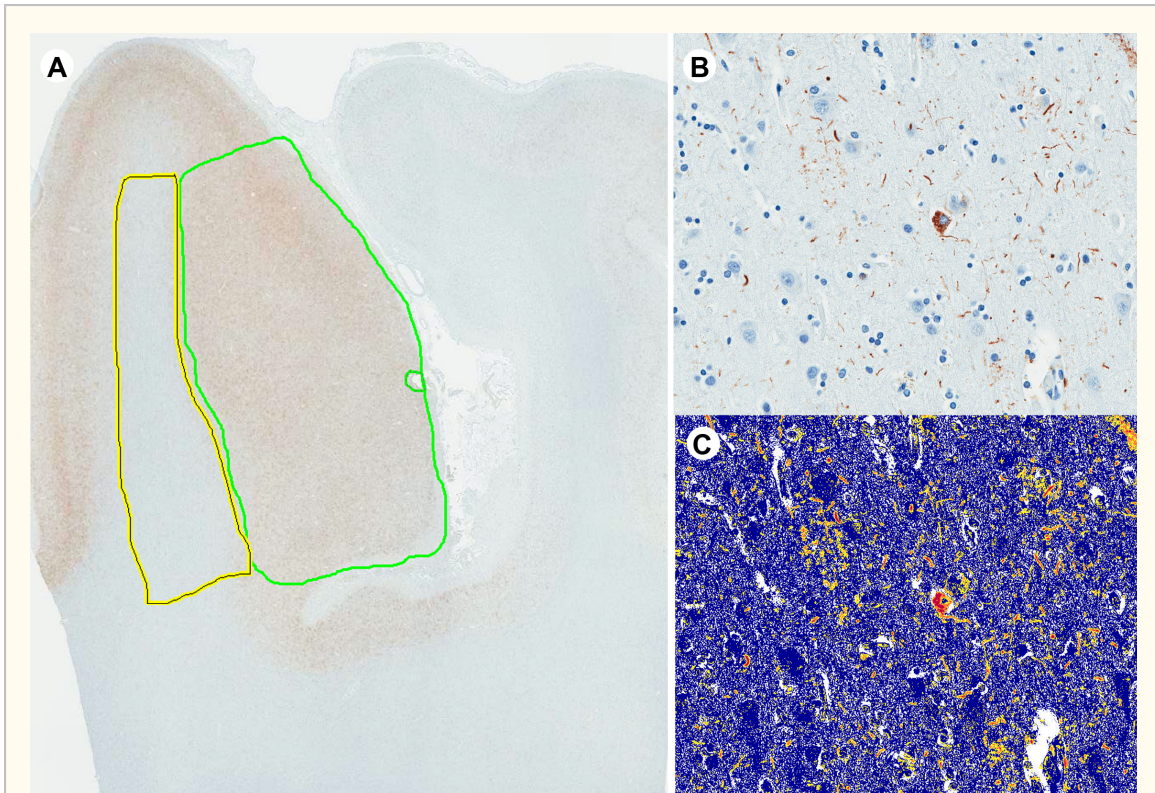
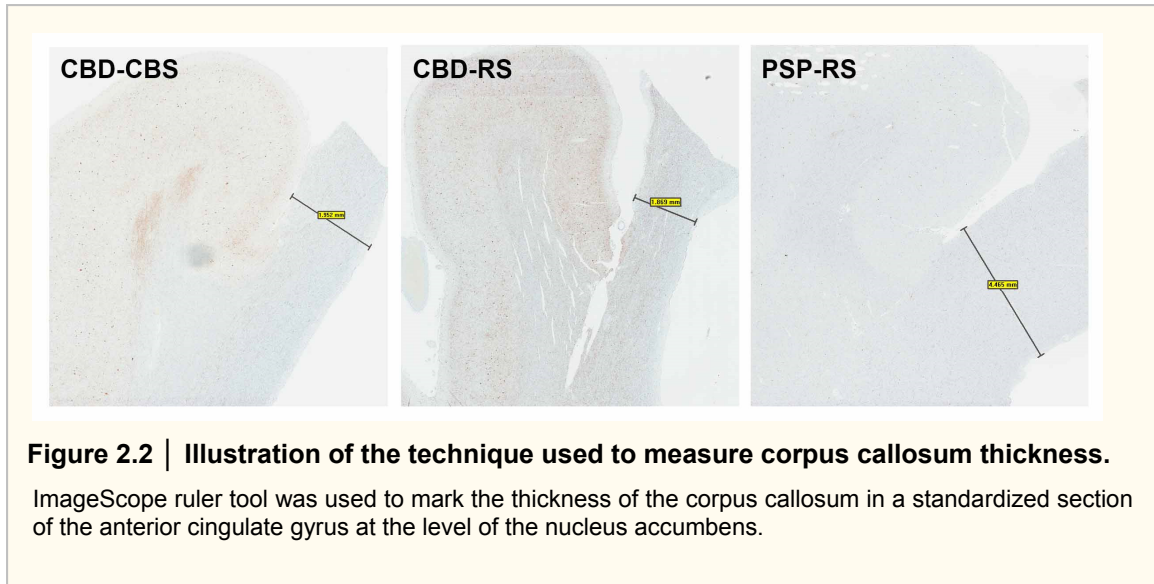


Figure 2.1 | Digital image analysis with ImageScope software.

A. Entire regions of interest are outlined using the pen tool. Here the gray matter (green outline) and white matter (yellow outline) of the primary motor cortex are illustrated. **B.** Higher magnification (20X) of the white matter immunostained with phospho-tau antibody shows tau-positive pretangles and neurites. **C.** When the color deconvolution algorithm is applied to the region of interest in panel B, tau-positive structures are detected (yellow, orange and red pixels) as a percent of the total area of tissue (yellow, orange and red plus blue pixels). Positive pixels are detected in a graded fashion where the strongest DAB chromogen in the image is red, medium intensity structures are orange and weakly positive structures are yellow.

Given that atrophy of the corpus callosum is common in CBD,^{31, 32} we also measured corpus callosum width in this study cohort. These measurements were made on digital images of 5- μ m thick paraffin-embedded tissue sections that included the anterior cingulate gyrus, obtained from coronal brain slices at the level of nucleus accumbens. The ImageScope ruler feature was used to measure the thickness (expressed in millimeters) at a consistent location in all cases (**Figure 2.2**).



The degree of neuronal loss in the STN and SN was assessed semi-quantitatively using the following scheme: 0 = none; 1 = mild; 2 = moderate; 3 = severe; 4 = almost complete. The STN was assessed in both medial (limbic) and lateral (sensorimotor) regions of the nucleus, separately. The SN neuronal population was recorded for both the ventrolateral cell groups (A9) and the medial neuronal cell groups or ventral tegmental area (A10).³³ During assessment of neuronal loss, the neuropathologist was blind to the clinical status.

2.3.4. Tau biochemistry

Brain tissue from 8 cases (2 CBD-CBS, 3 CBD-RS, and 3 PSP-RS) was homogenized in 10 volumes of tris (hydroxymethyl) aminomethane (Tris)-buffered saline containing protease and phosphatase inhibitors (50 mM Tris base, pH 8.0, 274 mM sodium chloride, 5 mM potassium chloride – TE buffer) and centrifuged at 26,300g for 20 min at 4°C. Supernatants were collected as S1 fractions, and the pellets (P1) were re-homogenized in 5 volumes of salt/sucrose buffer (10 mM Tris pH 7.4, 800 mM sodium chloride, 10% sucrose, 1 mM ethylene glycol tetraacetic acid, 1mM phenylmethylsulfonyl fluoride) and centrifuged as before. The resulting supernatants were incubated with 1% sarkosyl for 1 h at 37°C and centrifuged at 150,000g for 1 h at 4°C. The resulting pellet (P3) was resuspended in TE buffer (10mM Tris pH 8.0, 1 mM ethylenediaminetetraacetic acid).

Electrophoresis and immunoblotting were performed as previously described.³⁴ The samples were diluted with an equivalent volume of 2×Novex Tris-glycine sodium-dodecyl sulfate (SDS) sample buffer (Invitrogen), and equal volumes were run on 10% SDS-polyacrylamide gels (Invitrogen), transferred to Immobilon membranes (Millipore), and immunoblotted. The primary antibody used against phosphorylated tau was PHF-1 (1:1,000; kind gift of Dr. Peter Davies) and anti-mouse IgG secondary antibody (1:5,000).

2.3.5. Statistical analyses

All statistical analyses were performed with SigmaPlot 11.0 (Systat Software, Inc., San Jose, CA, USA) with significance set at $P < 0.05$. The Student's *t*-test was used to compare continuous variables (age at onset, age at death and disease duration) between CBD-CBS and CBD-RS. Chi-square or Fisher exact tests were used to compare categorical variables including initial presenting signs and symptoms, frequency of clinical features, referral source, and neurologist type (*e.g.* movement disorder specialist or cognitive and behavioral neurologist) of the three study groups. Tau burden percent and neuronal loss scores were compared with the Mann-Whitney rank sum test. The effect of the side of brain evaluated on tau burden was tested with two-way analysis of variance for CBD cases with either CBS or RS presentations, adjusting for side examined (contralateral side of brain considered 1 and ipsilateral side of brain considered 0 with respect to predominant side affected clinically).

2.4. Results

2.4.1. Demographic and initial presentation

Eleven CBS patients (7 male, 4 female) and 15 RS patients (7 male, 8 female) with a pathologic diagnosis of CBD met inclusion and exclusion criteria (**Table 2.4**). Fifteen PSP patients (8 male, 7 female) were selected who had typical RS clinical presentation.^{23, 35} The mean age at onset, disease duration and age at death did not differ between CBD-RS and CBD-CBS. The mean disease duration for PSP-RS was 7.7 years, which was slightly longer compared to both CBD groups. CBD-CBS and CBD-RS did not differ with respect to presence of concomitant Alzheimer type pathology – Braak neurofibrillary tangle stage [median (25th, 75th %-tile)]: CBD-CBS 1.5 (1, 2) versus CBD-

RS 2 (1, 2.5); $P = 0.96$ and presence of argyrophilic grain disease: CBD-CBS 64% versus CBD-RS 53%; $P = 0.70$.

Table 2.4 Demographics and final clinical diagnosis			
Demographic feature	CBD-CBS	CBD-RS	PSP-RS
Cases, n	11	15	15
Sex (M/F)	7/4	7/8	8/7
Mean age at onset (years)	64.3 ± 7.8 (53-79)	62.9 ± 5.6 (55-74)	62.1 ± 7.5 (47-75)
Mean disease duration (years)	5.8 ± 2.9 (2-11)	6.1 ± 2.5 (3-11)	7.7 ± 2.6 (5-13)
Age of death (years)	70.2 ± 9.8 (57-87)	68.9 ± 6.6 (60-82)	69.0 ± 7.6 (52-83)

Data are mean ± standard deviation (with range); CBS = clinical corticobasal syndrome; RS = clinical Richardson syndrome

Initial symptoms and signs are detailed in **Table 2.5**. At initial presentation, nine (60%) of the CBD-RS and 10 (67%) of the PSP-RS patients had unexplained falls and gait disturbance, whereas motor complaints of CBD-CBS patients were related most commonly to having difficulty using an upper limb. Memory complaints were noted in 40% of CBD-RS patients as indicated by caregivers and from information obtained from medical records. Early behavioral changes were noted in 20% of both CBD-RS and PSP-RS patients, which was not observed in CBD-CBS patients. Similarly, initial symptoms of depression were noted in one-third of CBD-RS patients, 27% of PSP-RS, and none of the CBD-CBS patients presented with symptoms of depression.

Table 2.5 Initial clinical presenting signs and symptoms			
Clinical feature	CBD-CBS n = 11 (%)	CBD-RS n = 15 (%)	PSP-RS n = 15 (%)
Symptoms			
Unilateral limb dysfunction	7 (64)	0	0
Falls/gait difficulty	0	9 (60)	10 (67)
Eye movement abnormalities	0	1 (7)	4 (27)
Behavioral changes	0	3 (20)	3 (20)
Memory problems	0	6 (40)	0
Depression	0	5 (33)	4 (27)
Signs			
Bradykinesia	1 (9)	1 (7)	2 (13)
Dysarthria	0	0	3 (20)
Aphasia	1 (9)	1 (7)	0
Astereognosis	1 (9)	0	0
Action tremor	1 (9)	1 (7)	0

2.4.2. Clinical features of CBD and PSP

Clinical assessment of symptoms and signs are summarized in **Table 2.3**. Given that the groups were included if they fit accepted clinical criteria for CBS and RS, the majority of differences between CBD-CBS and CBD-RS were expected. For example, CBD-CBS more often exhibited asymmetric limb rigidity and apraxia, focal limb dystonia, myoclonus and cortical sensory deficits than CBD-RS. CBD-CBS patients had less early unexplained falls, vertical gaze palsy, and dysphagia. Limb apraxia was not a common feature in either CBD-RS or PSP-RS, but when present, was bilateral; which contrasted with the marked asymmetry of limb apraxia in CBD-CBS. Pyramidal and extrapyramidal signs were noted at similar frequencies across the three groups.

Table 2.6 | Symptoms/signs in pathologically confirmed corticobasal degeneration and progressive supranuclear palsy

Symptoms/signs	CBD-CBS n = 11 (%)		CBD-RS n = 15 (%)		PSP-RS n = 15 (%)	
	present	absent	present	absent	present	absent
CBS features						
Appendicular rigidity	11 (100)	0	15 (100)	0	14 (93)	0
Asymmetric	11 (100)*	0	3 (20)	4	0	4
Limb apraxia	10 (91)*	0	3 (20)	3	2 (13)	1
Asymmetric	10 (91)*	0	0	0	1 (7)	0
Limb dystonia	9 (82)*	0	1 (7)	5	1 (7)	6
Myoclonus	7 (64)*	2	0	3	0	4
Cortical sensory	8 (73)*	3	3 (20)	10	0	7
Alien limb	4 (36)*	0	0	0	0	0
Aphasia	4 (36)*	3	1 (7)	5	0	2
RS features						
Vertical gaze palsy	2 (18)*	7	14 (93)	1	15 (100)	0
Dysphagia	3 (27)*	7	12 (80)	2	11 (73)	2
Falls/gait difficulty	9 (82)	1	15 (100)	0	15 (100)	0
Falls (within 1 year of onset)	2 (18)	1	4 (27)	0	7 (47)	0
Falls (within 2 year of onset)	3 (27)	1	8 (47)	0	12 (80)	0
Axial rigidity	5 (45)	3	12 (80)	1	15 (100)	0
Cognitive or behavioral disorder						
Behavioral abnormality	5 (45)	4	14 (93)*†	0	7 (47)	5
Memory impairment	2 (18)*	5	10 (67)	1	4 (27)	1
Frontal release signs	5 (45)	0	6 (40)	1	6 (40)	0
Movement disorder						
Bradykinesia	11 (100)	0	15 (100)	0	15 (100)	0
Postural instability	8 (73)	3	15 (100)	0	15 (100)	0
Dysarthria	11 (100)	0	12 (80)	2	14 (93)	0
Rest tremor	1 (9)	7	4 (27)	11	0	15
Other tremor	7 (64)	2	9 (60)	2	6 (40)	9
Handwriting difficulty	7 (64)	0	7 (47)	0	10 (67)	0
Cervical dystonia	0	0	2 (13)	0	1 (7)	0
Blepharospasm	0	0	3 (20)	0	1 (7)	0
Pyramidal signs	7 (64)	4	7 (47)	5	7 (47)	1
Other						
Urinary incontinence	1 (9)	8	11 (73)*†	1	3 (20)	5
Depression	5 (45)	4	10 (67)	1	8 (53)	1

* $P < 0.05$ comparing CBD-RS and CBD-CBS using Chi-square test; † $P < 0.05$ comparing CBD-RS and PSP-RS.

CBD-RS patients could not be distinguished from PSP-RS patients based on the presence of core features of RS. The frequency of unexplained falls within the first year of disease onset, a key diagnostic feature of the NINDS-SPSP research criteria for PSP, was more frequent in PSP-RS (47%) compared to CBD-RS (27%), but this frequency was not significantly different ($P = 0.45$). Vertical gaze palsy and dysphagia were common in both CBD-RS and PSP-RS.

There were, however, some unexpected clinical differences between CBD-RS and PSP-RS. For example, all but one CBD-RS patient had executive and behavioral abnormalities during the disease course, which was significantly more common than in PSP-RS patients ($P = 0.014$). The behavioral features often noted disinhibition, social withdrawal, apathy, agitation, and impatience. In addition, urinary incontinence was reported in 73% of CBD-RS patients, but this was noted in only three (20%) PSP-RS patients ($P = 0.01$).

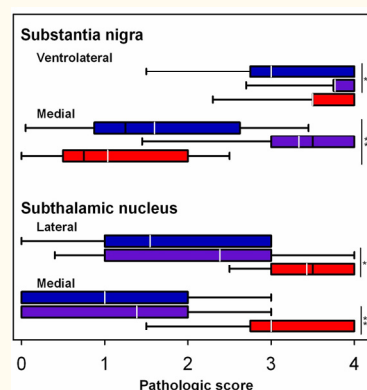
2.4.3. Neuropathologic findings

2.4.3.1. Neuronal loss in subthalamic nucleus and substantia nigra

Neuronal loss was semi-quantitatively assessed in the SN and STN blinded to clinical and pathologic diagnosis (**Figure 2.3**). The STN had similar neuronal loss in medial and lateral parts in CBD-CBS and CBD-RS, but more severe neuronal loss in PSP-RS, which fits with the known selective vulnerability of the STN in PSP. The ventrolateral cell group of the SN, which is selectively affected in Parkinsonian disorders, was severely affected in both CBD-RS and PSP-RS, but less affected in CBD-CBS. In contrast, the medial cell group of the SN, which forms part of the mesolimbic ventral tegmental area, was selectively decreased in CBD-RS compared to both CBD-CBS and PSP-RS.

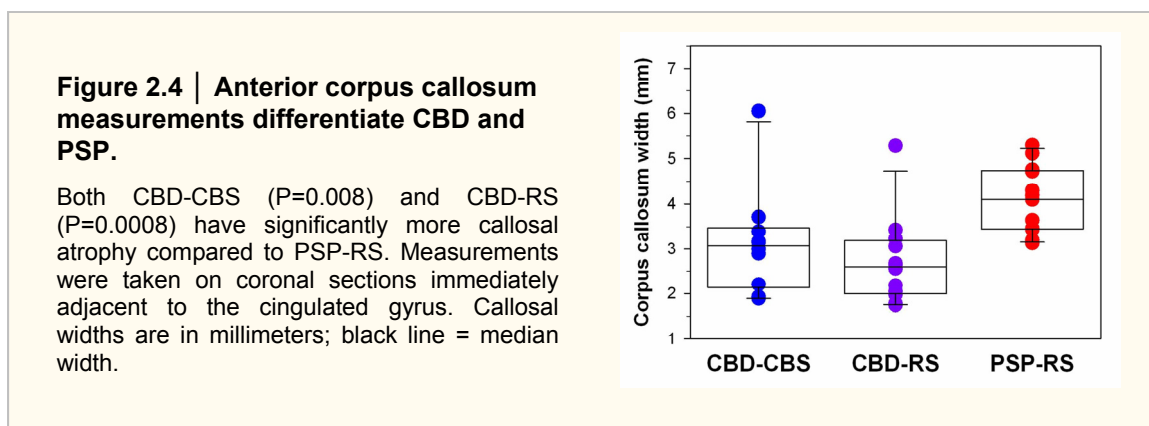
Figure 2.3 | Semi-quantitative assessment of neuronal loss in the substantia nigra and subthalamic nucleus

CBD-CBS (blue), CBD-RS (purple) and PSP-RS (red). The lateral portion of the SN refers to ventrolateral neuronal population (A9) and medial SN corresponds to ventral tegmental area (A10). Pathologic scoring scheme: 0 = none; 1 = mild; 2 = moderate; 3 = severe; 4 = almost complete; Black line = median pathologic score; White line = mean. * $P < 0.05$; ** $P < 0.001$.



2.4.3.2. Atrophy of the corpus callosum

Callosal width (in millimeters) was measured with ImageScope on digital images of 5- μ m thick tissue sections at the level of the anterior cingulate gyrus and nucleus accumbens (**Figure 2.4**). Both CBD-CBS (median) and CBD-RS (median) had marked atrophy of the anterior corpus callosum compared to PSP-RS (median values: CBD-CBS, 3.1 mm; CBD-RS, 2.6 mm; PSP-RS, 4.1 mm; $P = 0.0008$). In contrast, the width of the corpus callosum was not different between CBD-CBS and CBD-RS ($P = 0.31$).



2.4.3.3. Distribution and severity of tau immunoreactivity

Tau burden was quantified by digital image analysis in 25 anatomical regions in the neocortex, basal ganglia, brainstem and cerebellum. **Figure 2.5** illustrates tau pathology in representative brain regions, and **Figure 2.6** summarizes quantification of tau pathology by brain region. In CBD-CBS the regions with the most severe tau pathology, mostly in the form of neuronal pretangles and thread-like processes, were the primary motor cortex, putamen, globus pallidus externa and STN. Primary motor and somatosensory cortices had significantly greater tau burden in both gray and white matter in CBD-CBS compared to CBD-RS ($P < 0.001$), whereas both groups had similar tau burden in superior frontal cortex. CBD-CBS also had increased tau pathology in the putamen compared to CBD-RS ($P = 0.005$).

Gray matter of the superior frontal cortex was the most severely affected cortical region in CBD-RS; however, the greatest burden of tau pathology was in the hippocampus, STN, amygdala, and white matter tracts in the brainstem (e.g., tegmentum of the medulla and superior colliculus). These components of the extended

limbic system and hindbrain structures had greater tau pathology in CBD-RS compared to CBD-CBS. The regions that had significantly higher tau burden in CBD-RS compared to CBD-CBS are hippocampal CA2 ($P = 0.012$), dentate gyrus of the hippocampus ($P = 0.007$), anterior nucleus of the thalamus ($P = 0.037$), tegmentum of the medulla ($P = 0.026$), and cerebellar white matter ($P = 0.008$).

The overall severity of tau pathology in both CBD-CBS and CBD-RS was much greater than in PSP-RS. The most affected regions in CBD ranged from approximately 10-20% tau burden, whereas in PSP-RS, the regions with the highest percentage of tau immunoreactivity ranged from 5-10%. As expected, the brunt of tau pathology in PSP-RS was in brainstem regions, followed by the basal ganglia. Other than a mild involvement of the primary motor cortex, there was little cortical tau pathology in PSP-RS. The greatest cortical burden in PSP-RS was in the primary motor cortex gray matter (3% mean tau burden) and white matter (1% mean tau burden). All other cortical regions assessed in PSP-RS had <0.5% mean tau burden.

For CBD-CBS cases, the hemisphere opposite the side of greater clinical involvement was evaluated in 5 of 11 cases. When side was taken into consideration for the regions that were significantly different between CBD-CBS and CBD-RS using a two way analysis of variance adjusting for side, there was no significant effect on tau burden in any of these regions except for gray and white matter of somatosensory cortex and for the putamen (**Table 2.2**), consistent with less parietal tau burden for cases in which the ipsilateral cortex was evaluated and greater putaminal tau burden for cases in which the ipsilateral basal ganglia was evaluated.

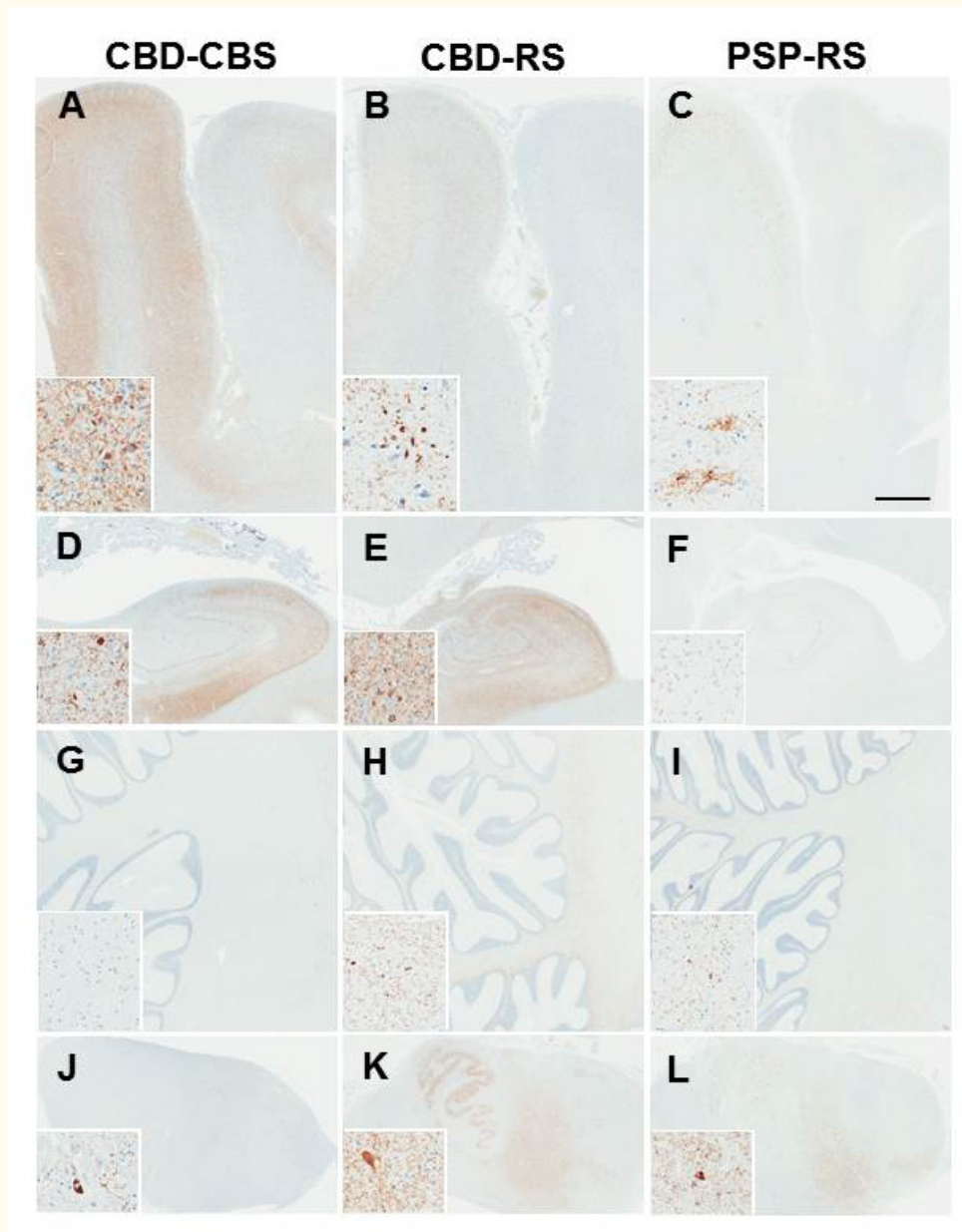


Figure 2.5 | Tau immunohistochemistry in representative brain regions.

CBD-RS has relative sparing of motor and somatosensory cortices (**A-C**; inset primary motor cortex) and greater tau pathology in the hippocampus (**D-F**; inset CA2) compared to CBD-CBS. CBD-RS tau burden in the cerebellar white matter (**G-I**) and medulla (**J-L**; inset tegmentum) is more comparable to PSP-RS. Bar in panel C represents 3 mm in all panels and 60 μ m in all insets.

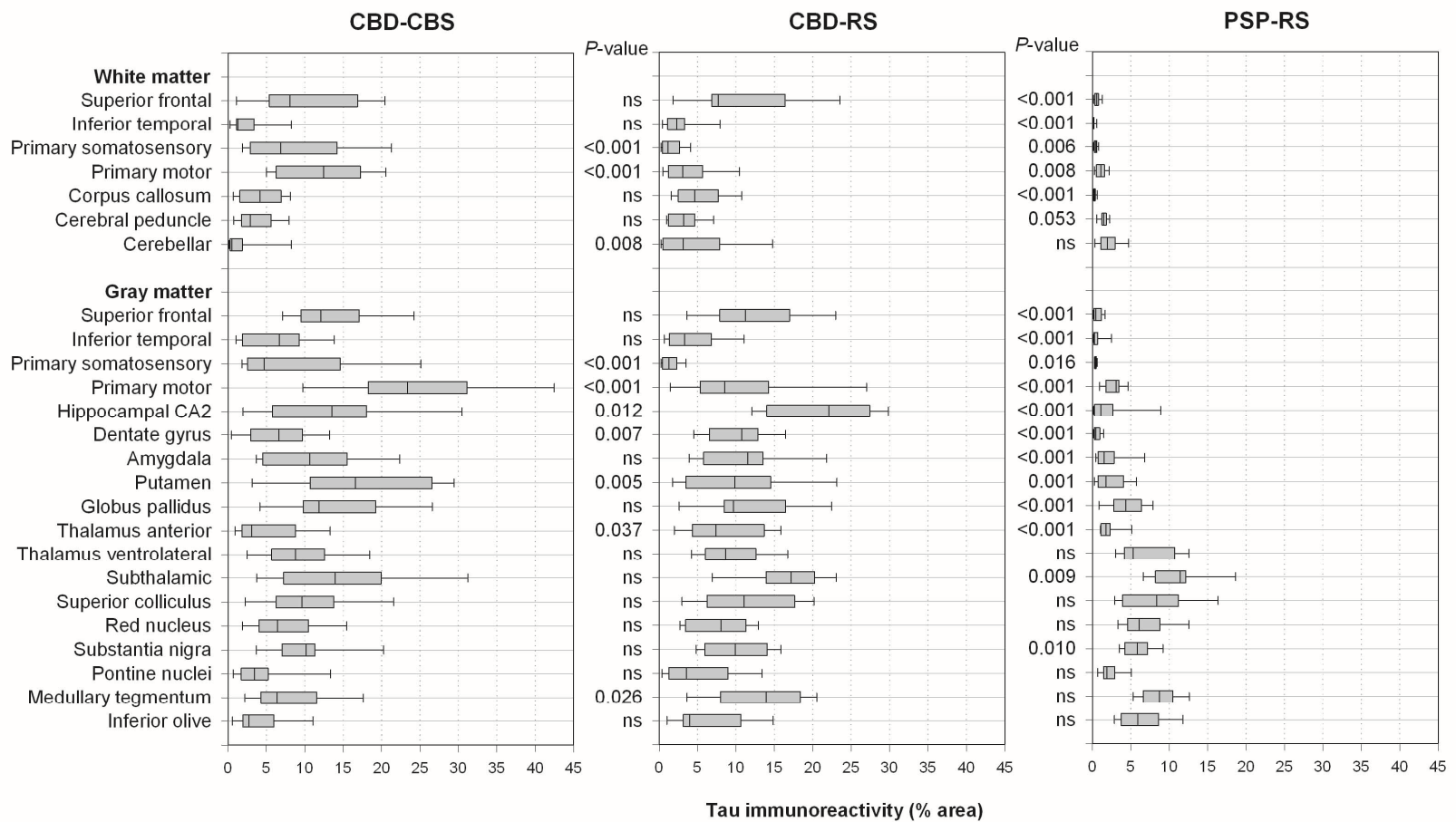
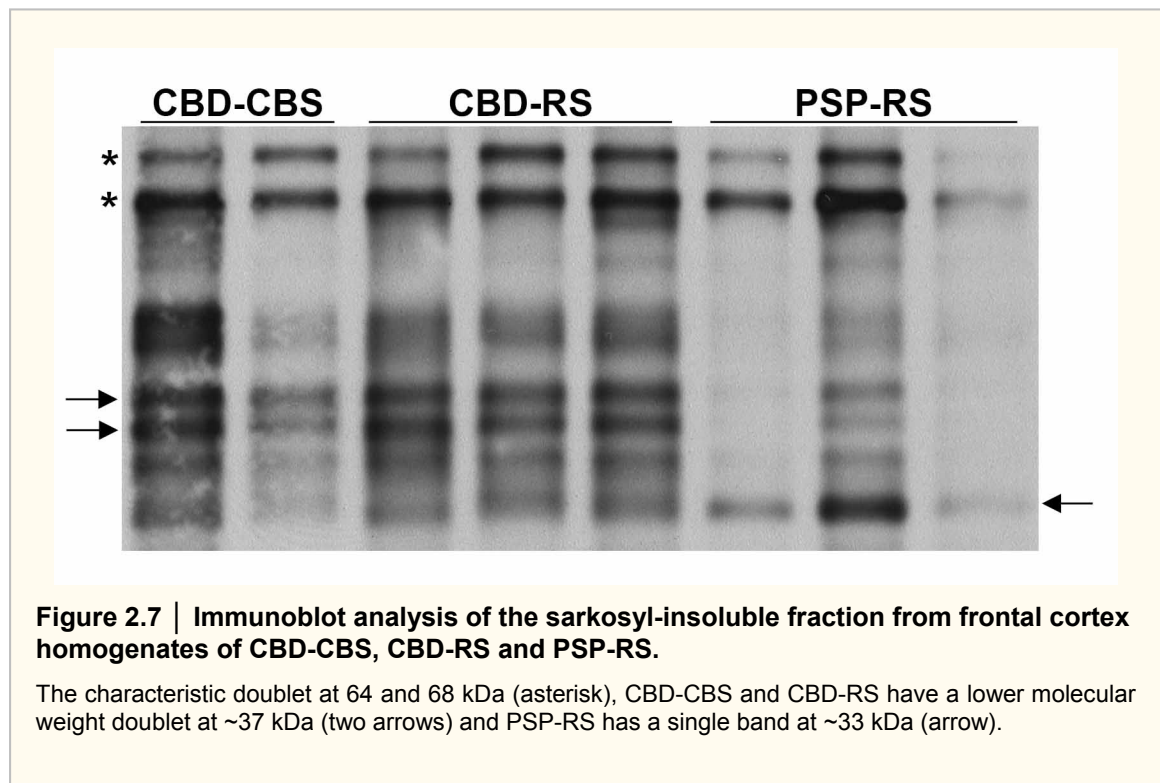


Figure 2.6 | Regional distribution of tau immunoreactivity as assessed by image analysis in CBD-CBS, CBD-RS and PSP-RS.

The Mann-Whitney rank sum test was used to compare tau burden in CBD-RS to either CBD-CBS or PSP-RS.

2.4.3.4. Tau biochemistry

Homogenates from frontal cortex of eight cases were prepared. Since soluble tau species in CBD and PSP do not differ,²² their sarkosyl-insoluble fractions were analyzed by immunoblot using the phosphorylation-dependent tau PHF-1 antibody (**Figure 2.7**). The typical doublet at 64 and 68 kDa was seen in all cases; however, the lower molecular weight tau species differed between CBD and PSP. CBD-CBS and CBD-RS both had predominantly two closely associated bands around 37 kDa, whereas the major lower molecular weight species in PSP-RS was at 33 kDa.



2.5. Discussion

This study investigated two distinct clinical phenotypes (CBS and RS) of pathologically-confirmed CBD and found regional differences in tau pathology burden using state-of-the-art digital imaging methods, which correlated with the two clinical presentations. All patients, regardless of clinical presentation, met neuropathologic criteria for CBD, including presence of pathognomonic astrocytic plaques and numerous thread-like processes in gray and white matter of cortical and subcortical regions.^{1, 37} Additionally, both CBD-CBS and CBD-RS cases had the same low molecular weight tau fragments in

sarkosyl-insoluble fractions of brain, a molecular fingerprint that differentiates CBD from PSP.²² Protein sequence analysis using Edman chemistry and immunohistochemical analysis using multiple tau antibodies spanning tau protein showed that the 33kDa band and 37kDa doublet were composed of the carboxyl terminus with different amino termini.²² In CBD the 37kDa bands begin at amino acid residue 169 of the longest tau isoform (middle of *MAPT* exon 7) and the PSP 33kDa tau cleavage fragment begins at amino acid 187 (beginning of *MAPT* exon 9). Altogether suggesting that there is differential proteolytic processing of abnormal tau in CBD and PSP.

CBD is clinically characterized by both motor and cognitive disturbances that can present with a variety of syndromes, including CBS, progressive nonfluent aphasia, behavioral variant frontotemporal dementia, and RS.⁵ Due to the rarity of autopsy-confirmed CBD, the exact proportion of the various clinical presentations is unknown. As a close estimate, when the 26 CBD patients in the present study are included with four large clinicopathologic studies of CBD, for a total of 98 autopsy-confirmed CBD patients, 36% presented with CBS and 27% with RS. This, of course, may not reflect the actual proportion of all CBD patients given the inevitable bias of autopsy studies in parkinsonian disorders.³⁸

The present study adds to increasing evidence that CBD can be the pathologic substrate for RS and for the first time, has specifically identified the neuropathologic features which explain differences in clinical presentation.^{15, 39} By definition, CBD-RS had early unexplained falls, early cognitive dysfunction, vertical supranuclear gaze palsy, and postural instability. Since this was not a longitudinal, prospective research study and clinical information was collected by retrospective review of medical records, we chose to use more lenient clinical criteria for RS proposed by Williams *et al.* rather than NINDS-SPSP research criteria for probable PSP.^{23, 26} A recent study that used the same criteria reviewed the clinical features of pathologically confirmed CBD presenting with either CBS or RS.¹⁵ In that study, CBD-RS had an earlier age at symptom onset (62.8 versus 69.0 years-of-age) compared with CBD-CBS. In the present series, we noted a similar trend, with CBD-RS being slightly younger than CBD-CBS (62.3 versus 64.3 years-of-age). They also found a delayed onset of vertical gaze palsy and infrequent occurrence of predominant downgaze palsy in their CBD-RS cases.¹⁵ In a meta-analysis of pathologically-confirmed CBD, Litvan *et al.* suggested that eye movement problems in CBD are more often characterized by oculomotor apraxia preceding vertical gaze palsy and typically have equal severity of both vertical and horizontal gaze palsy,

whereas PSP patients have greater involvement of vertical gaze without oculomotor apraxia.⁶ The presence or absence of oculomotor apraxia and the degree of severity of upward compared to downward vertical gaze palsy were not well documented in the medical records of all the cases in this study. Thus, it remains to be determined if eye movement abnormalities can differentiate CBD-RS from PSP-RS.

2.5.1. Corticobasal degeneration – pathologic basis for clinical heterogeneity

The anatomical distribution of brain atrophy, which reflects neuronal loss and tau pathology, determines the clinical syndrome in CBD, as is true for other neurodegenerative disorders.⁴⁰⁻⁴² In the present study, distribution of CBD-related tau pathology differed between CBD presenting with CBS compared with those presenting with RS. In CBD-CBS, tau pathology was marked in posterior frontal and anterior parietal (e.g. peri-Rolandic cortex), which includes primary motor and somatosensory cortices. In CBD-RS had more tau pathology compared with CBD-CBS in limbic structures, including the hippocampal subfields, dentate gyrus, and the anterior nucleus of the thalamus, as well as hindbrain structures including tegmentum of the medulla and cerebellar white matter. The greater tau burden in the lower brainstem and cerebellum in CBD-RS may explain the clinical overlap with PSP-RS, whereas the relative sparing of the peri-Rolandic cortices may explain the absence of hallmark cortical signs of CBS.

Involvement of the frontal and especially parietal cortices has been emphasized in CBD since the original description of the disorder,² and these cortical regions were markedly affected in CBD-CBS, with a three-fold greater tau burden in the primary motor cortex compared with that in CBD-RS. In the present series, tau pathology in the primary somatosensory cortex in CBD-CBS was 10-fold greater in white matter and six-fold greater in gray matter compared to CBD-RS, which had mild tau pathology in the parietal lobe. In CBD-RS, minimal involvement of parietal lobe may correlate with absence of cortical signs, such as limb apraxia and cortical sensory loss.

A highly characteristic clinical feature of CBS is asymmetry,⁴³ but symmetrical clinical presentations of CBD are increasingly recognized.¹³ The majority of CBD-CBS patients in the present series had clinical asymmetry. The inability to document laterality of tau pathology, given that only one hemisphere was studied in each case, is a limitation of the present study. Neuropathologic analyses were on the side predicted to be more

severely affected (*i.e.* contralateral to clinically most affected side) in 5 of the 11 CBD-CBS cases (**Table 2.1**). Had the ‘correct’ hemisphere been evaluated, one might predict that differences in cortical tau burdens would have been even greater between CBD-CBS and CBD-RS. Support for this contention was strengthened with a two way analysis of variance adjusting for side of the brain evaluated, with a significant effect of side detected for parietal lobe gray and white matter (**Table 2.2**). Of unknown significance, the opposite effect was noted for burden of tau in the putamen.

Symmetry of cortical involvement, although not specifically addressed in this study, may also have contributed to the RS clinical phenotype. Of note is the fact that symmetrical CBD may have clinical features that overlap with RS.¹³ Also, behavioral and cognitive deficits are clinically more significant in symmetrical clinical presentations of CBD.¹³ It is thus of interest that cognitive and behavioral changes were also more frequent in our patients with CBD-RS. One might speculate that this is due to greater tau burden in limbic structures in CBD-RS compared with CBD-CBS.

In addition to differences in anatomical distribution of tau pathology, CBD-CBS and CBD-RS had distinct patterns of neuronal loss in the STN and SN. Severe neuronal loss and gliosis in the STN is a defining neuropathologic feature of PSP, while there is less consistent neuronal loss in the STN in CBD.^{1,24} It was therefore not surprising that both CBD-CBS and CBD-RS had less neuronal loss in the STN than PSP-RS. The SN has variable neuronal loss and gliosis in CBD.¹ Neuronal loss affecting the medial portion of the SN has been shown to correlate with dementia in parkinsonian disorders.⁴⁴ In accord with this observation, CBD-RS had more severe neuronal loss in medial SN than CBD-CBS. This correlates with the observed increased frequency of cognitive and frontal behavioral deficits in CBD-RS compared with CBD-CBS. Both PSP-RS and CBD-RS had severe neuronal loss in the ventrolateral cell groups of the SN, which is known to correlate with extrapyramidal features in parkinsonian disorders.^{33,45}

2.5.2. Richardson syndrome – pathological heterogeneity

RS is the most common presentation of PSP, but there is increasing recognition of clinical heterogeneity of PSP, with some patients presenting with pure akinesia with gait freezing, progressive nonfluent aphasia, or even Parkinson’s disease.^{27, 35, 46} Moreover, there are other pathologic processes that can produce the RS clinical phenotype, including CBD, Lewy body disease, multiple system atrophy, and cerebrovascular disease.^{39, 47, 48} Results of the present study suggest that RS patients who also have

severe cognitive impairment may have underlying pathology of CBD, but confirmation requires additional longitudinal studies coupled with postmortem examination.

Despite considerable overlap in clinical features of CBD-RS and PSP-RS, there were significant differences with respect to distribution and severity of tau pathology, morphology of tau lesions, lower molecular weight sarkosyl-insoluble tau species and pattern of neuronal loss in the STN and SN. There were also significant differences between CBD-RS and PSP-RS with respect to degree of corpus callosum atrophy. Previous neuroimaging studies of CBS patients have noted atrophy of the corpus callosum,^{31, 32} but this may not be specific since this can also be detected in frontotemporal lobar degeneration.^{49, 50} On the other hand, few studies addressing callosal atrophy in CBD have been on pathologically verified cases.⁵⁰ It thus remains a possibility that in patients presenting with RS presence of corpus callosum atrophy may assist in differential diagnosis of underlying pathology.

2.6. Conclusion

Both CBD and PSP are 4R tauopathies with a range of clinical presentations that correlate with differences in distribution of brain atrophy and tau pathology. The explanation for selective vulnerability in 4R tauopathies is unknown, but contribution of genetic background can be hypothesized. Further studies are needed to determine genetic variants that might contribute to these differences. Clinicopathologic studies suggest that CBD and PSP represent a disease spectrum, and the results of the present study support this concept. In particular, the present study indicates that CBD can be the pathologic substrate of RS, just as previous studies have shown that PSP can be the pathologic substrate of CBS.⁵¹ Although there is clinical and pathologic overlap in CBD and PSP, most cases have distinct pathologic, biochemical, and clinical features that warrant retention of their current classification.^{17, 52} If future disease-modifying therapies are discovered that generally target 4R tau dysfunction, there would be little significance in differentiating CBD-RS from PSP-RS. On the other hand, if the factors that drive cellular and anatomical specificity in CBD differ meaningfully from PSP, making this distinction may eventually be of more than academic interest. To that end, it remains to be determined if CBD and PSP have the same pathogenesis, but current evidence supports that CBD and PSP have distinct disease processes.

2.7. References

1. Dickson, DW, Bergeron, C, Chin, SS, Duyckaerts, C, Horoupian, D, Ikeda, K, Jellinger, K, Lantos, PL, Lippa, CF, Mirra, SS, Tabaton, M, Vonsattel, JP, Wakabayashi, K & Litvan, I. Office of Rare Diseases neuropathologic criteria for corticobasal degeneration. *J Neuropathol Exp Neurol* 61, 935-46 (2002).
2. Rebeiz, JJ, Kolodny, EH & Richardson, EP, Jr. Corticodentatonigral degeneration with neuronal achromasia. *Arch Neurol* 18, 20-33 (1968).
3. Gibb, WR, Luthert, PJ & Marsden, CD. Clinical and pathological features of corticobasal degeneration. *Adv Neurol* 53, 51-4 (1990).
4. Riley, DE, Lang, AE, Lewis, A, Resch, L, Ashby, P, Hornykiewicz, O & Black, S. Cortical-basal ganglionic degeneration. *Neurology* 40, 1203-12 (1990).
5. Kouri, N, Whitwell, JL, Josephs, KA, Rademakers, R & Dickson, DW. Corticobasal degeneration: a pathologically distinct 4R tauopathy. *Nat Rev Neurol* 7, 263-72 (2011).
6. Litvan, I, Grimes, DA & Lang, AE. Phenotypes and prognosis: clinicopathologic studies of corticobasal degeneration. *Adv Neurol* 82, 183-96 (2000).
7. Josephs, KA, Petersen, RC, Knopman, DS, Boeve, BF, Whitwell, JL, Duffy, JR, Parisi, JE & Dickson, DW. Clinicopathologic analysis of frontotemporal and corticobasal degenerations and PSP. *Neurology* 66, 41-8 (2006).
8. Kertesz, A, McMonagle, P, Blair, M, Davidson, W & Munoz, DG. The evolution and pathology of frontotemporal dementia. *Brain* 128, 1996-2005 (2005).
9. Bergeron, C, Pollanen, MS, Weyer, L, Black, SE & Lang, AE. Unusual clinical presentations of cortical-basal ganglionic degeneration. *Ann Neurol* 40, 893-900 (1996).
10. Grimes, DA, Lang, AE & Bergeron, CB. Dementia as the most common presentation of cortical-basal ganglionic degeneration. *Neurology* 53, 1969-74 (1999).
11. Murray, R, Neumann, M, Forman, MS, Farmer, J, Massimo, L, Rice, A, Miller, BL, Johnson, JK, Clark, CM, Hurtig, HI, Gorno-Tempini, ML, Lee, VM, Trojanowski, JQ & Grossman, M. Cognitive and motor assessment in autopsy-proven corticobasal degeneration. *Neurology* 68, 1274-83 (2007).
12. Boeve, BF, Lang, AE & Litvan, I. Corticobasal degeneration and its relationship to progressive supranuclear palsy and frontotemporal dementia. *Ann Neurol* 54 Suppl 5, S15-9 (2003).
13. Hassan, A, Whitwell, JL, Boeve, BF, Jack, CR, Jr., Parisi, JE, Dickson, DW & Josephs, KA. Symmetric corticobasal degeneration (S-CBD). *Parkinsonism Relat Disord* 16, 208-14 (2010).
14. Rinne, JO, Lee, MS, Thompson, PD & Marsden, CD. Corticobasal degeneration. A clinical study of 36 cases. *Brain* 117 (Pt 5), 1183-96 (1994).
15. Ling, H, O'Sullivan, SS, Holton, JL, Revesz, T, Massey, LA, Williams, DR, Paviour, DC & Lees, AJ. Does corticobasal degeneration exist? A clinicopathological re-evaluation. *Brain* 133, 2045-57 (2010).
16. Shiozawa, M, Fukutani, Y, Sasaki, K, Isaki, K, Hamano, T, Hirayama, M, Imamura, K, Mukai, M, Arai, N & Cairns, NJ. Corticobasal degeneration: an autopsy case clinically diagnosed as progressive supranuclear palsy. *Clin Neuropathol* 19, 192-9 (2000).
17. Feany, MB, Mattiace, LA & Dickson, DW. Neuropathologic overlap of progressive supranuclear palsy, Pick's disease and corticobasal degeneration. *J Neuropathol Exp Neurol* 55, 53-67 (1996).

18. Buee, L & Delacourte, A. Comparative biochemistry of tau in progressive supranuclear palsy, corticobasal degeneration, FTDP-17 and Pick's disease. *Brain Pathol* 9, 681-93 (1999).
19. Dickson, DW. Neuropathologic differentiation of progressive supranuclear palsy and corticobasal degeneration. *Journal of Neurology* 246 Suppl 2, II6-15 (1999).
20. Feany, MB & Dickson, DW. Widespread cytoskeletal pathology characterizes corticobasal degeneration. *Am J Pathol* 146, 1388-96 (1995).
21. Yamada, T, McGeer, PL & McGeer, EG. Appearance of paired nucleated, Tau-positive glia in patients with progressive supranuclear palsy brain tissue. *Neurosci Lett* 135, 99-102 (1992).
22. Arai, T, Ikeda, K, Akiyama, H, Nonaka, T, Hasegawa, M, Ishiguro, K, Iritani, S, Tsuchiya, K, Iseki, E, Yagishita, S, Oda, T & Mochizuki, A. Identification of amino-terminally cleaved tau fragments that distinguish progressive supranuclear palsy from corticobasal degeneration. *Ann Neurol* 55, 72-9 (2004).
23. Williams, DR, Lees, AJ, Wherrett, JR & Steele, JC. J. Clifford Richardson and 50 years of progressive supranuclear palsy. *Neurology* 70, 566-73 (2008).
24. Hauw, JJ, Daniel, SE, Dickson, D, Horoupian, DS, Jellinger, K, Lantos, PL, McKee, A, Tabaton, M & Litvan, I. Preliminary NINDS neuropathologic criteria for Steele-Richardson-Olszewski syndrome (progressive supranuclear palsy). *Neurology* 44, 2015-9 (1994).
25. Riley, DE & Lang, AE. Clinical diagnostic criteria. *Adv Neurol* 82, 29-34 (2000).
26. Litvan, I, Agid, Y, Calne, D, Campbell, G, Dubois, B, Duvoisin, RC, Goetz, CG, Golbe, LI, Grafman, J, Growdon, JH, Hallett, M, Jankovic, J, Quinn, NP, Tolosa, E & Zee, DS. Clinical research criteria for the diagnosis of progressive supranuclear palsy (Steele-Richardson-Olszewski syndrome): report of the NINDS-SPSP international workshop. *Neurology* 47, 1-9 (1996).
27. Ahmed, Z, Josephs, KA, Gonzalez, J, DelleDonne, A & Dickson, DW. Clinical and neuropathologic features of progressive supranuclear palsy with severe pallido-nigro-luysial degeneration and axonal dystrophy. *Brain* 131, 460-72 (2008).
28. Barker, WW, Luis, CA, Kashuba, A, Luis, M, Harwood, DG, Loewenstein, D, Waters, C, Jimison, P, Shepherd, E, Sevush, S, Graff-Radford, N, Newland, D, Todd, M, Miller, B, Gold, M, Heilman, K, Doty, L, Goodman, I, Robinson, B, Pearl, G, Dickson, D & Duara, R. Relative frequencies of Alzheimer disease, Lewy body, vascular and frontotemporal dementia, and hippocampal sclerosis in the State of Florida Brain Bank. *Alzheimer Dis Assoc Disord* 16, 203-12 (2002).
29. Togo, T, Cookson, N & Dickson, DW. Argyrophilic grain disease: neuropathology, frequency in a dementia brain bank and lack of relationship with apolipoprotein E. *Brain Pathol* 12, 45-52 (2002).
30. Ishizawa, K & Dickson, DW. Microglial activation parallels system degeneration in progressive supranuclear palsy and corticobasal degeneration. *J Neuropathol Exp Neurol* 60, 647-57 (2001).
31. Yamauchi, H, Fukuyama, H, Nagahama, Y, Katsumi, Y, Dong, Y, Hayashi, T, Konishi, J & Kimura, J. Atrophy of the corpus callosum, cortical hypometabolism, and cognitive impairment in corticobasal degeneration. *Arch Neurol* 55, 609-14 (1998).
32. Groschel, K, Hauser, TK, Luft, A, Patronas, N, Dichgans, J, Litvan, I & Schulz, JB. Magnetic resonance imaging-based volumetry differentiates progressive supranuclear palsy from corticobasal degeneration. *Neuroimage* 21, 714-24 (2004).

33. Dickson, DW, Braak, H, Duda, JE, Duyckaerts, C, Gasser, T, Halliday, GM, Hardy, J, Leverenz, JB, Del Tredici, K, Wszolek, ZK & Litvan, I. Neuropathological assessment of Parkinson's disease: refining the diagnostic criteria. *Lancet Neurol* 8, 1150-7 (2009).
34. Sahara, N, Lewis, J, DeTure, M, McGowan, E, Dickson, DW, Hutton, M & Yen, SH. Assembly of tau in transgenic animals expressing P301L tau: alteration of phosphorylation and solubility. *J Neurochem* 83, 1498-508 (2002).
35. Williams, DR, de Silva, R, Paviour, DC, Pittman, A, Watt, HC, Kilford, L, Holton, JL, Revesz, T & Lees, AJ. Characteristics of two distinct clinical phenotypes in pathologically proven progressive supranuclear palsy: Richardson syndrome and PSP-parkinsonism. *Brain* 128, 1247-58 (2005).
36. Armstrong, MJ, Litvan, I, Lang, AE, Bak, TH, Bhatia, KP, Borroni, B, Boxer, AL, Dickson, DW, Grossman, M, Hallett, M, Josephs, KA, Kertesz, A, Lee, SE, Miller, BL, Reich, SG, Riley, DE, Tolosa, E, Troster, AI, Vidaihet, M & Weiner, WJ. Criteria for the diagnosis of corticobasal degeneration. *Neurology* 80, 496-503 (2013).
37. Komori, T, Arai, N, Oda, M, Nakayama, H, Mori, H, Yagishita, S, Takahashi, T, Amano, N, Murayama, S, Murakami, S, Shibata, N, Kobayashi, M, Sasaki, S & Iwata, M. Astrocytic plaques and tufts of abnormal fibers do not coexist in corticobasal degeneration and progressive supranuclear palsy. *Acta Neuropathol* 96, 401-8 (1998).
38. Bower, JH, Dickson, DW, Taylor, L, Maraganore, DM & Rocca, WA. Clinical correlates of the pathology underlying parkinsonism: a population perspective. *Mov Disord* 17, 910-6 (2002).
39. Josephs, KA & Dickson, DW. Diagnostic accuracy of progressive supranuclear palsy in the Society for Progressive Supranuclear Palsy brain bank. *Mov Disord* 18, 1018-26 (2003).
40. Boxer, AL, Geschwind, MD, Belfor, N, Gorno-Tempini, ML, Schauer, GF, Miller, BL, Weiner, MW & Rosen, HJ. Patterns of brain atrophy that differentiate corticobasal degeneration syndrome from progressive supranuclear palsy. *Arch Neurol* 63, 81-6 (2006).
41. Josephs, KA, Whitwell, JL, Dickson, DW, Boeve, BF, Knopman, DS, Petersen, RC, Parisi, JE & Jack, CR, Jr. Voxel-based morphometry in autopsy proven PSP and CBD. *Neurobiol Aging* 29, 280-9 (2008).
42. Whitwell, JL, Jack, CR, Jr., Boeve, BF, Parisi, JE, Ahlskog, JE, Drubach, DA, Senjem, ML, Knopman, DS, Petersen, RC, Dickson, DW & Josephs, KA. Imaging correlates of pathology in corticobasal syndrome. *Neurology* 75, 1879-87 (2010).
43. Litvan, I, Grimes, DA, Lang, AE, Jankovic, J, McKee, A, Verny, M, Jellinger, K, Chaudhuri, KR & Pearce, RK. Clinical features differentiating patients with postmortem confirmed progressive supranuclear palsy and corticobasal degeneration. *J Neurol* 246 Suppl 2, II1-5 (1999).
44. Rinne, JO, Rummukainen, J, Paljarvi, L & Rinne, UK. Dementia in Parkinson's disease is related to neuronal loss in the medial substantia nigra. *Ann Neurol* 26, 47-50 (1989).
45. Fearnley, JM & Lees, AJ. Ageing and Parkinson's disease: substantia nigra regional selectivity. *Brain* 114 (Pt 5), 2283-301 (1991).
46. Williams, DR, Holton, JL, Strand, K, Revesz, T & Lees, AJ. Pure akinesia with gait freezing: a third clinical phenotype of progressive supranuclear palsy. *Mov Disord* 22, 2235-41 (2007).
47. Hughes, AJ, Daniel, SE, Ben-Shlomo, Y & Lees, AJ. The accuracy of diagnosis of parkinsonian syndromes in a specialist movement disorder service. *Brain* 125, 861-70 (2002).

48. Williams, DR & Lees, AJ. What features improve the accuracy of the clinical diagnosis of progressive supranuclear palsy-parkinsonism (PSP-P)? *Mov Disord* 25, 357-62 (2010).
49. Yamauchi, H, Fukuyama, H, Nagahama, Y, Katsumi, Y, Hayashi, T, Oyanagi, C, Konishi, J & Shio, H. Comparison of the pattern of atrophy of the corpus callosum in frontotemporal dementia, progressive supranuclear palsy, and Alzheimer's disease. *J Neurol Neurosurg Psychiatry* 69, 623-9 (2000).
50. Josephs, KA, Tang-Wai, DF, Edland, SD, Knopman, DS, Dickson, DW, Parisi, JE, Petersen, RC, Jack, CR, Jr. & Boeve, BF. Correlation between antemortem magnetic resonance imaging findings and pathologically confirmed corticobasal degeneration. *Arch Neurol* 61, 1881-4 (2004).
51. Boeve, BF, Maraganore, DM, Parisi, JE, Ahlskog, JE, Graff-Radford, N, Caselli, RJ, Dickson, DW, Kokmen, E & Petersen, RC. Pathologic heterogeneity in clinically diagnosed corticobasal degeneration. *Neurology* 53, 795-800 (1999).
52. Wakabayashi, K & Takahashi, H. Pathological heterogeneity in progressive supranuclear palsy and corticobasal degeneration. *Neuropathology* 24, 79-86 (2004).

Chapter 3

Corticobasal degeneration with olivopontocerebellar atrophy and TDP-43 pathology: an unusual clinicopathologic variant of CBD

3.1. Abstract

CBD is a disorder affecting cognition and movement due to a progressive neurodegeneration associated with distinctive neuropathologic features, including abnormal phosphorylated tau protein in neurons and glia in cortex, basal ganglia, diencephalon and brainstem, as well as ballooned neurons and astrocytic plaques. We identified three cases of CBD with olivopontocerebellar atrophy (CBD-OPCA) that did not have α -synuclein-positive glial cytoplasmic inclusions of multiple system atrophy (MSA). Two patients had clinical features suggestive of progressive supranuclear palsy (PSP), and the third case had cerebellar ataxia thought to be due to idiopathic OPCA. Neuropathologic features of CBD-OPCA are compared to typical CBD, as well as MSA and PSP. CBD-OPCA and MSA had marked neuronal loss in pontine nuclei, inferior olivary nucleus, and Purkinje cell layer. Neuronal loss and grumose degeneration in the cerebellar dentate nucleus was comparable in CBD-OPCA and PSP. Image analysis of tau pathology showed greater infratentorial tau burden, especially in pontine base, in CBD-OPCA compared with typical CBD. Additionally, CBD-OPCA had TDP-43 immunoreactive neuronal and glial cytoplasmic inclusions and threads throughout the basal ganglia and in olivopontocerebellar system. CBD-OPCA met neuropathologic diagnostic criteria for CBD and shared tau biochemical characteristics with typical CBD. Here we describe CBD-OPCA as a distinct clinicopathologic variant of CBD with olivopontocerebellar TDP-43 pathology.

3.2. Introduction

Corticobasal degeneration (CBD) was first described in 1968 by Rebeiz, Kolodny, and Richardson as “corticodentatonigral degeneration with neuronal achromasia”¹ CBD is a sporadic, mid-to-late life, adult-onset, neurodegenerative disease typically presenting

with progressive levodopa-nonresponsive parkinsonism with focal cortical signs, such as apraxia, aphasia or frontal type dementia (reviewed in²). Pathologically, CBD is characterized by numerous neuropil threads in gray and white matter of affected cortices, basal ganglia, diencephalon, and brainstem; as well as characteristic astrocytic plaques,³ pleiomorphic neurofibrillary pretangles, and ballooned neurons (BNs).⁴ Biochemically, abnormal tau in CBD is enriched in a specific alternatively spliced form of tau, namely, tau containing four \approx 32 amino acid repeat motifs in the microtubule binding domain (4R tau), which is due to inclusion of exon 10.⁵ In addition to CBD, several other disorders are associated with abnormal accumulation of 4R tau, including progressive supranuclear palsy (PSP)⁵ and argyrophilic grain disease (AGD).⁶

Olivopontocerebellar atrophy (OPCA) is a group of diseases pathologically characterized by neuronal degeneration of the inferior olivary nuclei, pontine nuclei, and cerebellum. The most common form of sporadic OPCA is multiple system atrophy (MSA). Graham and Oppenheimer were the first to recognize MSA as a distinct clinicopathologic entity, with and varying degrees of parkinsonism, cerebellar ataxia, and autonomic dysfunction.⁷ Neuropathologic features of MSA include degeneration in substantia nigra, putamen, inferior olivary nucleus, pontine nuclei, and cerebellum, but with sparing of the cerebellar dentate neurons (reviewed in⁸). Intracytoplasmic argyrophilic and α -synuclein-immunoreactive inclusions of oligodendrocytes, referred to as glial cytoplasmic inclusions (GCIs), are found in affected regions in MSA.^{9,10}

In this study, we describe three patients with OPCA and pathologic features of CBD (CBD-OPCA) with no GCIs, an unusual combination that has not been previously reported. CBD-OPCA demographic, clinical, and neuropathologic features are compared to typical CBD, PSP, and MSA. Additionally, we examined the biochemical profile of tau in CBD-OPCA, CBD, and PSP.

3.3. Materials and methods

3.3.1. Case selection

Three CBD-OPCA cases were identified from a series of brains submitted for review or consultation to the neuropathology laboratory at Mayo Clinic Florida between 1998 and 2006. Out of 81 CBD cases observed during that time period, three out of 81 CBD cases (3.7%) had macroscopic and microscopic features of OPCA. These three cases are compared to a set of control cases, including CBD, MSA, PSP, and neurologically normal controls ($n = 11$ for each group).

3.3.2. Tissue sampling and pathologic assessment

Most brains submitted for neuropathologic evaluation include one half of the brain (usually left) divided in a mid-sagittal plane fixed in formaldehyde and the other half frozen for biochemical and genetic studies. Thioflavin S fluorescent microscopy was used to assess Alzheimer-type pathology,¹¹ and hematoxylin and eosin-stained sections were used to evaluate neuronal loss and gliosis. For quantitative analyses, samples were taken from pons and medulla, as well as a transverse section of cerebellar hemisphere (including deep white matter and dentate nucleus) and a sagittal section of the cerebellar vermis. Three non-overlapping images were randomly captured from H&E stained sections of pontine nuclei, inferior olivary nucleus, cerebellar dentate nucleus, cerebellar Purkinje cell layer, and vermis for each case (1.5 mm x 1.25 mm section for cerebellar Purkinje cell layer in cerebellar hemisphere and vermis: 0.6 mm x 0.5 mm section for inferior olivary nucleus, pontine nuclei and dentate nucleus). Mean value of the number of surviving neurons in each image was counted manually for each case.

Statistical analyses were performed with statistics software (GraphPad Prism 4.03, GraphPad Software, CA) and a probability value of $P < 0.05$ was regarded as significant for all analyses. The differences were examined with One Way Analysis of Variance on Ranks. When there was a significant difference, either Holm-Sidak or Dunn's method was performed for pair-wise comparisons.

3.3.3. Immunohistochemistry

Multiple cortical and subcortical areas, brainstem, and cerebellum were processed for α -synuclein and tau immunohistochemistry. Sections of formalin-fixed and paraffin-embedded specimens were cut a 5- μ m thickness and mounted on glass slides, immunostained with a polyclonal rabbit anti- α -synuclein antibody (NACP)¹²; a phospho-tau monoclonal antibody (CP13 from Peter Davies, Albert Einstein College of Medicine, NY)¹³; a phospho-TDP-43 monoclonal antibody (ps409/410, 1:5000, Cosmobio Co., Tokyo, Japan), or a p62/sequestosome (p62 Ick ligand, 1:1,000, BD Bioscience, Franklin Lakes, NJ, USA) and then processed on an autostainer (DAKO Autostainer Universal Staining System, DAKO) using 3, 3'-diaminobenzidine as a chromogen. After immunostaining, the sections were counterstained briefly with hematoxylin. The α -

synuclein immunohistochemical methods have previously been shown to have high sensitivity and specificity for Lewy body and MSA pathologies.^{14,15}

Tau pathology burden was analyzed in CBD-OPCA ($n = 3$) and typical CBD ($n = 11$). Three non-overlapping images were randomly captured from tau-immunostained sections of middle frontal gyrus, pontine nuclei, inferior olivary nucleus, and cerebellar dentate nucleus (0.3 mm x 0.25 mm section). The captured images were processed with image analysis software (MetaMorph Offline version 7.0r4, Molecular Devices Corporation, CA). A ratio of the immunoreactive pixels to the total pixels of the whole field was calculated to yield an estimate of lesion burden (%) and the mean value was calculated for each case. In addition, the mean value of infratentorial tau burden (pontine base, inferior olivary nucleus and dentate nucleus) was calculated for each case. The differences were examined with an unpaired t-test.

3.3.4. Genetic analysis

All *MAPT* exons were amplified from genomic DNA for Cases 1 and 2 (frozen tissue was not available for Case 3). PCR reactions of approximately 500 bp fragments were performed in 15 μ l reactions in 384 well plates. PCR products were purified using AMPure (Agencourt Biosciences) then sequenced in both directions using the BigDye Terminator cycle sequencing kit (Applied Biosystems). Sequencing reactions were purified using CleanSEQ (Agencourt Biosciences) and analyzed on an ABI 3730 Genetic Analyzer (Applied Biosystems). Base calling, sequence alignments and heterozygote detection was performed using Sequencher (Gene Codes Corporation). *C9ORF72* noncoding hexanucleotide repeats were examined with a repeat-primed PCR assay.¹⁶

3.3.5. Tau biochemistry

A biochemical protein extraction followed a previously reported protocol.¹⁷ Frozen brain samples from frontal cortex, pons, dentate nucleus of the cerebellum, and midbrain were homogenized into 2 volumes of TS buffer (50 mM Tris-HCl, pH 7.6, 150 mM NaCl, 10 mM PMSF, 1 mM EGTA) and centrifuged at 20,000 g for 20 min. The resultant pellet was resuspended and homogenized with 2 volumes of H buffer (10 mM Tris-HCl, pH 7.4, 0.8 M NaCl, 10 mM PMSF, 1 mM EGTA, 10% sucrose), and centrifuged at 100,000 g for 20 min. Resultant pellet (P1) was homogenized with 1% sarkosyl containing TS buffer and centrifuged at 100,000 g to obtain sarkosyl soluble supernatant (S3) and

insoluble pellet (P3). The sarkosyl-insoluble P3 fractions were extracted with 2% sodium dodecyl sulfate (SDS) containing TS buffer. Each sample was mixed with SDS and β -mercaptoethanol containing sample buffer, separated on 12.5% Tris-glycine gels, transferred to nitrocellulose membranes (Millipore Co., USA), and immunoblotted. The primary antibody used against phosphorylated tau was PHF-1 (1:1000, from Peter Davies, Albert Einstein College of Medicine, NY), which recognizes the C-terminal region of phosphorylated tau (p-Ser396/p-Ser404),¹⁸ and anti-mouse IgG secondary antibody (1:5000). MCID v6.0 image software (InterFocus Imaging, Cambridge, England) was used for densitometric analysis. The intensities of 37 and 40 kDa bands were calculated and divided by that of 33 kDa band in each case of CBD-OPCA, CBD, and PSP. The differences were examined by unpaired t-test.

3.4. Results

Here we give a summary of neuropathologic features that were similar for all three cases, as well as clinical vignettes of the three patients with CBD-OPCA. Demographic information and clinical characteristics are summarized in **Table 3.1**. DNA samples were available for Cases 1 and 2, and they were both negative for *MAPT* mutations in all coding exons. Because a CBD case has been reported to have the chromosome 9 open reading frame 72 (*C9ORF72*) hexanucleotide expansion, fluorescent fragment-length analysis was performed between noncoding *C9ORF72* exons 1a and 1b showed that both Cases 1 and 2 were heterozygous, and therefore, had hexanucleotide repeats of a nonpathogenic length. Only fixed tissue was available for study for Case 3. All three cases were of European descent. Immunohistochemistry for p62 was performed on cerebellum, medulla, and pons section and all three CBD-OPCA were negative for neuronal intranuclear inclusions.

Table 3.1 Summary of demographics, clinical, and neuropathology of CBD-OPCA			
	Case 1	Case 2	Case 3
Sex	female	male	female
Age at death, y	67	75	74
Disease duration, y	6	8	10
Family history	cousin: parkinsonism	brother: parkinsonism	mother: MS; 2 siblings: psychiatric
Initial clinical features	poor balance, unexplained falls; personality change	poor balance, unexplained falls; ataxic gait	gait ataxia, unexplained falls, hyperreflexia, high-arched feet
Later clinical features	ataxic gait, parkinsonism, vertical gaze palsy, cognitive impairment, dysphagia, hypophonia; L-DOPA nonresponsive	bradykinesia, vertical gaze palsy, hypophonia, mutism	ataxia, poor handwriting, pontocerebellar atrophy on MRI
Clinical diagnosis	probable PSP	probable PSP	idiopathic OPCA
Brain weight, g	1320	1220	1254
Braak NFT stage	0	II	I
Thal amyloid stage	1	3	0
Pathologic diagnoses	CBD-OPCA AGD	CBD-OPCA	CBD-OPCA AGD

3.4.1. Clinical features

Case 1: This 67-year-old woman had balance problems beginning at age 61, and she experienced multiple falls. Five years prior to her movement disorder, she suffered from depression following the death of her husband, and she became apathetic and withdrawn. One year into her illness, she exhibited a broad-based ataxic gait with an inability to tandem walk, abnormal Romberg, and a reduced stride length. Bradykinesia, rest tremor, and terminal fine tremor on finger-to-nose testing, and micrographia were observed. She was treated with carbidopa and levodopa with no apparent improvement. She then developed eye movement abnormalities including abnormal saccades, poor vision, reduced blink, and eyelid apraxia. Three years into her illness, she had vertical supranuclear gaze palsy, bilateral rigidity of the upper extremities, and cogwheel rigidity of the left arm. There was no apraxia, myoclonus, or aphasia noted. Four years into her illness, neuropsychiatric evaluation showed significant cognitive impairment, especially in the domain of expressive language, and she had reduced concentration and a flat affect. In the final stage of her illness, she had dysphagia, hypophonia, increased

rigidity, and urinary incontinence. She had episodes of confusion and agitation and did not spontaneously interact. She was diagnosed as clinically probable PSP.

Case 2: This 75-year-old man presented with balance problems at age 67. This progressively worsened, and he experienced several falls in the backward direction. His gait was wide-based, erect, and mildly ataxic. Five years into the disease, his speech became softened, and his extraocular motility showed vertical impairment. There was no resting or action tremor noted, but his reflexes were reduced throughout. He became bradykinetic, and his ataxic gait progressively worsened. There was a paucity of spontaneous language output, mask-like facies, and eye movement abnormalities affecting both up and down gaze, with reduced blink rate. There was a positive family history for Parkinsonism in his brother. He was diagnosed with clinically probable PSP.

Case 3: This 74-year-old woman presented with an unsteady, ataxic gait and unexplained falls that began at approximately age 64. Her gait was wide-based and she had difficulty walking in a straight line and on her toes and heels. She had normal jaw jerk, but had hyperreflexia of the upper extremities with bilateral Hoffmann signs. Reflexes were brisk at the knees and ankles without clonus. Detection of vibration at the toes and toe strength were slightly decreased. She had high-arched feet, with clawing of the toes. There was some difficulty on the finger-to-nose test with the upper limbs, right more than left, and there was no accentuation of this difficulty with the eyes being closed. There was mild dysarthria and mild weakness of the small muscles of the hands. Her speech became monotonic and did not modulate much. Decreased arm swing was noted with increased cogwheeling. Her handwriting deteriorated, and she had coordination difficulty with both of her hands. She had impaired alternative motion reactions of the right hand greater than left, but equally in both feet. **Brain magnetic resonance imaging from Case 3:** Brain MRI (1.5T GE Medical Systems Signa scanner, Milwaukee, WI) performed 5 years after the onset of symptoms showed a small brainstem, particularly from the pontomesencephalic junction to the pontomedullary junction (**Figure 3.1a**). Sagittal and coronal T3-1-weighted MRI scan performed 7 years after onset of symptoms showed progressive focal cerebellar atrophy **Figure 3.1a,b**). T2-weighted MR images demonstrated slightly increased signal within the transverse pontine fibers (**Figure 3.1c**). Diffusion weighted imaging and fluid attenuated inversion recovery (FLAIR) images showing enlargement of the fourth ventricle and

cerebellopontine cisterns (**Figure 3.1d**). The olivopontocerebellar atrophy was bilateral. Her disease course was slowly progressive, and she died after a 10-year disease duration. There was a possible history of multiple sclerosis in her mother and psychiatric illness in two siblings. The antemortem clinical diagnosis was idiopathic OPCA.

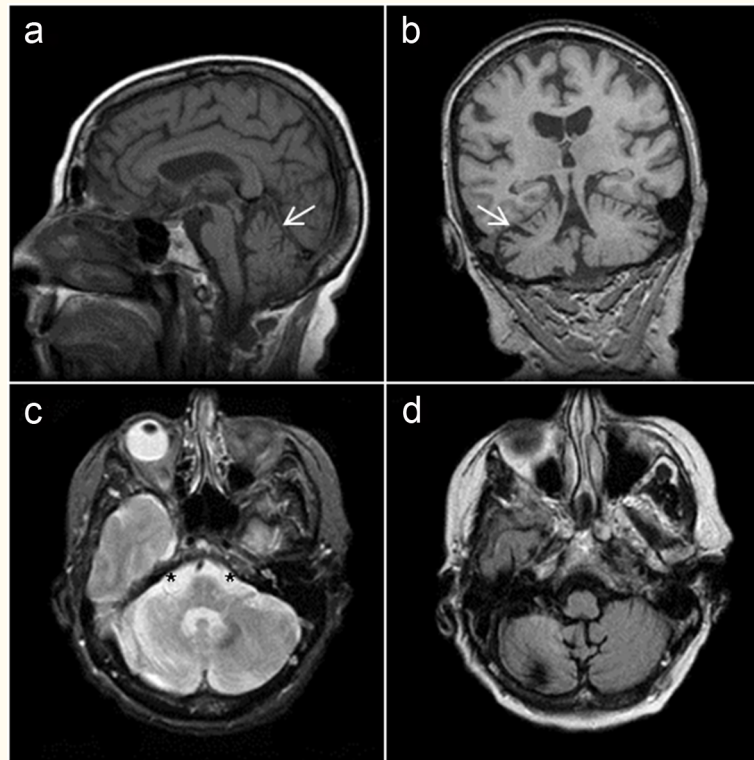


Figure 3.1 | Brain magnetic resonance imaging (MRI) from Case 3.

(a) T1-weighted mid-sagittal MRI section shows anterior cerebellar (*arrow*) and brainstem atrophy. (b) T1-weighted coronal section shows bilateral cerebellar atrophy. (c) Axial T2-weighted image and (d) fluid attenuated inversion recovery MRI showing enlargement of the fourth ventricle and cerebellopontine cisterns (*asterisks*).

3.4.2. Neuropathologic features

3.4.2.1. Macroscopic

Cerebral atrophy was moderate in frontal lobe, and the corpus callosum was thin. The midbrain had loss of neuromelanin pigment in the substantia nigra, and the pontine base had marked atrophy (**Figure 3.2a**). There was discoloration of transverse fibers of

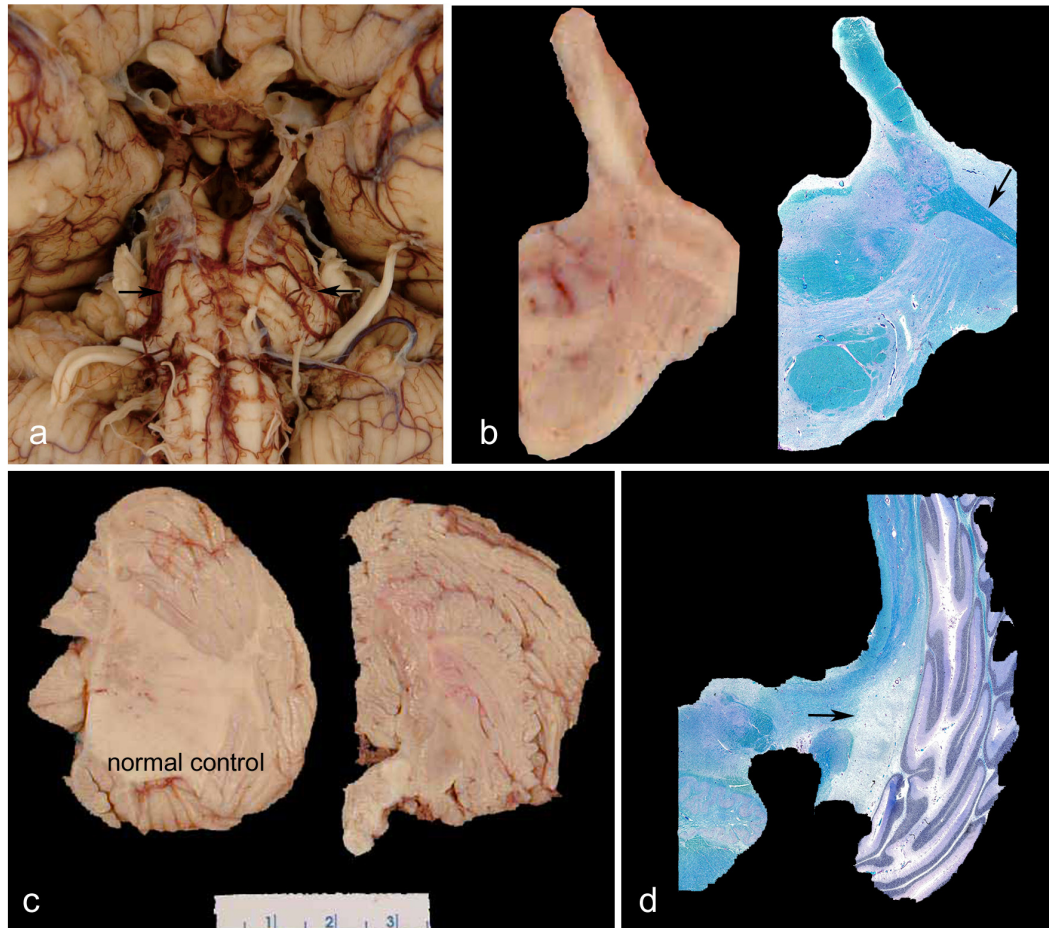


Figure 3.2 | CBD-OPCA macroscopic features.

The base of the brain shows prominent atrophy of the pons (arrows in **a**). A transverse section of the mid-pons shows marked atrophy of the pontine base, while the superior cerebellar peduncle is relatively preserved, and the trigeminal nerve (arrow in **b**) is prominent against the atrophic and has loss of myelin middle cerebellar peduncle (**b**). Cerebellum sections show marked white matter atrophy compared with normal control (**c**). Cerebellar white matter has loss of myelin (arrow in **d**). Luxol fast blue staining (**b, d**); case 1 (**b, c**); case 2 (**d**); case 3 (**a**).

the pontine base and middle cerebellar peduncle (**Figure 3.2b**) with relative sparing of the trigeminal nerve on Luxol fast blue (**Figure 3.2b**, arrow). The inferior cerebellar peduncle and cerebellar white matter were markedly atrophic with a dusky gray appearance (**Figure 3.2c**) and had significant myelin staining pallor on Luxol fast blue (**Figure 3.2d**, arrow).

3.4.2.2. CBD pathology

There were no GCIs with α -synuclein immunohistochemistry or Gallyas silver stains in all brain regions examined. On the other hand, the tau pathology in CBD-OPCA was consistent with CBD with the exception of an especially high tau pathology burden in the brainstem and cerebellum compared to that typically seen in CBD. Tau pathology distribution and degree of severity for all three cases is shown in **Tables 3.2-3.4**.

Pretangles, neuropil threads, astrocytic plaques (**Figure 3.3a**), and sparse coiled bodies were present in affected cortices and subjacent white matter. There were ballooned neurons in affected cortices (**Figure 3.3b**). Sections from the frontal lobe showed diffuse gliosis and minimal microvacuolation. The substantia nigra had marked neuronal loss with extraneuronal melanin (**Figure 3.3c**), axonal spheroids, and reactive astrocytosis. Some neurons in the substantia nigra and locus coeruleus had tau-positive inclusions typical of so-called “corticobasal bodies” (**Figure 3.3c**).¹⁹ The neuronal population of the subthalamic nucleus was relatively preserved, but there were numerous neuropil threads. Argyrophilic grains were present in medial temporal lobe structures, including the amygdala. Gliosis was observed in the striatum, globus pallidus, and thalamus.

Region	NFT & pre-NFT	Coiled bodies	Astrocytic plaques	Tau+ threads
Temporal cortex	++	+	++	+
Motor cortex	+++	+	+++	+++
Caudate/putamen	+++	++	+++	+++
Globus pallidus	++	+	-	+++
Basal nucleus	+++	-	-	+++
Hypothalamus	+++	-	-	+++
Ventral thalamus	++	+	-	+++
Subthalamic nucleus	+++	+	-	+++
Thalamic fasciculus	-	+	-	++
Red nucleus	++	+	-	++
Substantia nigra	+++	+	-	+++
Oculomotor complex	++	-	-	+++
Midbrain tectum	+	+	+	+++
Locus coeruleus	+++	-	-	+++
Pontine tegmentum	+++	++	-	+++
Pontine base	+	+++	-	+++
Medullary tegmentum	+++	-	-	+++
Inferior olive	++	-	-	+++
Dentate nucleus	+++	+	-	++
Cerebellar white matter	-	++	-	+++

Table 3.3 Tau pathology in Case 2				
Region	NFT & pre-NFT	Coiled bodies	Astrocytic plaques	Tau+ threads
Temporal cortex	++	+	++	+
Motor cortex	+++	+	+++	++
Caudate/putamen	+++	+	+++	+++
Globus pallidus	++	-	-	+++
Basal nucleus	++	-	-	++
Hypothalamus	+++	-	-	+
Ventral thalamus	+++	+	-	+++
Subthalamic nucleus	+	+	-	++
Thalamic fasciculus	-	+	-	++
Red nucleus	+	+	-	++
Substantia nigra	++	+	-	+++
Oculomotor complex	++	-	-	+
Midbrain tectum	++	+	-	+++
Locus coeruleus	+	-	-	+++
Pontine tegmentum	++	+	-	+++
Pontine base	+	++	-	++
Medullary tegmentum	++	+	-	++
Inferior olive	+	+	-	+++
Dentate nucleus	++	+	-	+++
Cerebellar white matter	-	++	-	+

Table 3.4 Tau pathology in Case 3				
Region	NFT & pre-NFT	Coiled bodies	Astrocytic plaques	Tau+ threads
Temporal cortex	++	+	++	+
Motor cortex	++	+	+++	++
Caudate/putamen	+++	-	++	+++
Globus pallidus	+++	+	+	+++
Basal nucleus	++	-	-	+++
Hypothalamus	+++	-	-	++
Ventral thalamus	+++	-	-	+++
Subthalamic nucleus	+++	+	+	+++
Thalamic fasciculus	-	+	-	++
Red nucleus	+	+	-	++
Substantia nigra	+++	-	-	+++
Oculomotor complex	++	-	-	+++
Midbrain tectum	+	-	++	+++
Locus coeruleus	++	-	-	+++
Pontine tegmentum	+++	-	-	+++
Pontine base	+++	+	-	+++
Medullary tegmentum	+++	-	-	+++
Inferior olive	++	++	-	+++
Dentate nucleus	+++	-	-	+++
Cerebellar white matter	-	++	-	+++

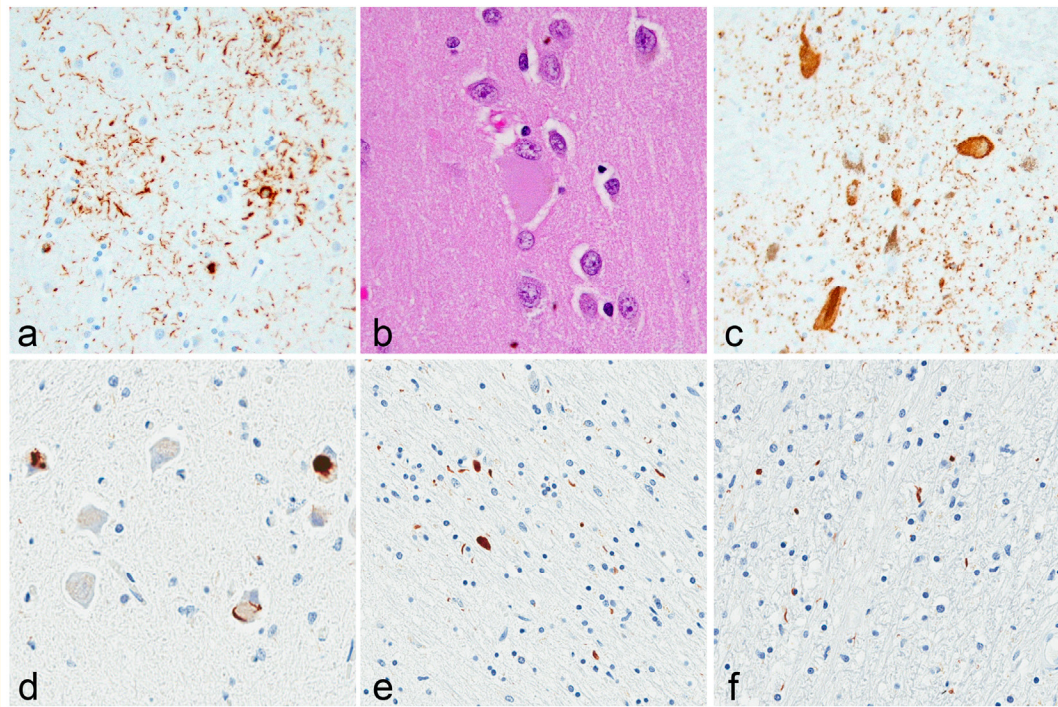


Figure 3.3 | Tau and TDP-43 immunohistochemistry in CBD-OPCA.

Affected cortical regions show tau-immunoreactive astrocytic plaques (a) and ballooned neurons (b). The substantia nigra has neuronal loss and tau-positive “corticobasal bodies” (c). Abundant TDP-43-positive pathology was seen throughout the olivopontocerebellar system in CBD-OPCA, including neuronal cytoplasmic inclusions in the inferior olivary nucleus (d) and numerous threads and oligodendroglial inclusions in the pontine base (e) and cerebellar white matter (f).

3.4.2.3. TDP-43 immunohistochemistry

Sections from the medulla had the most striking TDP-43 pathology with many neuronal cytoplasmic inclusions (NCIs) in the inferior olivary nucleus, but not in the hypoglossal nuclei (**Figure 3.3d**). Numerous TDP-43 immunoreactive glial cytoplasmic inclusions (GCIs) and threads were detected in the pontine base (especially pontocerebellar fibers), cerebellar white matter (**Figure 3.3e, f**), subthalamic nucleus, globus pallidus, and substantia nigra. There were sparse TDP-43 positive NCIs in the pontine nuclei, but not in the pontine tegmentum, Purkinje cells, and cerebellar dentate nucleus. Detailed semi-quantitative TDP-43 immunohistochemistry scores for CBD-OPCA compared to typical CBD ($n = 4$) are listed in **Tables 3.5-3.7**.

Table 3.5 TDP-43-positive neuronal cytoplasmic inclusions							
Region	CBD-OPCA 1	CBD-OPCA 2	CBD-OPCA 3	CBD 1	CBD 2	CBD 3	CBD 4
Caudate/putamen	++	++	+	+	-	+	++
Globus pallidus	++	+++	+	+++	-	+++	++
Basal nucleus	+	-	+	+	NA	+	+
Hypothalamus	++	++	+	+	NA	+++	-
Amygdala	++	-	-	-	NA	-	+
Subthalamic nucleus	+++	+++	+	++	+++	++	
Dentate of hippocampus	-	-	NA	-	-	-	-
Subiculum	++	-	-	-	-	-	-
Red nucleus	-	+	+	+	+	+	+
Substantia nigra	++	+++	++	+	++	+++	-
Locus coeruleus	++	+	+	+	+	++	NA
Pontine tegmentum	+	+	+	-	-	+	-
Pontine base	++	+++	+++	-	-	-	+
Inferior olive	+++	+++	+++	-	-	NA	-
Cerebellar white matter	-	-	-	-	-	-	-

Table 3.6 TDP-43-positive glial inclusions							
Region	CBD-OPCA 1	CBD-OPCA 2	CBD-OPCA 3	CBD 1	CBD 2	CBD 3	CBD 4
Caudate/putamen	+	+	+	+	-	++	+
Globus pallidus	++	+	++	-	-	-	-
Basal nucleus	++	+	+	+	NA	+	-
Hypothalamus	++	++	+	+	NA	+	-
Amygdala	+	-	+	-	NA	+	-
Subthalamic nucleus	+	+	++	-	-	++	+
Dentate of hippocampus	-	-	NA	-	-	-	-
Subiculum	+	-	-	-	-	-	-
Red nucleus	++	++	+	-	+	-	-
Substantia nigra	++	++	+	+	-	+	-
Locus coeruleus	+	++	+	-	-	-	NA
Pontine tegmentum	+	++	+	-	+	+	+
Pontine base	++	++	++	-	-	-	-
Inferior olive	+	++	++	-	-	NA	-
Cerebellar white matter	++	++	++	-	-	-	-

Table 3.7 TDP-43-positive threads							
Region	CBD-OPCA 1	CBD-OPCA 2	CBD-OPCA 3	CBD 1	CBD 2	CBD 3	CBD 4
Caudate/putamen	++	+	++	+	-	++	++
Globus pallidus	+	++	++	-	-	+	-
Basal nucleus	+++	+	+	+	NA	++	+
Hypothalamus	+++	-	++	+	NA	+++	-
Amygdala	++	+	+	-	NA	-	-
Subthalamic nucleus	+	+	++	-	-	+	-
Dentate of hippocampus	-	-	NA	-	-	-	-
Subiculum	+	+	-	-	-	-	-
Red nucleus	++	++	+	+	+	+	-
Substantia nigra	+++	+	+	+		+	-
Locus coeruleus	+	+	+	-	-	+	NA
Pontine tegmentum	+++	+++	++	-	+	++	+
Pontine base	+++	++	+++	-	-	-	-
Inferior olive	+	+	++	-	-	NA	-
Cerebellar white matter	-	-	-	-	-	-	-

3.4.2.4. Olivopontocerebellar system

Sections from the medulla revealed marked neuronal loss in the inferior olivary nucleus and significant degeneration of olivocerebellar fibers (**Figure 3.4a**). The pons was remarkable for severe neuronal loss in the pontine base and degeneration and gliosis of the transverse fibers (**Figure 3.4b**) with preservation of the longitudinal fibers. The cerebellar white matter was atrophic and had marked demyelination (**Figure 3.4c**). The cerebellum had patchy, but extensive neuronal loss in Purkinje and internal granular cell layers with many axonal torpedoes (**Figure 3.4c**) and empty baskets. Tau-immunoreactive pretangles and numerous neuropil threads were detected in inferior olivary nucleus (**Figure 3.4d**). Tau pathology was prominent in the pontocerebellar fibers (**Figure 3.4e**), pontine base, and pontine nuclei had numerous pretangles. The cerebellar dentate nucleus had many pretangles and cerebellar white matter had numerous tau-immunoreactive threads and sparse coiled bodies (**Figure 3.4f**). Cerebellar dentate nucleus had moderate neuronal loss and gliosis and pyknotic neurons with grumose degeneration.

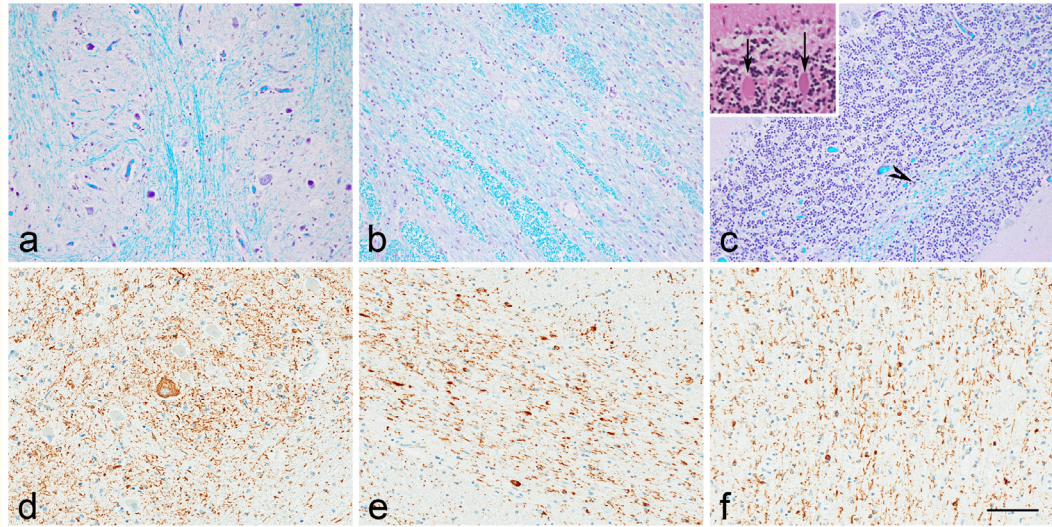


Figure 3.4 | CBD-OPCA olivopontocerebellar system pathology.

The inferior olivary nucleus has neuronal loss with degeneration of olivocerebellar fibers (a), marked degeneration of transverse fibers of the pontine base with preservation of longitudinal fibers (b), cerebellar white matter loss (c, arrowhead) and axonal torpedoes (c, inset arrows). The inferior olivary nucleus has many pretangles and threads (d). Pontine transverse fibers (e) and cerebellar white matter (f) with tau-immunoreactive threads. Luxol fast blue staining (a-c); H&E staining (c inset); tau immunohistochemistry (d-f); bar = 50 μ m.

3.4.3. Comparison of CBD-OPCA to MSA, typical CBD and PSP

3.4.3.1. Neuronal loss

Three CBD-OPCA cases were compared to CBD, MSA, PSP, and normal controls ($n = 11$ for each group) with respect to neuronal loss in key infratentorial nuclei involved in olivopontocerebellar degeneration. Neuronal loss was severe in the pontine nuclei and inferior olivary nucleus of CBD-OPCA and comparable to that seen in MSA (**Figure 3.5**). PSP cases had pretangles and sparse globose type of neurofibrillary tangles (NFTs), but minimal neuronal loss in pontine nuclei and inferior olivary nucleus. Purkinje cell neuronal loss was most marked in MSA; less in CBD-OPCA and PSP; and minimal or absent in typical CBD. The cerebellar vermis, like the pontine nuclei and olivary nuclei, had a similar degree of neuronal loss in CBD-OPCA and MSA. Axonal torpedoes were more numerous in CBD-OPCA and MSA compared to typical CBD and PSP, although they were observed in all neurodegenerative disorders examined in this study. The cerebellar dentate nucleus had neuronal loss and gliosis in CBD-OPCA, but the dentate nucleus was spared in MSA and typical CBD. There was marked neuronal loss of

dentate nucleus in PSP cases, which tended to be more severe than in CBD-OPCA. Grumose degeneration was frequent in both PSP and CBD-OPCA.

Table 3.8 Summary of cases and controls used for quantitative neuronal counts				
	M:F	Age at death, y (m ± SD)	Brain weight, g (m ± SD)	Braak NFT Stage (m ± SD)
CBD-OPCA	1:2	72.0 ± 4.4	1264 ± 51	1.0 ± 1.0
CBD	8:3	68.5 ± 7.8	1169 ± 111	1.2 ± 1.0
MSA	7:4	67.5 ± 7.5	1235 ± 141	1.4 ± 1.1
PSP	3:8	70.7 ± 7.85	1130 ± 95	1.7 ± 0.9
Normal controls	6:5	73.7 ± 12.8	1170 ± 159	1.6 ± 1.2

m ± SD = mean ± standard deviation

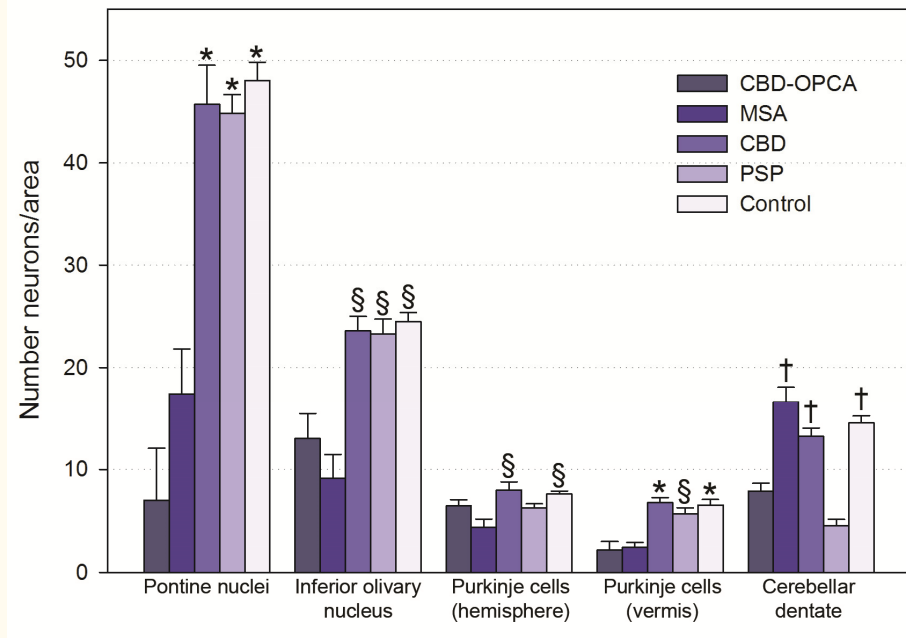


Figure 3.5 | Neuronal loss in CBD-OPCA, CBD, MSA, PSP, and normal controls.

Neuronal loss in CBD-OPCA, CBD, MSA, PSP, and normal controls. Three non-overlapping images were randomly captured from H&E stained sections (1.5 mm x 1.25 mm section for cerebellar Purkinje cell layer in cerebellar hemisphere and vermis; 0.6 mm x 0.5 mm section for inferior olivary nucleus, pontine nuclei and dentate nucleus). Bars represent mean and error bars show the standard error of the mean. CBD-OPCA = corticobasal degeneration with olivopontocerebellar atrophy, MSA = multiple system atrophy, CBD = typical corticobasal degeneration, PSP = progressive supranuclear palsy. * P < 0.001 versus CBD OPCA and MSA; § P < 0.05 (inferior olivary nucleus) and P < 0.001 (Purkinje and vermis) versus MSA; † P < 0.05 versus PSP

3.4.3.2. Tau immunohistochemistry image analysis

Image analysis of tau pathology was used to determine whether there were differences in severity of tau pathology in CBD-OPCA compared with typical CBD. Regional anatomical differences were assessed in middle frontal gyrus, pontine base, inferior olivary nucleus, and dentate nucleus of the cerebellum (**Figure 3.6**). CBD-OPCA had more severe tau pathology in the pontine base ($P = 0.003$) compared with typical CBD. Although the results did not meet statistical significance, tau burden in the inferior olivary nucleus and dentate nucleus also tended to be greater in CBD-OPCA compared with CBD. Since CBD-OPCA is rare and our cohort is small, we tested the mean tau burden of infratentorial structures by summing the burden in pontine base, inferior olivary nucleus and dentate nucleus; this analysis showed significantly greater tau burden in CBD-OPCA than in typical CBD ($P = 0.003$). CBD-OPCA also had significantly greater tau burden when including only the inferior olivary and dentate nuclei ($P < 0.05$, data not shown). In frontal cortex, the density of astrocytic plaques, coiled bodies, pretangles, and neuropil threads was similar in CBD-OPCA and typical CBD.

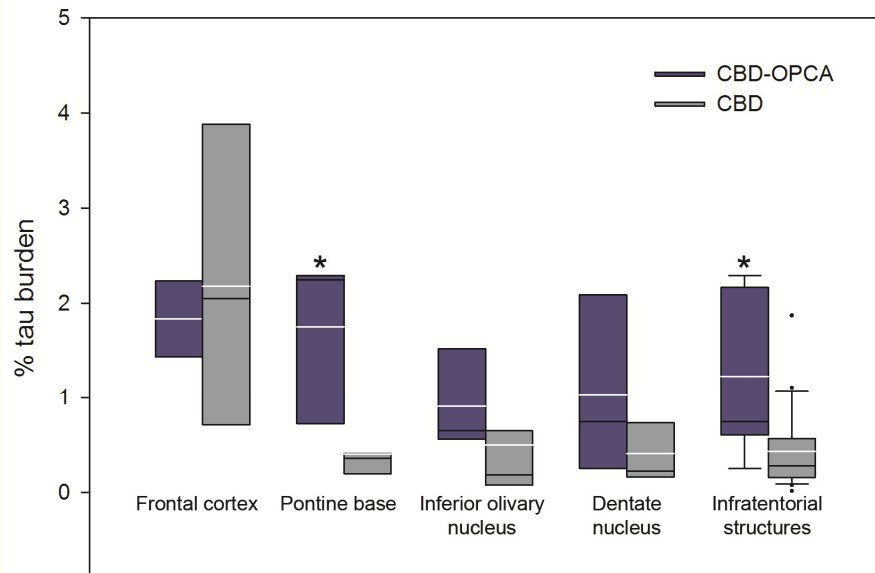


Figure 3.6 | Image analysis tau burden in CBD-OPCA and CBD.

The tau burden was quantified for CBD-OPCA (n = 3) and typical CBD (n = 11) on sections of middle frontal gyrus, pontine nuclei, inferior olivary nucleus, and cerebellar dentate nucleus (0.3 mm x 0.25 mm section). Boxes represent the ratio of tau immunoreactive pixels to total pixels as a % tau burden; median = black line; mean = white line; CBD-OPCA = corticobasal degeneration with olivopontocerebellar atrophy, CBD = typical corticobasal degeneration. * P = 0.003

3.4.3.3. Tau biochemistry

The biochemical profile of tau was analyzed to determine whether tau protein accumulating in CBD-OPCA was similar to typical CBD. Immunoblot analyses of sarkosyl-soluble fractions for CBD-OPCA, CBD, and PSP was performed. CBD-OPCA, CBD and PSP all had prominent tau immunoreactive bands at approximately 64 and 68 kDa (**Figure 3.7a**, asterisks). Both CBD-OPCA and typical CBD had prominent bands at 37 and 40 kDa (**Figure 3.7a**, double arrows), whereas PSP had a single prominent band at approximately 33 kDa (**Figure 3.7a**, single arrow). Quantitative analysis of PHF-1 immunoreactive tau bands showed significant differences in the ratio of 37 and 40 kDa tau to 33 kDa tau between both CBD-OPCA and typical CBD compared with PSP (**Figure 3.7b**). Immunoblot analysis of sarkosyl-insoluble tau fragments with PHF-1 disclosed similar results (data not shown).

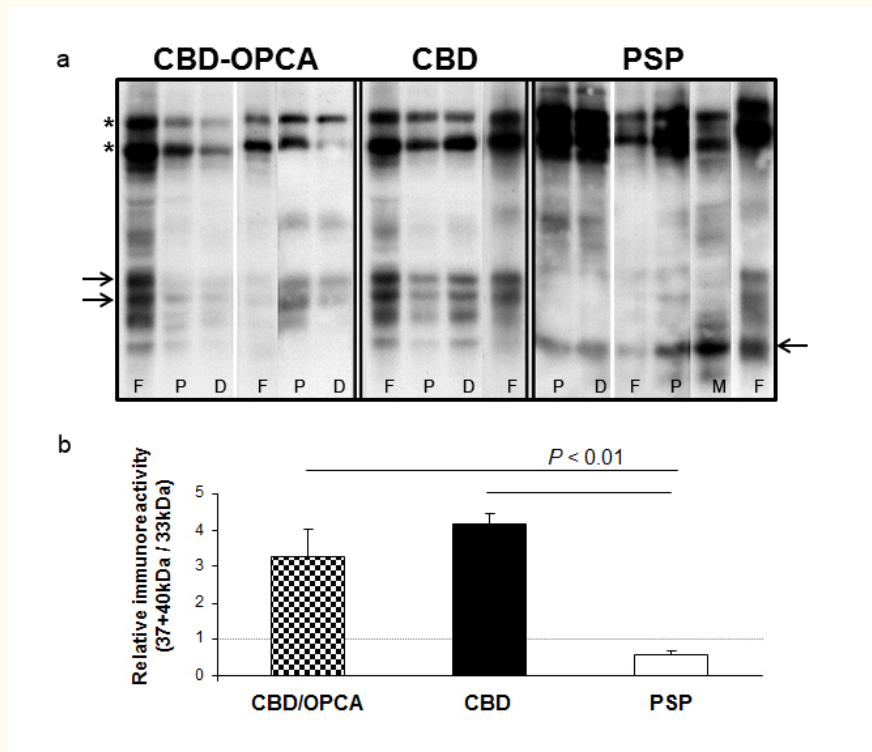


Figure 3.7 | Biochemical analysis of tau in CBD-OPCA, CBD, and PSP.

Biochemical analysis of tau in CBD-OPCA, CBD, and PSP. Proteins were extracted from frontal cortex (F), pons (P), dentate nucleus of the cerebellum (D), and midbrain (M) of CBD-OPCA, CBD, and PSP. Sarkosyl-soluble fractions were separated by SDS-PAGE and immunoblotted (a). Tau was present at the characteristic doublet (~64- and 68-kDa, asterisks) for all cases, CBD-OPCA and CBD have a lower molecular weight doublet at ~37-kDa (two arrows, left) and PSP has a single band at ~33-kDa (arrow, right). (b) Densitometric ratio of 37- and 40-kDa to 33-kDa tau. Bar charts show mean and error bars show the standard error of mean.

3.5. Discussion

This study identified patients with pathologically confirmed CBD who had OPCA that clinically presented with either a symmetrical, atypical parkinsonism suggestive of PSP or a slowly progressive cerebellar syndrome suggestive of idiopathic OPCA. The typical asymmetrical rigidity and apraxia syndrome (*i.e.* corticobasal syndrome) of CBD was not present in any of the three cases. CBD-OPCA had marked pontine and cerebellar atrophy associated with severe myelin loss of the pontocerebellar fibers, middle cerebellar peduncle, and cerebellar white matter. Yet, immunohistochemical analyses failed to show α -synuclein-positive GCIs that are pathognomonic of MSA,⁹ but instead

revealed tau-immunoreactive astrocytic plaques, thread-like processes in gray and white matter, and ballooned neurons, all neuropathologic features of CBD. The fact that CBD-OPCA has a tau biochemical profile as that observed in typical CBD, supports the idea that CBD-OPCA is a variant of CBD. A reexamination of the Mayo Clinic brain bank in 2014 shows that four of 180 CBD cases have CBD-OPCA (2.2%).

3.5.1. CBD-OPCA is one of several clinical variants of CBD

CBD can present with various clinical syndromes, with the particular clinical features dependent on the location of the greatest cortical involvement.² While many of the clinical presentations are asymmetric syndromes (*e.g.*, corticobasal syndrome or progressive nonfluent aphasia), symmetrical CBD is increasingly recognized²⁰ and such cases are often misdiagnosed as PSP, with an estimated frequency of 30% of all reported pathologically confirmed CBD.²¹ Disease duration and age of death were not significantly different between CBD-OPCA and other reported CBD demographic information.^{2,22}

Previously, we identified distinct pathologic differences that accounted for CBD presenting clinically like PSP (a clinical syndrome also referred to as Richardson syndrome),²³ including more severe tau burden in white matter of the cerebellum and inferior olivary nucleus compared with CBD presenting with corticobasal syndrome. In the present study, we report that CBD-OPCA also has greater tau pathology in infratentorial structures, especially the pontine base (**Figure 3.6**), indicating that greater hindbrain tau pathology plays a significant role in the RS clinical presentation of CBD. The two CBD-OPCA cases diagnosed as PSP both exhibited an ataxic gait at some point during their illness, an atypical feature for both CBS and Richardson syndrome, presumably reflecting the cerebellar involvement.

Cerebellar dentate pathology was highlighted in the first descriptions of CBD,¹ but it is not a consistent finding in all cases, and it is not included in neuropathologic diagnostic criteria for CBD.⁴ In contrast, dentate pathology, with grumose degeneration is very frequent in PSP.^{24,25} The clinical significance of cerebellar dentate nucleus pathology in PSP is unknown. All three cases of CBD-OPCA in this small series had cerebellar dentate pathology comparable to that seen in PSP, which was much different from MSA, where preservation of the dentate neuronal population was observed. The neuronal density of the dentate nucleus in MSA was not only greater than PSP, CBD, and CBD-OPCA, but also control cases. Fukutani and co-workers reported that the

increased neuronal density in the dentate nucleus in MSA is a counting artifact related to decreased dentate nucleus volume related to severe cerebellar atrophy,²⁶ and this likely explains the results of the present study.

A caveat of our study is that we didn't use stereology to assess neuronal loss in the various key nuclei and this could potentially cause bias in our neuropathologic evaluation. In order to ensure that randomly selected fields for neuronal counts were representative of the entire nucleus at the level where we sample the regions, we inspected the nuclei to ensure the neuronal loss was in fact diffuse and not focal. With the exception of the cerebellar dentate, macroscopic and light microscopic studies of CBD-OPCA have notable similarities to MSA with respect to neuronal loss in the olivopontocerebellar system. CBD-OPCA and MSA both had significant neuronal loss in pontine nuclei, inferior olivary nuclei, and cerebellar vermis. In MSA, it has been previously reported that the vermis is more severely affected than the cerebellar hemispheres,²⁷ and this was also observed for both CBD-OPCA and MSA in the present study. Although CBD-OPCA and PSP had some degree of Purkinje cell loss, this was most severe in MSA compared to other groups.

3.5.2. CBD-OPCA is an uncommon variant of CBD

While there are a number of rare disorders that can produce familial and sporadic OPCA (the most common being MSA), none have been reported to be associated with tau pathology. On the other hand, Iwasaki and co-workers recently reported a Japanese patient with pathologically confirmed PSP who had severe olivopontocerebellar involvement and an antemortem clinical diagnosis of spinocerebellar degeneration.²⁷ MRI findings showed progressive brainstem and cerebellar atrophy similar to our Case 3. To our knowledge, this is the only report of OPCA associated with a 4R tauopathy. Review of the database of the Mayo Clinic brain bank, which includes referral PSP cases from CurePSP | Society for Progressive Supranuclear Palsy, with over 900 PSP cases, PSP with OPCA has not been detected. Therefore, OPCA appears to be more common in CBD than in PSP, although it is also quite rare in a series of pathologically confirmed CBD (4 of 180 cases (2%)).

The results of immunohistochemical and biochemical examinations lead to the conclusion that CBD-OPCA can be considered an uncommon, atypical variant of CBD, rather than a distinct 4R tauopathy. Tau immunohistochemistry showed astrocytic plaques in CBD-OPCA, which are useful in neuropathologic diagnosis of CBD²⁸ and

different from the tufted astrocytes in PSP.²⁹ Different low molecular weight tau fragments originally reported in CBD and PSP by Arai and coworkers¹⁷ were confirmed in the present study. Moreover, we show for the first time that CBD-OPCA resembles typical CBD and not PSP, favoring it being a variant of CBD rather than another type of 4R tauopathy. In Chapter 2 where we studied CBD cases presenting clinically with Richardson syndrome, we showed the usefulness of tau biochemical profile in differential diagnosis. Despite clinical differences in CBD presenting with Richardson syndrome or with corticobasal syndrome, both had the same lower molecular weight tau species similar to those reported here.²¹

All three cases of CBD-OPCA also had medial temporal 4R tau pathology, two of which were consistent with argyrophilic grain disease (AGD).^{6,30} It is not uncommon to find AGD pathology in CBD, with >30% of CBD cases positive for AGD.³¹ Interestingly, many patients with pathologically confirmed CBD presenting with Richardson syndrome also have increased limbic system tau pathology, with many cases meeting diagnostic criteria for AGD.²¹ It is not clear if AGD *per se* is associated with a discrete clinical syndrome³² and even less certain how presence of AGD modifies the clinical presentation of disorders in which it is a concomitant pathologic finding. Given the small number of cases in this study, it remains to be determined if medial temporal AGD is consistently found in CBD-OPCA.

In addition to CBD and AGD pathology, all three cases of CBD-OPCA had abnormal TDP-43 immunoreactive neuronal and glial inclusions with a predilection for the olivopontocerebellar system. Because a single CBD case has been reported to have the *C9ORF72* hexanucleotide expansion³³ and the fact that these CBD-OPCA cases have significant TDP-43 pathology, fluorescent fragment-length analysis was performed on Cases 1 and 2 and the results were negative for a repeat expansion. TDP-43 has been inconsistently detected in 4R tauopathies, being uncommon in PSP,³⁴ but more frequent in AGD³⁵ and CBD.³⁶ The distribution of TDP-43 pathology in CBD-OPCA is unusual and, to our knowledge, has not been previously reported in CBD or any other neurodegenerative disorder. Given that it maps to the olivopontocerebellar system, which is severely affected by the disease process, suggests that it may be linked to neurodegeneration much as amygdala TDP-43 pathology is linked to neurodegeneration in Alzheimer's disease.^{37,38} As in Alzheimer's disease, it is not clear if the TDP-43 is directly linked to the neurodegeneration or if it is a secondary reaction to neurodegeneration. It is worth noting that we detected TDP-43 pathology in typical CBD

cases, as well, but it was predominantly in diencephalon and basal ganglia. Thus, distribution of TDP-43 pathology even in typical CBD differs from that seen in frontotemporal lobar degenerations³⁸ and Alzheimer's disease.⁴⁰ Clearly, much remains to be learned about factors that contribute to selective vulnerability and concomitant pathologies in CBD and its clinicopathologic variants, including CBD-OPCA.

3.6. References

1. Rebeiz, JJ, Kolodny, EH & Richardson, EP, Jr. Corticodentatonigral degeneration with neuronal achromasia: a progressive disorder of late adult life. *Trans Am Neurol Assoc* 92, 23-6 (1967).
2. Kouri, N, Whitwell, JL, Josephs, KA, Rademakers, R & Dickson, DW. Corticobasal degeneration: a pathologically distinct 4R tauopathy. *Nature reviews. Neurology* 7, 263-72 (2011).
3. Feany, MB & Dickson, DW. Widespread cytoskeletal pathology characterizes corticobasal degeneration. *Am J Pathol* 146, 1388-96 (1995).
4. Dickson, DW, Bergeron, C, Chin, SS, Duyckaerts, C, Horoupian, D, Ikeda, K, Jellinger, K, Lantos, PL, Lippa, CF, Mirra, SS, Tabaton, M, Vonsattel, JP, Wakabayashi, K & Litvan, I. Office of Rare Diseases neuropathologic criteria for corticobasal degeneration. *J Neuropathol Exp Neurol* 61, 935-46 (2002).
5. Buee, L & Delacourte, A. Comparative biochemistry of tau in progressive supranuclear palsy, corticobasal degeneration, FTDP-17 and Pick's disease. *Brain Pathol* 9, 681-93 (1999).
6. Togo, T, Sahara, N, Yen, SH, Cookson, N, Ishizawa, T, Hutton, M, de Silva, R, Lees, A & Dickson, DW. Argyrophilic grain disease is a sporadic 4-repeat tauopathy. *J Neuropathol Exp Neurol* 61, 547-56 (2002).
7. Graham, JG & Oppenheimer, DR. Orthostatic hypotension and nicotine sensitivity in a case of multiple system atrophy. *J Neurol Neurosurg Psychiatry* 32, 28-34 (1969).
8. Jellinger, KA & Lantos, PL. Papp-Lantos inclusions and the pathogenesis of multiple system atrophy: an update. *Acta neuropathologica* 119, 657-67 (2010).
9. Papp, MI, Kahn, JE & Lantos, PL. Glial cytoplasmic inclusions in the CNS of patients with multiple system atrophy (striatonigral degeneration, olivopontocerebellar atrophy and Shy-Drager syndrome). *J Neurol Sci* 94, 79-100 (1989).
10. Arima, K, Ueda, K, Sunohara, N, Arakawa, K, Hirai, S, Nakamura, M, Tonzuka-Uehara, H & Kawai, M. NACP/alpha-synuclein immunoreactivity in fibrillary components of neuronal and oligodendroglial cytoplasmic inclusions in the pontine nuclei in multiple system atrophy. *Acta neuropathologica* 96, 439-44 (1998).
11. Murray, ME, Graff-Radford, NR, Ross, OA, Petersen, RC, Duara, R & Dickson, DW. Neuropathologically defined subtypes of Alzheimer's disease with distinct clinical characteristics: a retrospective study. *Lancet Neurol* 10, 785-96 (2011).
12. Gwinn-Hardy, K, Mehta, ND, Farrer, M, Maraganore, D, Muentner, M, Yen, SH, Hardy, J & Dickson, DW. Distinctive neuropathology revealed by alpha-synuclein antibodies in hereditary parkinsonism and dementia linked to chromosome 4p. *Acta Neuropathol (Berl)* 99, 663-72 (2000).
13. Ishizawa, T, Mattila, P, Davies, P, Wang, D & Dickson, DW. Colocalization of tau and alpha-synuclein epitopes in Lewy bodies. *J Neuropathol Exp Neurol* 62, 389-97 (2003).
14. Fujishiro, H, Ahn, TB, Frigerio, R, DelleDonne, A, Josephs, KA, Parisi, JE, Eric Ahlskog, J & Dickson, DW. Glial cytoplasmic inclusions in neurologically normal elderly: prodromal multiple system atrophy? *Acta neuropathologica* 116, 269-75 (2008).
15. Beach, TG, White, CL, Hamilton, RL, Duda, JE, Iwatsubo, T, Dickson, DW, Leverenz, JB, Roncaroli, F, Buttini, M, Hladik, CL, Sue, LI, Noorigian, JV & Adler, CH. Evaluation of alpha-synuclein immunohistochemical methods used by invited experts. *Acta neuropathologica* 116, 277-88 (2008).

16. DeJesus-Hernandez, M, Mackenzie, IR, Boeve, BF, Boxer, AL, Baker, M, Rutherford, NJ, Nicholson, AM, Finch, NA, Flynn, H, Adamson, J, Kouri, N, Wojtas, A, Sengdy, P, Hsiung, GY, Karydas, A, Seeley, WW, Josephs, KA, Coppola, G, Geschwind, DH, Wszolek, ZK, Feldman, H, Knopman, DS, Petersen, RC, Miller, BL, Dickson, DW, Boylan, KB, Graff-Radford, NR & Rademakers, R. Expanded GGGGCC hexanucleotide repeat in noncoding region of C9ORF72 causes chromosome 9p-linked FTD and ALS. *Neuron* 72, 245-56 (2011).
17. Arai, T, Ikeda, K, Akiyama, H, Nonaka, T, Hasegawa, M, Ishiguro, K, Iritani, S, Tsuchiya, K, Iseki, E, Yagishita, S, Oda, T & Mochizuki, A. Identification of amino-terminally cleaved tau fragments that distinguish progressive supranuclear palsy from corticobasal degeneration. *Ann Neurol* 55, 72-9 (2004).
18. Greenberg, SG & Davies, P. A preparation of Alzheimer paired helical filaments that displays distinct tau proteins by polyacrylamide gel electrophoresis. *Proc Natl Acad Sci U S A* 87, 5827-31 (1990).
19. Gibb, WR, Luthert, PJ & Marsden, CD. Corticobasal degeneration. *Brain* 112 (Pt 5), 1171-92 (1989).
20. Hassan, A, Whitwell, JL, Boeve, BF, Jack, CR, Jr., Parisi, JE, Dickson, DW & Josephs, KA. Symmetric corticobasal degeneration (S-CBD). *Parkinsonism Relat Disord* 16, 208-14 (2010).
21. Kouri, N, Murray, ME, Hassan, A, Rademakers, R, Uitti, RJ, Boeve, BF, Graff-Radford, NR, Wszolek, ZK, Litvan, I, Josephs, KA & Dickson, DW. Neuropathologic features of corticobasal degeneration presenting as corticobasal syndrome or Richardson syndrome. *Brain : a journal of neurology* 134, 3264-75 (2011).
22. Josephs, KA, Petersen, RC, Knopman, DS, Boeve, BF, Whitwell, JL, Duffy, JR, Parisi, JE & Dickson, DW. Clinicopathologic analysis of frontotemporal and corticobasal degenerations and PSP. *Neurology* 66, 41-8 (2006).
23. Williams, DR, Lees, AJ, Wherrett, JR & Steele, JC. J. Clifford Richardson and 50 years of progressive supranuclear palsy. *Neurology* 70, 566-73 (2008).
24. Mizusawa, H, Yen, SH, Hirano, A & Llana, JF. Pathology of the dentate nucleus in progressive supranuclear palsy: a histological, immunohistochemical and ultrastructural study. *Acta neuropathologica* 78, 419-28 (1989).
25. Ishizawa, K, Lin, WL, Tiseo, P, Honer, WG, Davies, P & Dickson, DW. A qualitative and quantitative study of glumose degeneration in progressive supranuclear palsy. *J Neuropathol Exp Neurol* 59, 513-24 (2000).
26. Fukutani, Y, Nakamura, I, Matsubara, R, Kobayashi, K & Isaki, K. Pathology of the cerebellar dentate nucleus in sporadic olivopontocerebellar atrophy: a morphometric investigation. *J Neurol Sci* 137, 103-8 (1996).
27. Iwasaki, Y, Mori, K, Ito, M, Mimuro, M & Yoshida, M. [An autopsied case of progressive supranuclear palsy, initially diagnosed as spinocerebellar degeneration with severe olivopontocerebellar involvement]. *Rinsho shinkeigaku = Clinical neurology* 51, 756-60 (2011).
28. Dickson, DW. Neuropathologic differentiation of progressive supranuclear palsy and corticobasal degeneration. *J Neurol* 246 Suppl 2, I16-15 (1999).
29. Komori, T, Arai, N, Oda, M, Nakayama, H, Mori, H, Yagishita, S, Takahashi, T, Amano, N, Murayama, S, Murakami, S, Shibata, N, Kobayashi, M, Sasaki, S & Iwata, M. Astrocytic plaques and tufts of abnormal fibers do not coexist in corticobasal degeneration and progressive supranuclear palsy. *Acta neuropathologica* 96, 401-8 (1998).

30. Tolnay, M, Spillantini, MG, Goedert, M, Ulrich, J, Langui, D & Probst, A. Argyrophilic grain disease: widespread hyperphosphorylation of tau protein in limbic neurons. *Acta neuropathologica* 93, 477-84 (1997).
31. Togo, T, Cookson, N & Dickson, DW. Argyrophilic grain disease: neuropathology, frequency in a dementia brain bank and lack of relationship with apolipoprotein E. *Brain Pathol* 12, 45-52 (2002).
32. Jicha, GA, Petersen, RC, Knopman, DS, Boeve, BF, Smith, GE, Geda, YE, Johnson, KA, Cha, R, Delucia, MW, Braak, H, Dickson, DW & Parisi, JE. Argyrophilic grain disease in demented subjects presenting initially with amnesic mild cognitive impairment. *J Neuropathol Exp Neurol* 65, 602-9 (2006).
33. Snowden, JS, Rollinson, S, Thompson, JC, Harris, JM, Stopford, CL, Richardson, AM, Jones, M, Gerhard, A, Davidson, YS, Robinson, A, Gibbons, L, Hu, Q, DuPlessis, D, Neary, D, Mann, DM & Pickering-Brown, SM. Distinct clinical and pathological characteristics of frontotemporal dementia associated with C9ORF72 mutations. *Brain : a journal of neurology* 135, 693-708 (2012).
34. Yokota, O, Davidson, Y, Bigio, EH, Ishizu, H, Terada, S, Arai, T, Hasegawa, M, Akiyama, H, Sikkink, S, Pickering-Brown, S & Mann, DM. Phosphorylated TDP-43 pathology and hippocampal sclerosis in progressive supranuclear palsy. *Acta neuropathologica* 120, 55-66 (2010).
35. Fujishiro, H, Uchikado, H, Arai, T, Hasegawa, M, Akiyama, H, Yokota, O, Tsuchiya, K, Togo, T, Iseki, E & Hirayasu, Y. Accumulation of phosphorylated TDP-43 in brains of patients with argyrophilic grain disease. *Acta neuropathologica* 117, 151-8 (2009).
36. Uryu, K, Nakashima-Yasuda, H, Forman, MS, Kwong, LK, Clark, CM, Grossman, M, Miller, BL, Kretschmar, HA, Lee, VM, Trojanowski, JQ & Neumann, M. Concomitant TAR-DNA-binding protein 43 pathology is present in Alzheimer disease and corticobasal degeneration but not in other tauopathies. *J Neuropathol Exp Neurol* 67, 555-64 (2008).
37. Hu, WT, Josephs, KA, Knopman, DS, Boeve, BF, Dickson, DW, Petersen, RC & Parisi, JE. Temporal lobar predominance of TDP-43 neuronal cytoplasmic inclusions in Alzheimer disease. *Acta neuropathologica* 116, 215-20 (2008).
38. Josephs, KA, Whitwell, JL, Knopman, DS, Hu, WT, Stroh, DA, Baker, M, Rademakers, R, Boeve, BF, Parisi, JE, Smith, GE, Ivnik, RJ, Petersen, RC, Jack, CR, Jr. & Dickson, DW. Abnormal TDP-43 immunoreactivity in AD modifies clinicopathologic and radiologic phenotype. *Neurology* 70, 1850-7 (2008).
39. Josephs, KA, Stroh, A, Dugger, B & Dickson, DW. Evaluation of subcortical pathology and clinical correlations in FTL-DU subtypes. *Acta neuropathologica* 118, 349-58 (2009).
40. Amador-Ortiz, C, Lin, WL, Ahmed, Z, Personett, D, Davies, P, Duara, R, Graff-Radford, NR, Hutton, ML & Dickson, DW. TDP-43 immunoreactivity in hippocampal sclerosis and Alzheimer's disease. *Ann Neurol* 61, 435-45 (2007).

Chapter 4

Novel mutation in *MAPT* exon 13 (p.N410H) causes corticobasal degeneration

4.1. Abstract

In order to determine the frequency of microtubule associated protein tau gene (*MAPT*) mutations and rare variants in CBD, we performed a systematic sequence analysis of *MAPT* coding and 3' untranslated region (3'UTR) in a large cohort of autopsy-confirmed CBD patients ($n = 109$). This identified a novel *MAPT* mutation in exon 13, p.N410H, in a case that is neuropathologically indistinguishable from sporadic CBD. On immunoblot, the p.N410H mutation carrier had the same insoluble tau profile as seen in CBD. Additionally, tau expression analysis in brain tissue found a significant increase in the 4R/3R tau mRNA ratio ($P=0.04$), indicating that p.N410H disrupts tau isoform homeostasis. Biochemically, recombinant tau protein with p.N410H showed a marked increase in tau filament formation compared to wild-type tau ($P<0.001$), had a 19.2% decrease in rate of microtubule assembly ($P<0.05$), and a 10.3% reduction in the extent of total microtubule polymerization ($P<0.01$). Sequence analysis of the complete *MAPT* 3'UTR in autopsy-confirmed CBD cases further identified two rare variants with nominally significant association with CBD. An ATC nucleotide insertion ("MAPTv8") was found in 4.6% of CBD patients compared to 1.2% of controls ($P=0.031$, OR=3.71), and rs186977284 in 4.6% CBD patients, but only 0.9% of controls ($P=0.04$, OR=3.58). Rs186977284 was also present in 2.7% of a large cohort of autopsy-confirmed PSP patients ($n = 566$) and only 0.9% of an additional control series ($P=0.034$, OR=3.08), extending the association to PSP. Our findings show that mutations in *MAPT* can cause CBD and *MAPT* non-coding variants may increase the risk of complex 4R tauopathies.

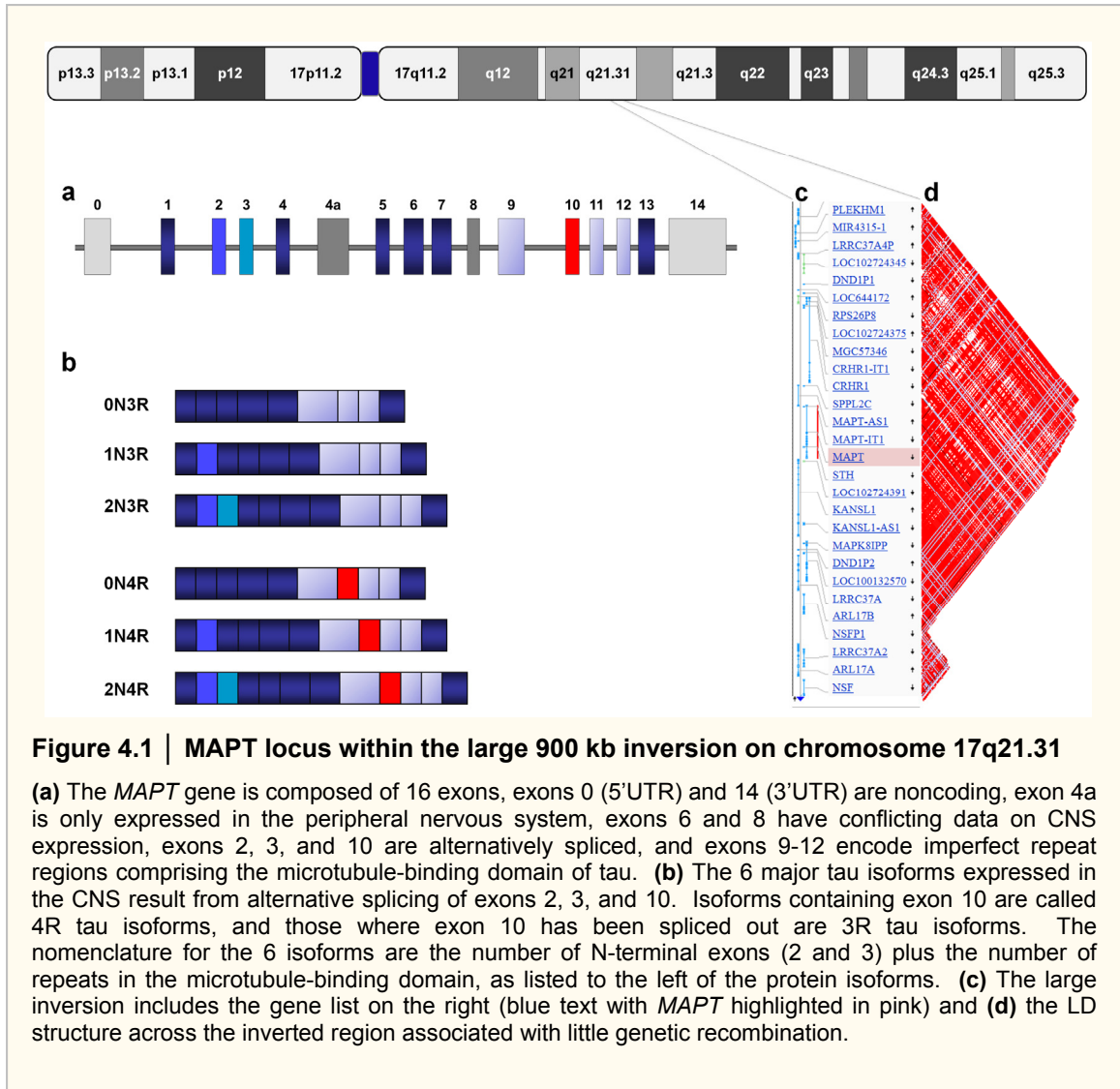
4.2. Introduction

Corticobasal degeneration (CBD) is a sporadic neurodegenerative disorder pathologically classified as a primary tauopathy due to neuronal and glial aggregates of hyperphosphorylated microtubule-associated protein tau throughout the brains of these patients.¹ CBD is associated with focal cortical atrophy and because of this, patients can

present with a wide range of clinical syndromes depending on the location of the most marked atrophy. Most commonly, CBD patients present with corticobasal syndrome, Richardson syndrome, or frontotemporal dementia.² Progressive supranuclear palsy (PSP) is a related tauopathy that has some overlapping clinical and pathologic features with CBD, yet represents a distinct disease entity.³⁻⁵

Microtubule associated protein tau encoded by the *MAPT* gene binds to microtubules and is important for maintaining neuronal morphology and function. Mutations in *MAPT* disrupt tau splicing and/or the binding of tau to microtubules, often increase the aggregation properties of tau, and lead to frontotemporal dementia with parkinsonism (FTDP-17), unequivocally demonstrating that tau dysfunction is sufficient to cause neurodegeneration.⁶⁻⁸ Though there are rare familial cases,⁹ CBD and PSP are considered sporadic disorders. Yet, despite their sporadic nature, common genetic variant at the *MAPT* locus are a strong risk factor for the development of CBD and PSP. Conrad, *et al.* reported an association of risk of PSP with a dinucleotide repeat located in intron 9 of *MAPT*.¹⁰ Subsequently, this association was extended to include CBD and shown to include multiple polymorphisms in complete linkage disequilibrium that are part of the extended *MAPT* H1 haplotype.¹¹⁻¹⁵ Findings from the recently completed PSP genome-wide association study confirmed that the H1 *MAPT* haplotype confers risk for developing PSP ($P=1.5 \times 10^{-116}$, OR=5.5).¹⁶

In this study, we performed systematic *MAPT* sequencing analyses in a large cohort of pathologically-confirmed CBD. To understand the role of rare variants, we performed sequence analysis of the *MAPT* coding region in 109 CBD patients as well as the entire ~4kb 3'UTR in 85 CBD patients. Excluding H1/H2-defining polymorphisms, a subset of 3'UTR variants were further tested for association in CBD and PSP case-control series.



4.3. Materials and methods

4.3.1. Subjects and samples

Patients with a neuropathologic diagnosis of corticobasal degeneration¹ and frozen tissue were identified from the Mayo Clinic Jacksonville brain bank between 1999 and 2010. Control series were ascertained at the Mayo Clinic Florida (MCF) and Mayo Clinic Arizona (MCA) and were diagnosed by a neurologist to be cognitively normal at the time of blood draw.

4.3.2. DNA sequencing

DNA from 109 CBD cases was screened for mutations in *MAPT* for all CNS-expressed coding exons (exons 1-7 and 9-13). To determine the genetic variability in the *MAPT* 3'UTR, 69 CBD cases homozygous for the *MAPT* H1 haplotype were further sequenced over the region encompassing ~4 kb of the *MAPT* 3'UTR (UCSC genome browser, chr17:44,101,538- 44,105,704, Feb. 2009 assembly) plus 200bp flanking the 3'UTR. Sixteen H1/H2 heterozygote CBD patients were also sequenced, but the presence of numerous insertion and deletion polymorphisms prohibited Sanger sequencing of the entire 3'UTR for these patients. Two individuals homozygous for *MAPT* H2 haplotype were included as a reference for haplotype-defining variants. PCR reactions of approximately 500bp fragments were performed in 15µl reactions in 384-well plates. PCR products were purified using AMPure (Agencourt Biosciences), then sequenced in both directions using the BigDye Terminator v3.1 Cycle Sequencing kit (Applied Biosystems, USA). Sequencing reactions were purified using CleanSEQ (Agencourt Biosciences) and analyzed on an ABI 3730 Genetic Analyzer (Applied Biosystems). Base calling, sequence alignments, and heterozygote detection were performed using Sequencher (Gene Codes).

4.3.3. Genotyping analysis

Genetic variants identified by sequence analysis were genotyped using MassArray iPLEX technology (Sequenom) and genotype calls were made using Typer 4.0 software following manufacturer's instructions. One H1/H2 haplotype-defining SNP, rs1052553, was included in the iPLEX SNP panel in order to use *MAPT* haplotype as a covariate in association analyses. The variants that did not multiplex in Sequenom assay design

(rs11331969, rs186977284, and rs75182761) were genotyped using custom Taqman SNP genotyping assays (Applied Biosystems), read on 7900HT Fast Real Time PCR system, and genotype calls were made using SDS v2.2 software.

4.3.4. Tissue sampling and neuropathologic assessment

Primary and association cortices, basal ganglia, diencephalon, brainstem and cerebellum were evaluated with tau immunohistochemistry as previously described.² Thioflavin S fluorescent microscopy was used to assess Alzheimer-type pathology, and haematoxylin and eosin (H&E) stained sections were used to evaluate neuronal loss and gliosis. For tau and TDP-43 immunohistochemistry, sections were processed using a DAKO Autostainer (Universal Staining System, Carpinteria, CA) using 3,3'-diaminobenzidine (DAB) as the chromogen and a phospho-tau antibody (CP13, mouse IgG1, 1:1000, kind gift of Peter Davies, Albert Einstein College of Medicine, Bronx, NY, USA), 3R tau antibody (RD3, Millipore, Temecula, CA), 4R tau antibody (RD4, Millipore, Temecula, CA), or a monoclonal phospho-TDP-43 antibody (ps409/410, 1:5000, Cosmobio Co., Tokyo, Japan). After immunostaining, the sections were counterstained with haematoxylin.

4.3.5. Recombinant tau purification

Recombinant tau was expressed and purified as previously described.¹⁷ Wild type and the p.N410H mutant 4R0N tau cDNA were cloned into pET30a and expressed in competent BL21 (DE3) cells. Briefly, overnight cultures were used to inoculate bulk media at 1/100, and these were grown to an OD (600) of 0.5 and induced by adding 0.5 mM IPTG for 2.5 hours. Cell pellets were collected, washed in 1X PBS and stored at -80°C. The cells were lysed with three freeze and thaw cycles, and the tau proteins were then purified by heating the lysates for 10 minutes at 80°C and isolating the tau proteins from clarified supernatants using ion exchange chromatography. The fractions containing tau proteins were then dialyzed overnight in 80 mM PIPES, 2mM MgCl₂ and 0.5mM EGTA at pH 6.8 with two buffer changes. These samples were further purified by HPLC C8 reverse phase chromatography if degraded fragments were detected following purification.¹⁸ The purity of the tau preparations was analyzed by SDS-polyacrylamide gel electrophoresis and Coomassie blue staining, and protein

concentrations were determined using the BCA protein assay kit with bovine serum albumin as a standard (Pierce, Rockford, IL).

4.3.6. Microtubule Assembly

Microtubule assembly with recombinant tau proteins was performed in a 96 well plate in a final volume of 100 μ l. Ice-cold tubulin at 1.5 mg/ml (30 μ M) (Cytoskeleton Inc.) was added to 0.12 mg/ml (3 μ M) of recombinant tau protein in assembly buffer (80 mM PIPES, 2 mM $MgCl_2$, 0.5 mM EGTA 1 mM GTP) also on ice and immediately transferred to a 96 well plate equilibrated to 37°C. The extent of microtubule assembly was monitored by turbidity assay per the manufacturer's recommendation, and the absorbance (optical density) was measured at 340 nm on a SpectraMax M5 Multi-Mode Microplate Readers (Molecular Devices, California). Reactions were run in quadruplicate, and this allowed both the rate and extent of microtubule polymerization to be assessed.

4.3.7. Tau filament formation

Polyglycosaminoglycan-induced tau aggregation reactions were performed as previously described.¹⁷ Briefly, 8 μ M of tau and 0.04 mg/ml of low molecular weight heparin or dextran sulfate were set up in 10 mM HEPES at pH 7.4, 100 mM NaCl. Samples were incubated at 37°C and analyzed at 30 and 90 minute time points. Tau filament polymerization was measured directly by adsorption of 10 μ l of reaction mixture onto a carbon/Formvar grid (EM Sciences Inc.) for 60 seconds and staining with 2% uranyl acetate for 60 seconds. Electron micrographs were captured using a Phillips EM208S electron microscope and camera. Tau filament length measurements and quantification were performed blinded to genotype by one analyzer using ImageScope software (version 11.2; Aperio Technologies). Each genotype had nine electron micrograph images captured from a set of predetermined grid regions per time point. This allowed for the number of tau filaments to be counted for each field, and their individual length and the total polymer mass could then be determined. Tau aggregation properties were confirmed independently using the diagnostic Thioflavin-S fluorescence which provides a measure of the cross β -sheet secondary structure that is formed as tau proteins polymerize into filaments.

4.3.8. Western blot

Sarkosyl insoluble protein fractions were extracted from frontal cortex of sporadic CBD cases and the p.N410H mutation carrier, samples were prepared and separated on 10% Tris-glycine gels (Invitrogen Life Technologies, USA), transferred to PVDF membrane, and immunoblotted as previously described.² The primary antibody used against phosphorylated tau was PHF-1 (1:1000, from Peter Davies, Albert Einstein College of Medicine, NY), which recognizes the C-terminal region of phosphorylated tau (p-Ser396/p-Ser404) and anti-mouse IgG secondary antibody (1:5000).

4.3.9. Tau Quantitative Real-Time PCR

Total RNA was extracted from gray matter of the frontal cortex with the RNeasy Plus Mini Kit (Qiagen, USA) and RNA integrity was checked on an Agilent 2100 Bioanalyzer (Agilent Technologies, USA). The Power SYBR Green RNA-to-CT 1-Step RT-PCR kit (Invitrogen Life Technologies, USA) was used according to manufacturer protocol. Isoform-specific primers were used for 3R tau (F: AGGCGGGAAGGTGCAAATAG; R: TCCTGGTTTATGATGGATGTT) and 4R tau (F: GAAGCTGGATCTTAGCAACG; R: GACGTGTTTGATATTATCCT).¹⁹ Total RNA (30 ng) was used in 10 μ l reactions and qRT-PCR was performed on a 7900HT Fast Real-Time PCR System (Applied Biosystems) and data were imported and analyzed in SDS v2.2. All samples were run in triplicate and tau mRNA 4R:3R tau ratios in the p.N410H carrier were compared to a pathologically normal individual. Relative expression was determined using the $\Delta\Delta C_t$ method after normalization to the geometric mean of GAPDH and RPLPO expression.

4.3.10. Statistical analysis

All genetic association analyses were performed with PLINK, open-source whole genome association analysis toolset: <http://pngu.mgh.harvard.edu/purcell/plink/>.²⁰ Association of *MAPT* variants with CBD or PSP was tested under an additive model adjusting for age at death, sex, and for the number of *MAPT* H1 haplotypes (0, 1, or 2). Statistical analyses of all functional studies were performed using Student's t-test.

4.4. Results

4.4.1. Sequencing and association studies of MAPT in CBD

Sequence analysis of the entire coding region of the *MAPT* gene in 109 pathology-confirmed CBD cases identified a novel coding *MAPT* mutation in exon 13, c.1228A>C (relative to *MAPT* isoform 2 NM_005910) predicted to result in p.N410H substitution (**Figure 4.2**). This mutation has not been previously reported in dbSNP or the 1000 Genomes databases and genotyping using a custom-designed ABI Taqman assay excluded this mutation from 1224 healthy controls and 566 PSP cases. Sequence analysis of the *MAPT* coding region additionally identified the rare p.A152T polymorphism in *MAPT* exon 7 in one pathologically-confirmed CBD case, which has been previously reported.²¹

Sequence analysis of *MAPT* 3'UTR in 85 CBD cases identified 31 genetic variants of which 27 were known SNPs, four were novel SNPs, and 21/27 variants were *MAPT* H1/H2 haplotype-defining SNPs. Of the remaining six non-H1/H2 SNPs, three were common and occurred only on the H1 haplotype, and three were rare variants in the CBD population (minor allele frequency, MAF<5%). Two of the four novel variants were rare (CBD MAF<5%), identified in five CBD patients or less and the other two novel variants were identified in only one CBD case each. To determine whether any of the non-H1/H2 defining SNPs in the *MAPT* 3'UTR were implicated in CBD risk, we genotyped these 10 variants in 643 controls and a total of 108 autopsy-confirmed CBD patients, including the 85 patients we used for sequencing (**Table 4.1**). The variants are listed in **Table 4.2** and genotype counts and frequencies are provided in **Table 4.3**.

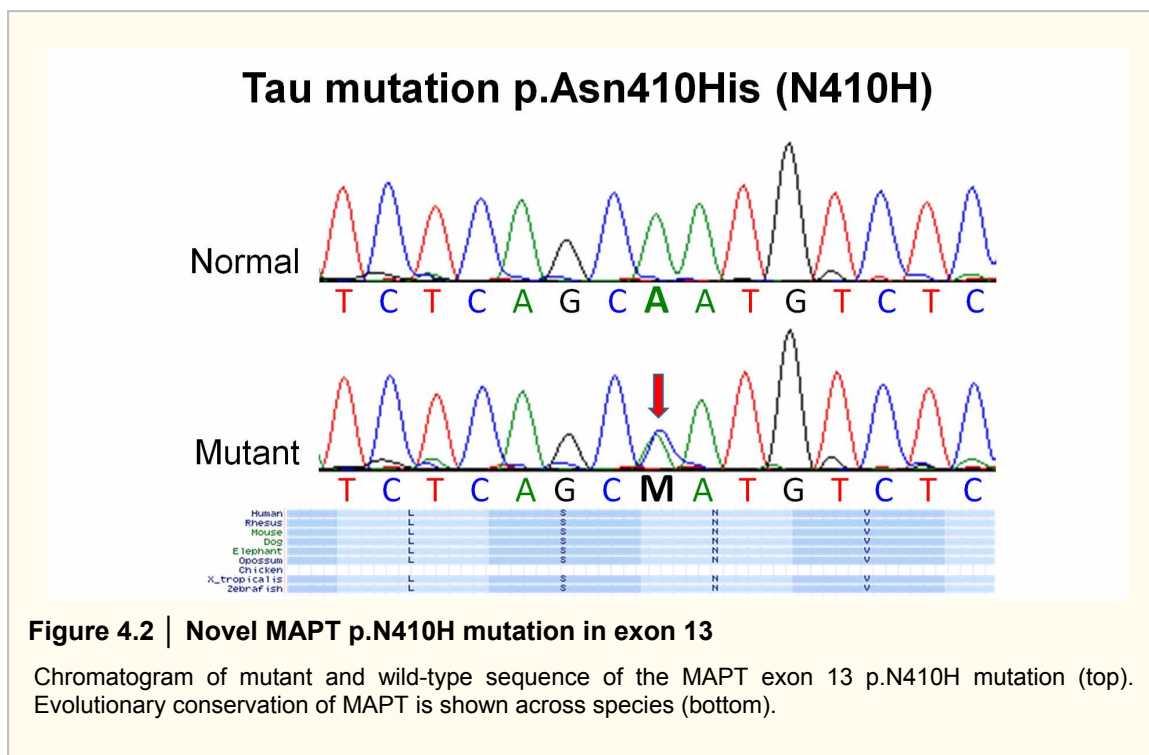


Table 4.1 | Cohort description

Cohort	N	Age ^a (years)	Females (%)	Sample Source
CBD cases	109	69.7 ± 8.7	47.7	Mayo Clinic Florida
Control series 1	643	73.7 ± 11.8	52.3	Mayo Clinic Florida
PSP cases	566	75.1 ± 7.9	48.2	Mayo Clinic Florida
Control series 2	660	70.4 ± 12.0	58.3	Mayo Clinic Arizona

^aAge is shown as the mean ± standard deviation representing the age at death of cases in the autopsy-confirmed CBD and PSP cohorts and the age at blood draw of subjects in the control series. Subjects included in the control series were healthy non-Hispanic white individuals in whom clinical history of neurological disease and cognitive impairment were excluded. Subjects from all cohorts agreed to be in the study and biological samples were obtained after informed consent with ethical committee approval from the respective institution.

When controlling for *MAPT* haplotype (using rs1052553), the common variants that occur on the H1 haplotype did not show association with CBD. In contrast, two of the rare variants, an ATC insertion (“MAPTv8”; chr17: 44104155:44104157; UCSC Genome Browser February 2009 (GRCh37/hg19) assembly) and rs186977284 showed nominally significant association with CBD as assessed by logistic regression analysis using an additive model with age, sex, and number of H1 alleles as covariates (**Table 4.2**). The effects observed for the two variants were similar, with overlapping odds ratio (OR) and 95% confidence intervals (95% CI), indicating an increased risk of CBD in the presence

of their minor allele. Although the MAPTv8 and rs186977284 association with CBD does not surpass the significance threshold for multiple testing correction, MAPTv8 was present in 4.6% of CBD compared to 1.2% frequency in Control Series 1 ($P = 0.031$, OR = 3.71) and rs186977284 was present in 4.6% CBD patients compared to 0.9% frequency in Control Series 2 ($P = 0.045$, OR = 3.58). To provide additional evidence for the involvement of these two non-coding variants in tauopathies, we next tested for association in 566 autopsy-confirmed PSP patients and Control Series 2 consisting of 659 individuals. Logistic regression analysis using an additive model with age, sex, and number of H1 alleles as covariates found rs186977284 to also associate with PSP (OR = 3.07, 95% CI = 1.08-8.71, $P = 0.035$), but MAPTv8 did not show evidence of an association with PSP (**Table 4.2**).

Table 4.2 Description of variants in the 3'UTR of <i>MAPT</i> and logistic regression results for association test with CBD and PSP						
Variant name	Position	Major allele	Minor allele	dbSNP MAF	CBD vs Control Series 1	
					OR (95% CI)	P-value
MAPTv4	44101605:44101607	AAT	-	NA	2.52 (0.22-28.28)	0.454
rs5820605	44102682:44102683	-	T	NA	0.88 (0.60-1.29)	0.499
rs16940802	44103704	G	A	0.050	0.58 (0.20-1.69)	0.318
MAPTv7	44103803:44103804	CT	-	NA	NA	NA
MAPTv8	44104155:44104157	-	ATC	NA	3.71 (1.12-12.25)	0.031
rs11331969	44104616:44104617	-	G	NA	0.94 (0.67-1.33)	0.734
rs186977284	44104972	T	C	NA	3.58 (1.03-12.43)	0.045
MAPTv11	44105107	T	C	NA	NA	NA
rs114213384	44105635	A	G	0.025	1.43 (0.27-7.49)	0.680
rs7521	44105395	G	A	0.429	1.24 (0.90-1.70)	0.193
					PSP vs Control Series 2	
Variant name	Position	Major allele	Minor allele	dbSNP MAF	OR (95% CI)	P-value
MAPTv8	44104155:44104157	-	ATC	NA	2.39 (0.38-15.17)	0.356
rs186977284	44104972	T	C	NA	3.07 (1.08-8.71)	0.035

Chromosome position is relative to the UCSC Genome Browser February 2009 (GRCh37/hg19) assembly. The dbSNP minor allele frequency (MAF) based on the 1000 genomes project (NA, not available). Logistic regression analyses were performed using an additive model with age, sex, and number of H1 haplotype alleles as covariates. *MAPTv7* and *MAPTv11* were not identified in controls precluding statistical analyses on these variants.

Table 4.3 | Genotype counts and frequencies for MAPT 3'UTR variants in CBD, PSP, Control Series 1, and Control Series 2.

Variant name	CBD			Control Series 1		
	22 (%)	12 (%)	11 (%)	22 (%)	12 (%)	11 (%)
rs1052553 ^a	0 (0)	17 (15.7)	91 (84.3)	34 (5.3)	234 (36.6)	372 (58.1)
MAPTv4	0 (0)	1 (0.9)	106 (99.1)	0 (0)	2 (0.3)	639 (99.7)
rs5820605	7 (6.5)	43 (40.2)	57 (53.3)	105 (16.4)	315 (49.1)	221 (34.5)
rs16940802	0 (0)	4 (3.7)	104 (96.3)	0 (0)	38 (5.9)	604 (94.1)
MAPTv7	0 (0)	1 (0.9)	107 (99.1)	0 (0)	0 (0)	642 (0)
MAPTv8	0 (0)	5 (4.6)	103 (95.4)	0 (0)	8 (1.2)	634 (98.8)
rs11331969	7 (6.4)	28 (25.7)	74 (67.9)	65 (10.3)	123 (19.4)	446 (70.3)
rs186977284	0 (0)	5 (4.6)	104 (95.4)	0 (0)	6 (0.9)	632 (99.1)
MAPTv11	0 (0)	1 (0.9)	107 (99.1)	0 (0)	0 (0)	643 (0)
rs75182761	0 (0)	1 (0.9)	107 (99.1)	0 (0)	7 (1.1)	636 (98.9)
rs7521	38 (34.9)	49 (45.0)	22 (20.2)	118 (18.4)	324 (50.4)	201 (31.3)
Variant name	PSP			Control Series 2		
	22 (%)	12 (%)	11 (%)	22 (%)	12 (%)	11 (%)
MAPTv8	0 (0)	5 (0.9)	561 (99.1)	0 (0)	2 (0.3)	658 (99.7)
rs186977284	0 (0)	15 (2.7)	551 (97.3)	0 (0)	6 (0.9)	654 (99.1)

^aH1/H2 haplotype-defining SNP used as a covariate in logistic regression analyses

4.4.2. p.N410H MAPT mutation in pathologically-confirmed CBD

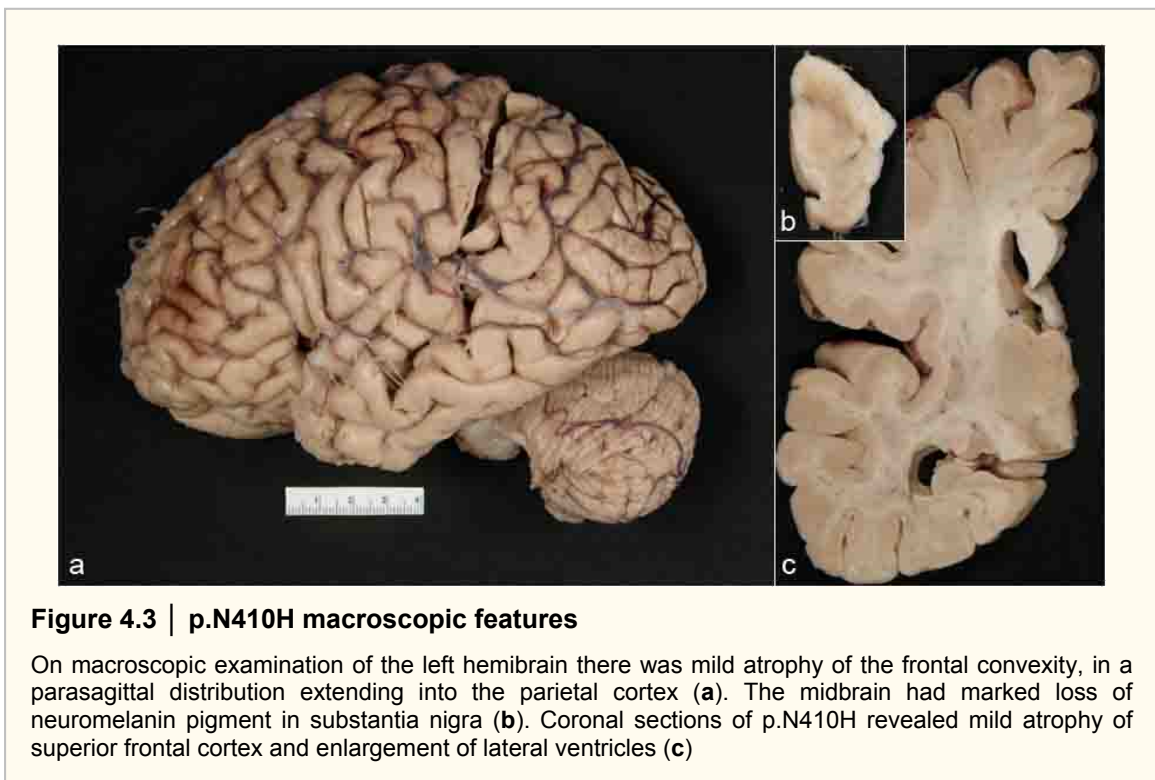
4.4.2.1. Clinical history

The female patient carrying this mutation had an age at onset of 63 years, with the chief complaint being forgetfulness and problems with mood and memory. There was a positive family history for dementia in an aunt. On initial neurological examination one year after onset, she had mild cognitive impairment and parkinsonism. She later developed a flat affect. Her movements became slowed; she lost facial expression; and her voice softened. Three years after disease onset, memory impairment became more severe, and she began falling. The following year, she had gait freezing, and she became aggressive, with increasingly poor insight, concentration, and comprehension. On examination, she was abulic and her gait was unsteady and stooped with small steps. Ocular exam was noted for abnormal saccades and smooth pursuit. Three years into the disease, she was practically aphonic with impaired eye movement, and some postural hand tremor. She developed obsessive use of hands either picking her nose or scratching her hair. A year later, she became mute and did not answer questions or

follow commands. She had hypokinesia and progressive rigidity on the left more than right side. Behavioral dyscontrol progressed and she became incontinent of urine. Her differential diagnosis was progressive supranuclear palsy syndrome versus corticobasal syndrome. She died at age 67 after a four year disease course.

4.4.2.2. Neuropathology

The fixed brain weighed 1000 grams. Macroscopic examination revealed mild atrophy of the frontal convexity (**Figure 4.3a**) and the midbrain showed marked loss of pigment in the substantia nigra (**Figure 4.3b**). On coronal sections there was mild atrophy of the superior frontal cortex (**Figure 4.3c**) and slight enlargement of frontal horn of the lateral ventricle. On microscopic examination, tau immunohistochemistry revealed fine, granular inclusions, or tau pretangles, most notably in small neurons of layer II. There was a high density of 4R tau-positive and argyrophilic astrocytic plaques throughout affected cortical regions (**Figure 4.4a, b**) and accompanied by thread-like tau pathology in both gray and white matter (**Figure 4.4d, e**), basal ganglia, and thalamus. Superior frontal gyrus had spongiosis, gliosis, and ballooned neurons (**Figure 4.4d**), most numerous in superior frontal and cingulate gyri.



The frontal white matter had myelin staining pallor and patchy gliosis. Putamen and globus pallidus had numerous 4R tau-immunoreactive pretangles, astrocytic plaques, and thread-like processes. White matter structures, including anterior commissure, internal capsule, and pencil fibers in the putamen had tau positive thread-like processes and oligodendrocyte coiled bodies. Globus pallidus had neuronal loss and gliosis with hemosiderin-like pigment and axonal spheroids. Thalamus was histologically unremarkable on H&E, but had extensive tau-immunoreactive lesions in the anterior nuclei, medial and dorsal nuclei, as well as ventral lateral nuclei. Subthalamic nucleus had moderate neuronal loss and gliosis in the medial portion of the nucleus and to a lesser extent in the lateral portion of the nucleus. There were numerous tau neuronal pretangles in the amygdala, basal nucleus of Meynert, and hypothalamus. Amygdala also had many tau-immunoreactive threads, grains, astrocytes, and ballooned neurons. The substantia nigra had marked pigment loss due to dopaminergic nerve cell degeneration. There were significant tau-immunoreactive lesions in the pons and cerebellum, especially a high density of oligodendroglial coiled bodies and tau pretangles in the cerebellar dentate.

Immunohistochemistry for 3R tau was negative in superior frontal, motor, cingulate, temporal, and somatosensory cortices, posterior hippocampus, putamen, globus pallidus, amygdala, nucleus basalis, and hypothalamus. Neocortical and hippocampal sections were negative for senile plaques and neurofibrillary tangles by Thioflavin-S fluorescent microscopy, but there were numerous threads and grains in the CA1 and subiculum.

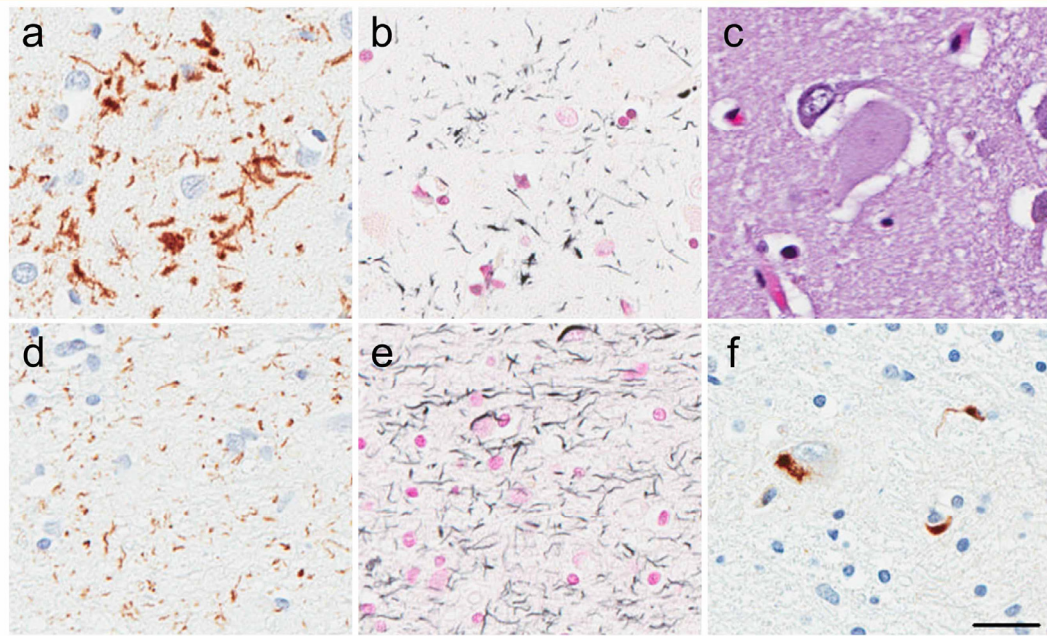


Figure 4.4 | Neuropathology of a CBD case with p.N410H MAPT mutation

Sections from motor cortex of p.N410H mutation carrier showed 4R tau-immunoreactive astrocytic plaques (a) and numerous threads in gray and white matter (d), both inclusion types were argyrophilic on Gallyas silver stain (b, e). Ballooned neurons were abundant in superior frontal cortex (c). Sections from the caudate nucleus of the p.N410H case had TDP-43 immunoreactive neuronal cytoplasmic and oligodendroglial cytoplasmic inclusions with thread-like processes (f). Bar=50µm

The p.N410H carrier had significant TDP-43 pathology. The severity and neuroanatomical distribution of tau and TDP-43-immunoreactivity are summarized in **Table 4.4**. There were scarce TDP-43 immunoreactive lesions in neocortical regions in contrast to sections from the basal ganglia, which had numerous TDP-43 neuronal cytoplasmic inclusions, especially in striatum, globus pallidus, and subthalamic nucleus. Additionally, TDP-43-immunoreactive oligodendroglial inclusions and thread-like processes were found in several brain regions, including striatum, diencephalon, midbrain tectum, and pontine tegmentum (**Figure 4.4f**). There were numerous tau-positive neurons in the granule cells of the dentate fascia and pyramidal layer, but no TDP-43 positive inclusions were observed. In a larger CBD cohort we screened a section of basal forebrain with TDP-43 immunohistochemistry and found TDP-43 pathology in 34/117 (29%) cases. Semiquantitative lesion scores in four sporadic CBD cases (Section 3.4.3.3.) revealed that TDP-43 inclusion density was greatest in caudate/putamen, globus pallidus, hypothalamus, subthalamic nucleus, substantia nigra,

and locus coeruleus (**Table 4.5**). There were no TDP-43 inclusions in the dentate gyrus of the hippocampus or subiculum. TDP-43 pathology burden in the p.N410H case did not significantly differ sporadic CBD (**Figure 4.5**). In contrast, CBD-OPCA had significantly more TDP-43 immunoreactive thread pathology compared to both sporadic CBD and p.N410H mutation carrier ($P < 0.05$). TDP-43 glial cytoplasmic inclusions were more numerous in CBD-OPCA compared to sporadic CBD ($P < 0.05$), but there was not a significant difference in oligodendroglial TDP-43 pathology when comparing p.N410H to CBD-OPCA.

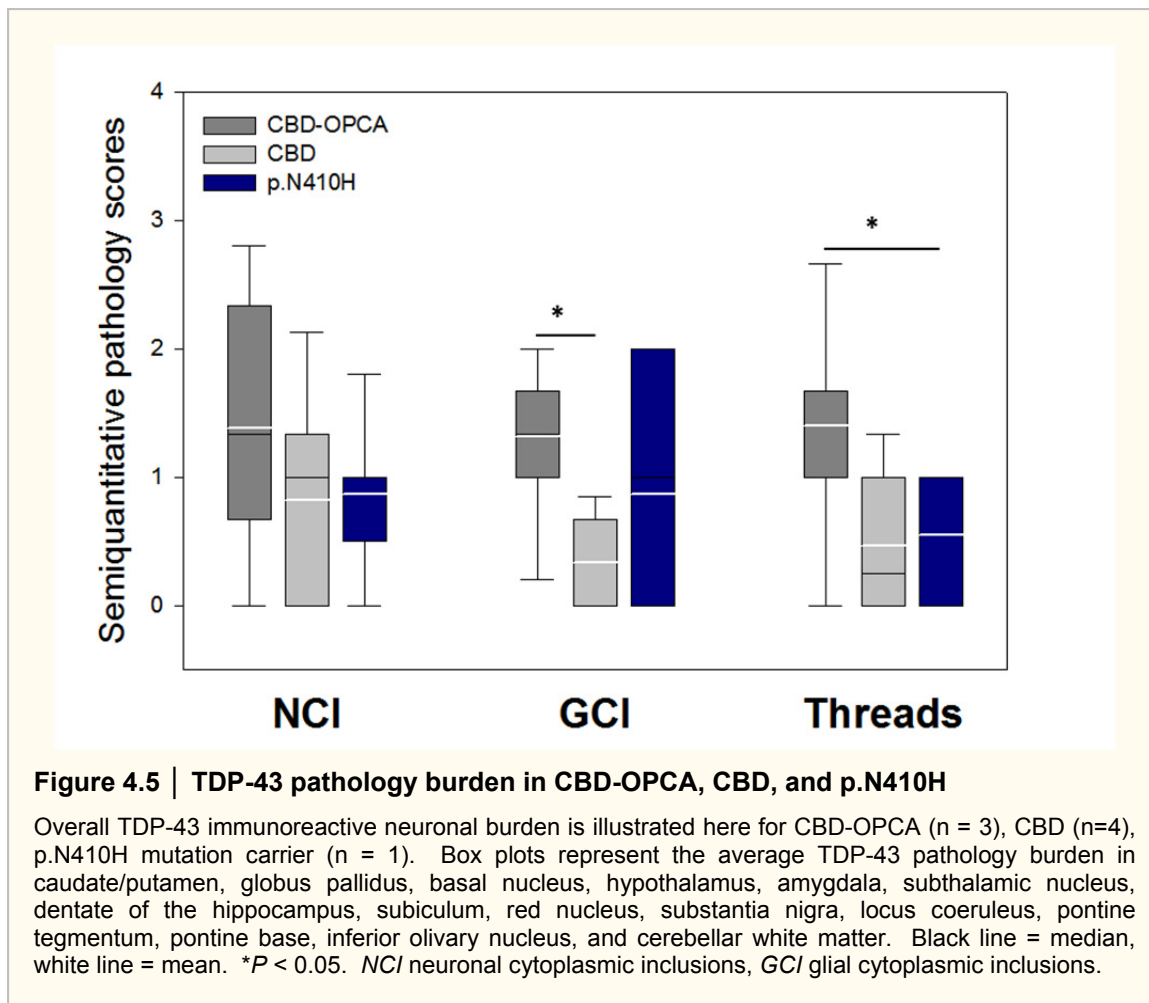
Table 4.4 | Semiquantitative assessment of tau and TDP-43 pathology in p.N410H case

Region	<u>Tau immunohistochemistry</u>				<u>TDP-43 Immunohistochemistry</u>		
	NFT & pre-NFT	Coiled bodies	Astrocytic plaques	Tau+ threads	NCI	GCI	TDP+ threads
Temporal cortex	+++	++	++	+++	0 - +	-	-
Superior frontal cortex	+++	++	+++	+++	+	+	-
Motor cortex	++	+	++	++	-	-	-
Caudate/putamen	+++	++	++	+++	+	+	+
Globus pallidus	++	+++	-	+++	+	++	+
Basal nucleus	++	+	-	+++	+	-	-
Hypothalamus	+++	+	-	+++	+	+	-
Ventral thalamus	+++	+	+	+++	+	++	+
Subthalamic nucleus	++	+	-	+++	++	++	+
Thalamic fasciculus	-	+	-	+++	-	-	-
Red nucleus	+	+	-	+	-	-	-
Substantia nigra	+	+	-	+++	+	+	+
Oculomotor complex	++	+	-	+++	-	+	-
Midbrain tectum	+++	+	+	+++	+	+	+
Locus coeruleus	+++	-	-	+++	+	-	+
Pontine tegmentum	+++	+	-	+++	+	++	+
Pontine base	++	++	-	+++	0 - +	-	-
Medullary tegmentum	NA	NA	NA	NA	NA	NA	NA
Inferior olive	NA	NA	NA	NA	NA	NA	NA
Dentate nucleus	++	-	-	+	-	-	-
Cerebellar white matter	-	++	-	+++	-	0 - +	-

NFT neurofibrillary tangles, *NCI* neuronal cytoplasmic inclusions, *GCI* glial cytoplasmic inclusions, *NA* not available

Table 4.5 | TDP-43 pathology severity and distribution separated by inclusion type in four sporadic CBD cases.

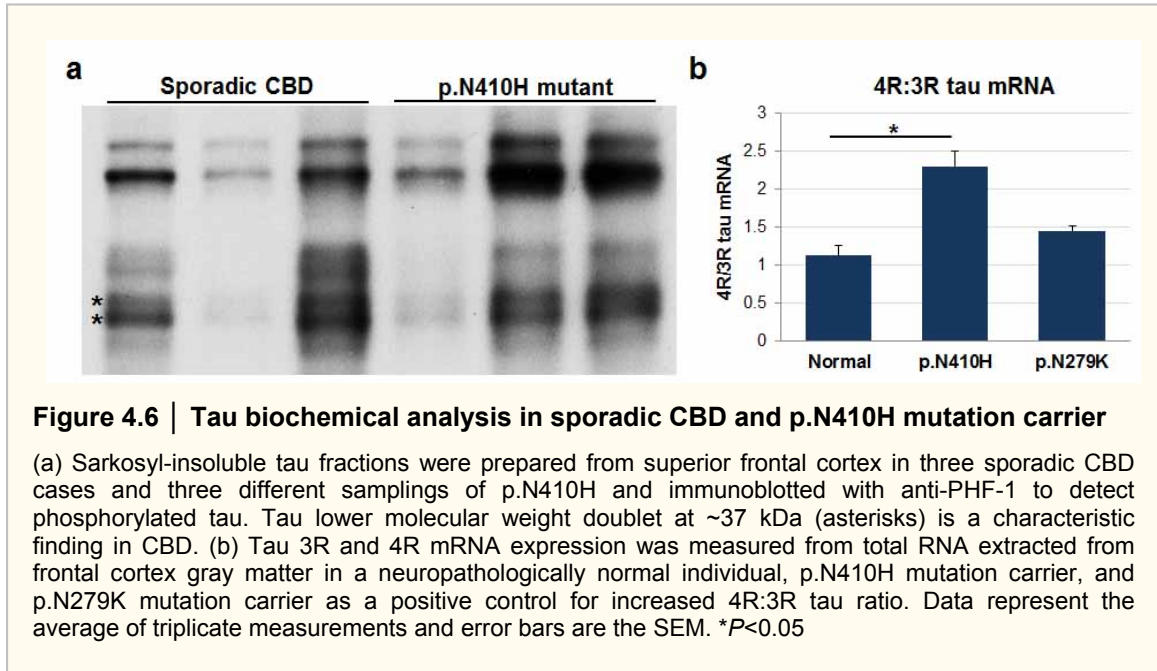
Region	Neuronal cytoplasmic inclusions				Glial cytoplasmic inclusions				TDP+ threads			
	CBD 1	CBD 2	CBD 3	CBD 4	CBD 1	CBD 2	CBD 3	CBD 4	CBD 1	CBD 2	CBD 3	CBD 4
Caudate/putamen	+	-	+	++	+	-	++	+	+	-	++	++
Globus pallidus	+++	-	+++	++	-	-	-	-	-	-	+	-
Basal nucleus	+	NA	+	+	+	NA	+	-	+	NA	++	+
Hypothalamus	+	NA	+++	-	+	NA	+	-	+	NA	+++	-
Amygdala	-	NA	-	+	-	NA	+	-	-	NA	-	-
Subthalamic nucleus	++	+++	++		-	-	++	+	-	-	+	-
Dentate of hippocampus	-	-	-	-	-	-	-	-	-	-	-	-
Subiculum	-	-	-	-	-	-	-	-	-	-	-	-
Red nucleus	+	+	+	+	-	+	-	-	+	+	+	-
Substantia nigra	+	++	+++	-	+	-	+	-	+		+	-
Locus coeruleus	+	+	++	NA	-	-	-	NA	-	-	+	NA
Pontine tegmentum	-	-	+	-	-	+	+	+	-	+	++	+
Pontine base	-	-	-	+	-	-	-	-	-	-	-	-
Inferior olive	-	-	NA	-	-	-	NA	-	-	-	NA	-
Cerebellar white matter	-	-	-	-	-	-	-	-	-	-	-	-



4.4.2.3. *In vivo* characterization of p.N410H mutant tau in patient brain samples

Immunoblot analysis was performed on sarkosyl-insoluble fractions prepared from superior frontal cortex in three sporadic CBD cases and the p.N410H mutation carrier (protein extracted from three different frontal cortex sections). Using the phosphorylation-dependent PHF-1 antibody, the typical doublet at 64 and 68 kDa composed of 4R tau was observed in all cases (**Figure 4.6a**). Most importantly, the p.N410H case showed the same lower molecular weight tau species, two bands at ~37 kDa, as those found in sporadic CBD that characterize the disease biochemically with regard to aggregated lower molecular weight tau species (**Figure 4.6a**, asterisks). To determine the effect of p.N410H on tau expression, quantitative real-time PCR for 4R tau and 3R tau was performed on total RNA isolated from the frontal cortices of a neuropathologically normal individual and the p.N410H carrier. A p.N279K mutation

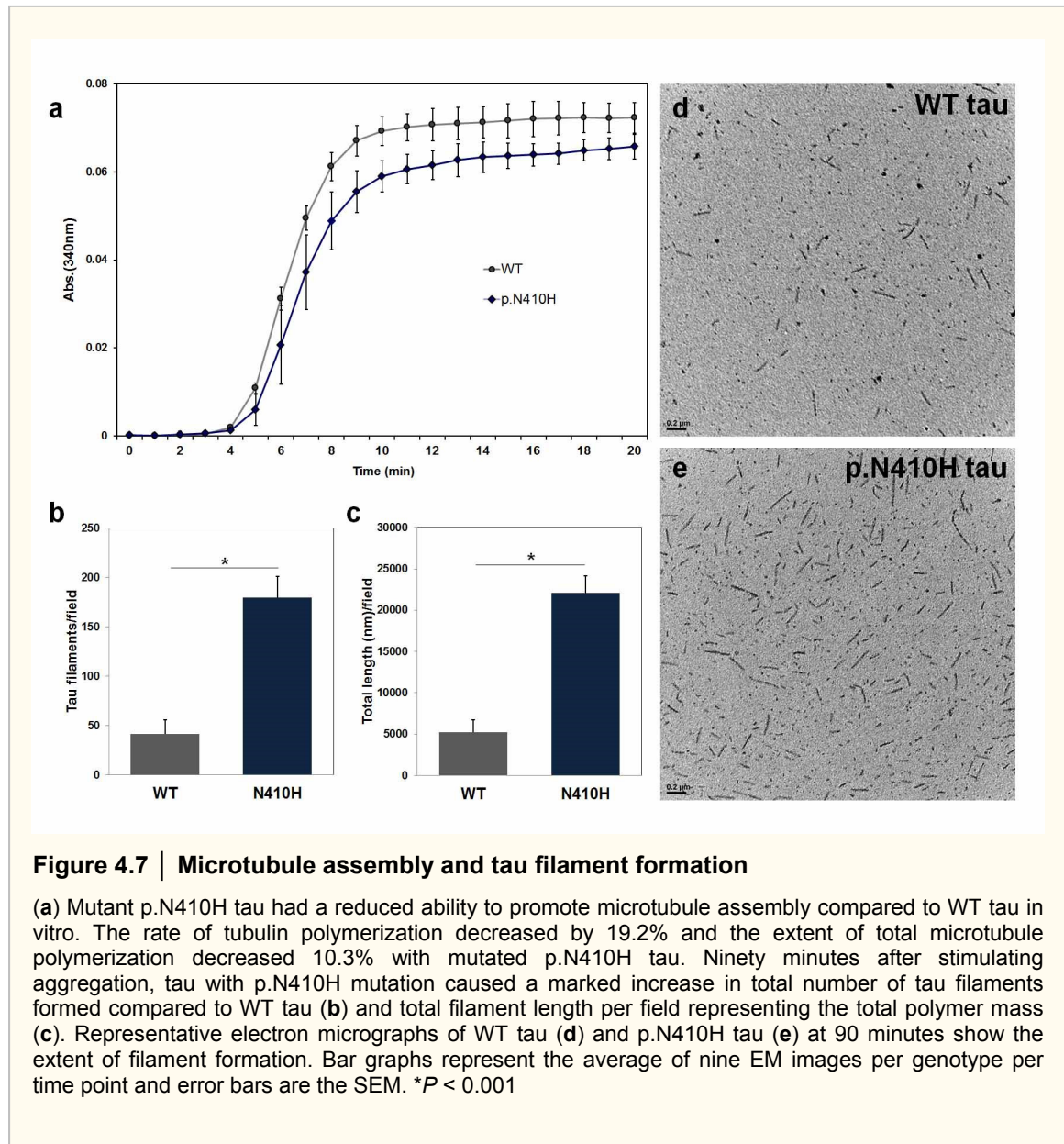
carrier was included as an enhancer of exon 10 splicing positive control. Expression analysis showed that the p.N410H mutation carrier had a significant increase in the 4R:3R tau mRNA ratio compared to the normal case ($P = 0.04$) (**Figure 4.6b**).



4.4.2.4. p.N410H tau has impaired ability to promote microtubule assembly

In order to assess the functional consequences of this increased 4R tau with the p.N410H mutation, the effects on tubulin polymerization and tau aggregation properties of mutant tau were compared to wild-type (WT) tau using *in vitro* assays. Microtubule assembly and tau filament formation assays were performed comparing WT and p.N410H tau in the 4R0N isoform which aggregates preferentially in CBD. Tau protein with the p.N410H mutation showed a decrease in its ability to promote microtubule assembly when compared to WT tau as both the rate and extent of tubulin polymerization were shown to be modestly, but significantly reduced (**Figure 4.7a**). The rate of tubulin polymerization decreased from $0.00032 \pm 0.000030 \Delta OD_{340}/min$ in WT tau to $0.000260 \pm 0.000043 \Delta OD_{340}/min$ ($P < 0.05$) when the p.N410H mutation was introduced, and the steady state levels of polymerized microtubules decreased from $0.0722 \pm 0.0028 \Delta OD_{340}$ to $0.0648 \pm 0.0031 \Delta OD_{340}$ ($P < 0.01$) with the p.N410H mutation. These represent a significant loss of normal tau function, as the rate of

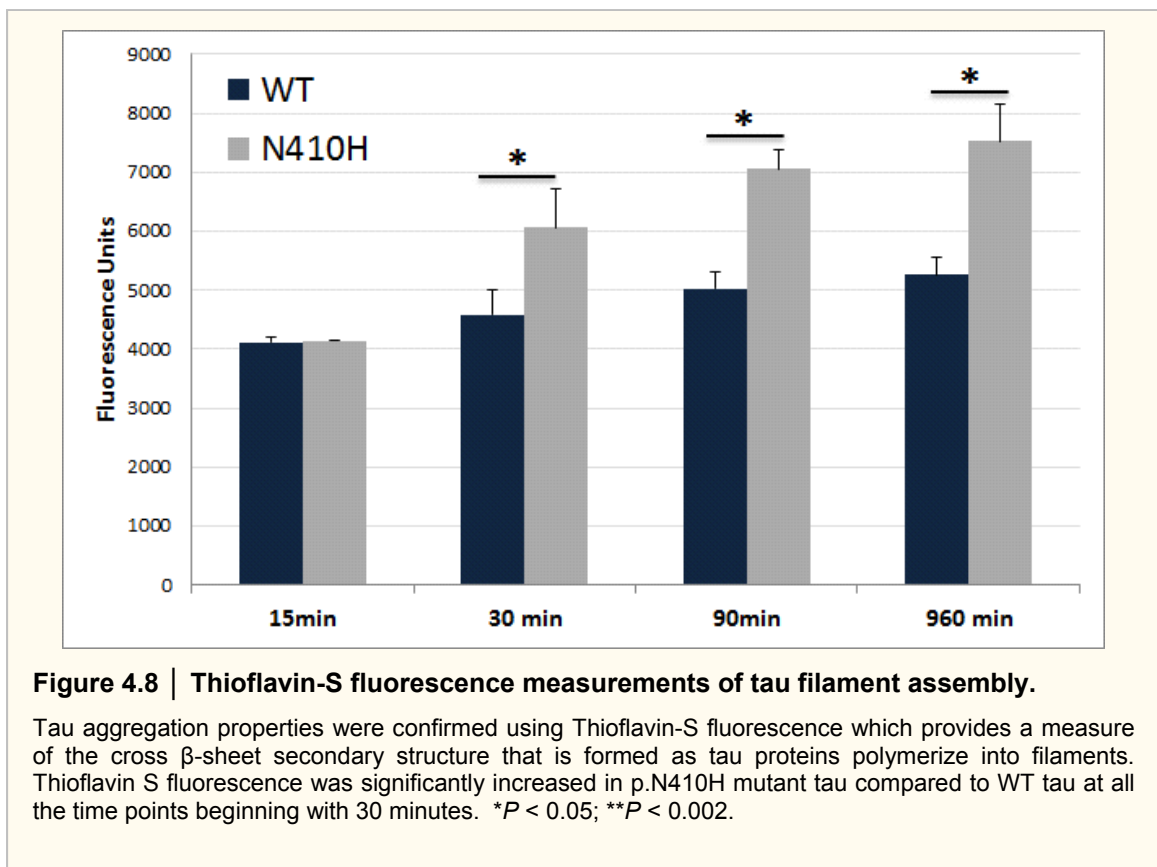
microtubule assembly decreased by 19.2% and the extent of total microtubule polymerization decreased 10.3% with mutated p.N410H tau.



4.4.2.5. p.N410H induces tau filament formation

The effects of the p.N410H mutation in the 4R0N isoform on tau filament assembly were also examined as this toxic gain of function is commonly observed in tauopathies, and it appears the tau aggregates themselves or their precursors are specifically toxic.²³ Upon inducing filament formation *in vitro*, the extent of p.N410H tau filament assembly after 30

minutes incubation was assessed directly using electron microscopy and observed to be statistically unchanged compared to WT tau with no effects on tau filament nucleation or total polymer mass per field observed (data not shown). However as shown in **Figure 4.7b, c**, by 90 minutes both the rate of nucleation and the extent of aggregation were markedly increased as the number of tau filaments observed per field increased from 41 ± 14 to 179 ± 21 ($P < 0.001$) when the p.N410H mutation was introduced and the total tau filament length per field increased from 5200 ± 1540 nm/field to 22110 ± 2060 nm/field ($P < 0.001$). Representative electron micrographs of WT tau (**Figure 4.7d**) and p.N410H tau (**Figure 4.7e**) at 90 minutes illustrate the extent of tau filament formation. These p.N410H filament assembly effects appeared to be largely nucleation driven as the average filament length was unchanged between WT (126 ± 36 nm) and p.N410H tau (123 ± 50 nm) at the 90 minute time point. These large increases in tau aggregation with the p.N410H mutation were supported by data collected using Thioflavin S fluorescence as a measure of tau folding into fibrillogenic forms (**Figure 4.8**).



4.5. Discussion

In a cohort of autopsy-confirmed CBD patients, we report the identification of a patient with a novel *MAPT* mutation in exon 13, p.N410H, located at a highly conserved amino acid residue. The only mention of family history of neurological disease was dementia in an aunt, and although we were unable to test other family members for segregation, 1224 normal controls and 566 PSP cases, and genome databases were all negative for p.N410H. We showed that sporadic CBD and p.N410H have the same neuropathologic features and aggregated tau protein species on immunoblot analysis, further illustrating the similarities between p.N410H and sporadic CBD. To the best of our knowledge, this is the first case meeting neuropathologic diagnostic criteria for CBD harboring a *MAPT* mutation.

Our *in vivo* and *in vitro* studies of p.N410H strongly support the pathogenic nature of this novel mutation. We showed that the p.N410H *MAPT* mutation in exon 13 disrupts tau alternative splicing, as evidenced by a more than two-fold increase in the 4R/3R tau mRNA ratio compared to a normal individual. Comparably, the p.E342V exon 12 tau mutation has also been shown to increase 4R tau mRNA,²⁴ demonstrating that it is possible to alter 3R and 4R tau mRNA levels through a mutation located outside of exon 10. This suggests that even though the p.N410H mutation is located distal to exon 10, it may contribute to disease through a tau alternative splicing mechanism that disturbs the normal tau 3R and 4R ratios. Alternatively, differential pathogenic effects of p.N410H on 3R tau isoforms versus 4R tau isoforms may be contributing to the altered 4R/3R tau ratio in the frontal cortex of the p.N410H carrier. In addition to altered tau mRNA expression levels in brain tissue, our *in vitro* studies showed that p.N410H has concomitant microtubule assembly impairment and increased tau aggregation properties. Tau protein with the p.N410H mutation showed a significant loss of normal tau function, as the rate of microtubule assembly decreased by 19.2% and the extent of total microtubule polymerization decreased 10.3% with mutated p.N410H tau compared to WT tau. Additionally, p.N410H caused a marked increase in tau filament formation, demonstrating that this mutation also acts through a toxic gain of function mechanism. Filament assembly effects appeared to be largely nucleation driven since the average filament lengths were unchanged between WT and p.N410H tau. There were significant increases in Thioflavin S fluorescence at 30 minutes when changes in filament number and mass were not detectable by electron microscopy which further supports the hypothesis that p.N410H accelerates the folding of tau proteins into assembly-competent

subunits. The Thioflavin S data also show that tau polymerization with the p.N410H mutation persist, as they are still observed with steady state readings at 960 minutes. In conclusion, the p.N410H mutation seems to affect tau on multiple levels, leading to an increased 4R/3R tau mRNA ratio, a reduced ability to promote microtubule assembly, and an increased propensity to aggregate into filaments compared to WT tau.

The p.N410H mutation carrier and sporadic CBD were indistinguishable on neuropathologic examination using tau and TDP-43 immunohistochemistry. TDP-43 pathology has been described in CBD pathology and other tauopathies, but the significance of co-occurring tau and TDP-43 pathology is not clear.^{22, 25-27} Of the 117 pathologically-confirmed CBD cases we screened, 29% had TDP-43 pathology (**Tables 3.5-7, pg. ##**). Upon mapping the distribution of TDP-43 pathology in four sporadic CBD cases, we observed a similar distribution as in the p.N410H mutation carrier. The neuroanatomical distribution of TDP-43 pathology observed in CBD was greatest in basal ganglia, thalamus, midbrain, and pons. The distribution of TDP-43 pathology in CBD has not been previously described, but one study found TDP-43 immunoreactivity in the dentate fascia as in FTLTDP as well as TDP-43 colocalization with tau pathology in astrocytic plaques and oligodendroglial white matter pathology.²⁵ In the present study, we did observe oligodendroglial TDP-43 immunoreactive inclusions, yet we did not find TDP-43 pathology in granule cells of the dentate fascia or astrocytic inclusions in any of the 117 CBD cases.

Compared to the three CBD cases with olivopontocerebellar atrophy (CBD-OPCA) described in Chapter 3, the distribution and severity of TDP-43 pathology in p.N410H was more similar to sporadic CBD compared to CBD-OPCA.

A review of the literature for FTDP-17 cases with CBD resulted in a limited number of reported cases, none of which met neuropathologic criteria for CBD. The most convincing *MAPT* mutation carrier with CBD pathology is a patient with an exon 9 mutation, p.I260V, who presented clinically with FTD and pathologically had a 4R tauopathy.²⁸ This p.I260V carrier had tau-immunoreactive astrocytic processes and argyrophilic thread-like lesions in white matter, yet swollen achromatic or ballooned neurons were absent. Other *MAPT* mutations have been described to have features of CBD pathology, but because of additional pathologic features, these cases do not meet research diagnostic criteria for CBD.²⁹⁻³¹ Some members of the pallidopontonigral degeneration family harboring the p.N279K mutation present with corticobasal syndrome, but they have neuropathologic features not fitting with CBD.³² A p.P301S

carrier presented with corticobasal syndrome, but a pathologic assessment was not performed.³³ Due to the heterogeneity of pathology underlying corticobasal syndrome, this raises the question if this case was in fact CBD.³⁴ Taken together, we believe that the p.N410H is the first *MAPT* mutation carrier that meets neuropathologic diagnostic criteria for CBD.

In addition to the *MAPT* coding regions, our study also systematically assessed the *MAPT* 3'UTR in pathologically-confirmed CBD patients. We identified two rare genetic variants (MAPTv8 and rs186977284) that nominally associate with risk of developing CBD. Furthermore, rs186977284 was found to be associated with an increased risk of developing PSP. Although this association of *MAPT* 3'UTR variants with CBD and PSP does not hold up upon correction for multiple testing, confirmatory studies in other CBD and PSP cohorts are warranted. We did note an unusually high number of neuropathologically atypical CBD and PSP cases harboring the MAPTv8 and rs186977284 risk alleles. One case had CBD with olivopontocerebellar atrophy (CBD-OPCA)²² and three cases had PSP with pallido-nigro-luysial degeneration which is an atypical pathologic variant of PSP.^{35,36} The contribution of rare *MAPT* variants to the development of neurodegenerative disease is currently not clear, but there is evidence that the p.A152T variant causes tauopathy, including CBD.^{21,37,38} CBD and PSP are considered to lie on a 4R tauopathy spectrum, and the fact that we find association of rare variants in the *MAPT* 3'UTR with risk of CBD and PSP further supports this notion. On the other hand, the MAPTv8 association was unique to CBD, providing additional evidence of how CBD and PSP are distinct clinicopathologic disorders.

In conclusion, performing an in-depth sequence analysis of *MAPT* in a large autopsy-confirmed CBD cohort identified the novel p.N410H tau mutation, indicating that *MAPT* sequencing should be considered in CBD patients. Functional characterization of this mutation demonstrated that p.N410H disrupts tau isoform homeostasis and has a reduced ability to promote microtubule assembly, with a potentially toxic gain of function demonstrated by a four-fold increase in its ability to polymerize into tau filaments. Additional functional characterization of this mutation may lead to a better molecular understanding of CBD pathogenesis and models for studying CBD-specific propagation.

4.6. References

1. Dickson, DW, Bergeron, C, Chin, SS, Duyckaerts, C, Horoupian, D, Ikeda, K, Jellinger, K, Lantos, PL, Lippa, CF, Mirra, SS, Tabaton, M, Vonsattel, JP, Wakabayashi, K & Litvan, I. Office of Rare Diseases neuropathologic criteria for corticobasal degeneration. *Journal of neuropathology and experimental neurology* 61, 935-46 (2002).
2. Kouri, N, Murray, ME, Hassan, A, Rademakers, R, Uitti, RJ, Boeve, BF, Graff-Radford, NR, Wszolek, ZK, Litvan, I, Josephs, KA & Dickson, DW. Neuropathological features of corticobasal degeneration presenting as corticobasal syndrome or Richardson syndrome. *Brain : a journal of neurology* 134, 3264-75 (2011).
3. Baker, M, Litvan, I, Houlden, H, Adamson, J, Dickson, D, Perez-Tur, J, Hardy, J, Lynch, T, Bigio, E & Hutton, M. Association of an extended haplotype in the tau gene with progressive supranuclear palsy. *Hum Mol Genet* 8, 711-5 (1999).
4. Dickson, DW. Neuropathologic differentiation of progressive supranuclear palsy and corticobasal degeneration. *Journal of neurology* 246 Suppl 2, II6-15 (1999).
5. Kouri, N, Whitwell, JL, Josephs, KA, Rademakers, R & Dickson, DW. Corticobasal degeneration: a pathologically distinct 4R tauopathy. *Nature reviews. Neurology* 7, 263-72 (2011).
6. Hutton, M, Lendon, CL, Rizzu, P, Baker, M, Froelich, S, Houlden, H, Pickering-Brown, S, Chakraverty, S, Isaacs, A, Grover, A, Hackett, J, Adamson, J, Lincoln, S, Dickson, D, Davies, P, Petersen, RC, Stevens, M, de Graaff, E, Wauters, E, van Baren, J, Hillebrand, M, Joosse, M, Kwon, JM, Nowotny, P, Che, LK, Norton, J, Morris, JC, Reed, LA, Trojanowski, J, Basun, H, Lannfelt, L, Neystat, M, Fahn, S, Dark, F, Tannenberg, T, Dodd, PR, Hayward, N, Kwok, JB, Schofield, PR, Andreadis, A, Snowden, J, Craufurd, D, Neary, D, Owen, F, Oostra, BA, Hardy, J, Goate, A, van Swieten, J, Mann, D, Lynch, T & Heutink, P. Association of missense and 5'-splice-site mutations in tau with the inherited dementia FTDP-17. *Nature* 393, 702-5 (1998).
7. Poorkaj, P, Bird, TD, Wijsman, E, Nemens, E, Garruto, RM, Anderson, L, Andreadis, A, Wiederholt, WC, Raskind, M & Schellenberg, GD. Tau is a candidate gene for chromosome 17 frontotemporal dementia. *Annals of neurology* 43, 815-25 (1998).
8. Spillantini, MG, Murrell, JR, Goedert, M, Farlow, MR, Klug, A & Ghetti, B. Mutation in the tau gene in familial multiple system tauopathy with presenile dementia. *Proceedings of the National Academy of Sciences of the United States of America* 95, 7737-41 (1998).
9. Fekete, R, Bainbridge, M, Baizabal-Carvallo, JF, Rivera, A, Miller, B, Du, P, Kholodovych, V, Powell, S & Ondo, W. Exome sequencing in familial corticobasal degeneration. *Parkinsonism & related disorders* (2013).
10. Conrad, C, Andreadis, A, Trojanowski, JQ, Dickson, DW, Kang, D, Chen, X, Wiederholt, W, Hansen, L, Masliah, E, Thal, LJ, Katzman, R, Xia, Y & Saitoh, T. Genetic evidence for the involvement of tau in progressive supranuclear palsy. *Annals of neurology* 41, 277-81 (1997).
11. Baker, M, Litvan, I, Houlden, H, Adamson, J, Dickson, D, Perez-Tur, J, Hardy, J, Lynch, T, Bigio, E & Hutton, M. Association of an extended haplotype in the tau gene with progressive supranuclear palsy. *Human molecular genetics* 8, 711-5 (1999).
12. Ezquerra, M, Pastor, P, Valdeoriola, F, Molinuevo, JL, Blesa, R, Tolosa, E & Oliva, R. Identification of a novel polymorphism in the promoter region of the tau gene highly associated to progressive supranuclear palsy in humans. *Neuroscience letters* 275, 183-6 (1999).

13. Houlden, H, Baker, M, Morris, HR, MacDonald, N, Pickering-Brown, S, Adamson, J, Lees, AJ, Rossor, MN, Quinn, NP, Kertesz, A, Khan, MN, Hardy, J, Lantos, PL, St George-Hyslop, P, Munoz, DG, Mann, D, Lang, AE, Bergeron, C, Bigio, EH, Litvan, I, Bhatia, KP, Dickson, D, Wood, NW & Hutton, M. Corticobasal degeneration and progressive supranuclear palsy share a common tau haplotype. *Neurology* 56, 1702-6 (2001).
14. Pastor, P, Ezquerra, M, Perez, JC, Chakraverty, S, Norton, J, Racette, BA, McKeel, D, Perlmutter, JS, Tolosa, E & Goate, AM. Novel haplotypes in 17q21 are associated with progressive supranuclear palsy. *Annals of neurology* 56, 249-58 (2004).
15. Rademakers, R, Melquist, S, Cruts, M, Theuns, J, Del-Favero, J, Poorkaj, P, Baker, M, Sleegers, K, Crook, R, De Pooter, T, Bel Kacem, S, Adamson, J, Van den Bossche, D, Van den Broeck, M, Gass, J, Corsmit, E, De Rijk, P, Thomas, N, Engelborghs, S, Heckman, M, Litvan, I, Crook, J, De Deyn, PP, Dickson, D, Schellenberg, GD, Van Broeckhoven, C & Hutton, ML. High-density SNP haplotyping suggests altered regulation of tau gene expression in progressive supranuclear palsy. *Human molecular genetics* 14, 3281-92 (2005).
16. Hoglinger, GU, Melhem, NM, Dickson, DW, Sleiman, PM, Wang, LS, Klei, L, Rademakers, R, de Silva, R, Litvan, I, Riley, DE, van Swieten, JC, Heutink, P, Wszolek, ZK, Uitti, RJ, Vandrovцова, J, Hurtig, HI, Gross, RG, Maetzler, W, Goldwurm, S, Tolosa, E, Borroni, B, Pastor, P, Cantwell, LB, Han, MR, Dillman, A, van der Brug, MP, Gibbs, JR, Cookson, MR, Hernandez, DG, Singleton, AB, Farrer, MJ, Yu, CE, Golbe, LI, Revesz, T, Hardy, J, Lees, AJ, Devlin, B, Hakonarson, H, Muller, U & Schellenberg, GD. Identification of common variants influencing risk of the tauopathy progressive supranuclear palsy. *Nature genetics* 43, 699-705 (2011).
17. Adams, SJ, DeTure, MA, McBride, M, Dickson, DW & Petrucelli, L. Three repeat isoforms of tau inhibit assembly of four repeat tau filaments. *PloS one* 5, e10810 (2010).
18. Di Noto, L, DeTure, MA & Purich, DL. Disulfide-cross-linked tau and MAP2 homodimers readily promote microtubule assembly. *Molecular cell biology research communications* : MCBRC 2, 71-6 (1999).
19. Ingelsson, M, Ramasamy, K, Cantuti-Castelvetri, I, Skoglund, L, Matsui, T, Orne, J, Kowa, H, Raju, S, Vanderburg, CR, Augustinack, JC, de Silva, R, Lees, AJ, Lannfelt, L, Growdon, JH, Frosch, MP, Standaert, DG, Irizarry, MC & Hyman, BT. No alteration in tau exon 10 alternative splicing in tangle-bearing neurons of the Alzheimer's disease brain. *Acta neuropathologica* 112, 439-49 (2006).
20. Purcell, S, Neale, B, Todd-Brown, K, Thomas, L, Ferreira, MA, Bender, D, Maller, J, Sklar, P, de Bakker, PI, Daly, MJ & Sham, PC. PLINK: a tool set for whole-genome association and population-based linkage analyses. *American journal of human genetics* 81, 559-75 (2007).
21. Coppola, G, Chinnathambi, S, Lee, JJ, Dombroski, BA, Baker, MC, Soto-Ortolaza, AI, Lee, SE, Klein, E, Huang, AY, Sears, R, Lane, JR, Karydas, AM, Kenet, RO, Biernat, J, Wang, LS, Cotman, CW, Decarli, CS, Levey, AI, Ringman, JM, Mendez, MF, Chui, HC, Le Ber, I, Brice, A, Lupton, MK, Preza, E, Lovestone, S, Powell, J, Graff-Radford, N, Petersen, RC, Boeve, BF, Lippa, CF, Bigio, EH, Mackenzie, I, Finger, E, Kertesz, A, Caselli, RJ, Gearing, M, Juncos, JL, Ghetti, B, Spina, S, Bordelon, YM, Tourtellotte, WW, Frosch, MP, Vonsattel, JP, Zarow, C, Beach, TG, Albin, RL, Lieberman, AP, Lee, VM, Trojanowski, JQ, Van Deerlin, VM, Bird, TD, Galasko, DR, Masliah, E, White, CL, Troncoso, JC, Hannequin, D, Boxer, AL, Geschwind, MD, Kumar, S, Mandelkow, EM, Wszolek, ZK, Uitti, RJ, Dickson, DW, Haines, JL, Mayeux, R, Pericak-Vance, MA, Farrer, LA, Ross, OA, Rademakers, R, Schellenberg, GD, Miller, BL, Mandelkow, E & Geschwind, DH. Evidence for a role of the rare p.A152T variant in MAPT in increasing the risk for FTD-spectrum and Alzheimer's diseases. *Human molecular genetics* 21, 3500-12 (2012).

22. Kouri, N, Oshima, K, Takahashi, M, Murray, ME, Ahmed, Z, Parisi, JE, Yen, SH & Dickson, DW. Corticobasal degeneration with olivopontocerebellar atrophy and TDP-43 pathology: an unusual clinicopathologic variant of CBD. *Acta neuropathologica* 125, 741-52 (2013).
23. Santacruz, K, Lewis, J, Spire, T, Paulson, J, Kotilinek, L, Ingelsson, M, Guimaraes, A, DeTure, M, Ramsden, M, McGowan, E, Forster, C, Yue, M, Orne, J, Janus, C, Mariash, A, Kuskowski, M, Hyman, B, Hutton, M & Ashe, KH. Tau suppression in a neurodegenerative mouse model improves memory function. *Science* 309, 476-81 (2005).
24. Lippa, CF, Zhukareva, V, Kawarai, T, Uryu, K, Shafiq, M, Nee, LE, Grafman, J, Liang, Y, St George-Hyslop, PH, Trojanowski, JQ & Lee, VM. Frontotemporal dementia with novel tau pathology and a Glu342Val tau mutation. *Annals of neurology* 48, 850-8 (2000).
25. Uryu, K, Nakashima-Yasuda, H, Forman, MS, Kwong, LK, Clark, CM, Grossman, M, Miller, BL, Kretschmar, HA, Lee, VM, Trojanowski, JQ & Neumann, M. Concomitant TAR-DNA-binding protein 43 pathology is present in Alzheimer disease and corticobasal degeneration but not in other tauopathies. *Journal of neuropathology and experimental neurology* 67, 555-64 (2008).
26. McKee, AC, Gavett, BE, Stern, RA, Nowinski, CJ, Cantu, RC, Kowall, NW, Perl, DP, Hedley-Whyte, ET, Price, B, Sullivan, C, Morin, P, Lee, HS, Kubilus, CA, Daneshvar, DH, Wulff, M & Budson, AE. TDP-43 proteinopathy and motor neuron disease in chronic traumatic encephalopathy. *Journal of neuropathology and experimental neurology* 69, 918-29 (2010).
27. Geser, F, Winton, MJ, Kwong, LK, Xu, Y, Xie, SX, Igaz, LM, Garruto, RM, Perl, DP, Galasko, D, Lee, VM & Trojanowski, JQ. Pathological TDP-43 in parkinsonism-dementia complex and amyotrophic lateral sclerosis of Guam. *Acta neuropathologica* 115, 133-45 (2008).
28. Grover, A, England, E, Baker, M, Sahara, N, Adamson, J, Granger, B, Houlden, H, Passant, U, Yen, SH, DeTure, M & Hutton, M. A novel tau mutation in exon 9 (1260V) causes a four-repeat tauopathy. *Experimental neurology* 184, 131-40 (2003).
29. Nasreddine, ZS, Loginov, M, Clark, LN, Lamarche, J, Miller, BL, Lamontagne, A, Zhukareva, V, Lee, VM, Wilhelmsen, KC & Geschwind, DH. From genotype to phenotype: a clinical pathological, and biochemical investigation of frontotemporal dementia and parkinsonism (FTDP-17) caused by the P301L tau mutation. *Annals of neurology* 45, 704-15 (1999).
30. Spillantini, MG, Yoshida, H, Rizzini, C, Lantos, PL, Khan, N, Rossor, MN, Goedert, M & Brown, J. A novel tau mutation (N296N) in familial dementia with swollen achromatic neurons and corticobasal inclusion bodies. *Annals of neurology* 48, 939-43 (2000).
31. Zarranz, JJ, Ferrer, I, Lezcano, E, Forcadas, MI, Eizaguirre, B, Atares, B, Puig, B, Gomez-Esteban, JC, Fernandez-Maiztegui, C, Rouco, I, Perez-Concha, T, Fernandez, M, Rodriguez, O, Rodriguez-Martinez, AB, de Pancorbo, MM, Pastor, P & Perez-Tur, J. A novel mutation (K317M) in the MAPT gene causes FTDP and motor neuron disease. *Neurology* 64, 1578-85 (2005).
32. Wszolek, ZK, Tsuboi, Y, Farrer, M, Uitti, RJ & Hutton, ML. Hereditary tauopathies and parkinsonism. *Advances in neurology* 91, 153-63 (2003).
33. Bugiani, O, Murrell, JR, Giaccone, G, Hasegawa, M, Ghigo, G, Tabaton, M, Morbin, M, Primavera, A, Carella, F, Solaro, C, Grisoli, M, Savoirdo, M, Spillantini, MG, Tagliavini, F, Goedert, M & Ghetti, B. Frontotemporal dementia and corticobasal degeneration in a family with a P301S mutation in tau. *Journal of neuropathology and experimental neurology* 58, 667-77 (1999).

34. Boeve, BF, Maraganore, DM, Parisi, JE, Ahlskog, JE, Graff-Radford, N, Caselli, RJ, Dickson, DW, Kokmen, E & Petersen, RC. Pathologic heterogeneity in clinically diagnosed corticobasal degeneration. *Neurology* 53, 795-800 (1999).
35. Ahmed, Z, Josephs, KA, Gonzalez, J, DelleDonne, A & Dickson, DW. Clinical and neuropathologic features of progressive supranuclear palsy with severe pallido-nigro-luysial degeneration and axonal dystrophy. *Brain : a journal of neurology* 131, 460-72 (2008).
36. Williams, DR, Holton, JL, Strand, K, Revesz, T & Lees, AJ. Pure akinesia with gait freezing: a third clinical phenotype of progressive supranuclear palsy. *Movement disorders : official journal of the Movement Disorder Society* 22, 2235-41 (2007).
37. Kovacs, GG, Wohrer, A, Strobel, T, Botond, G, Attems, J & Budka, H. Unclassifiable tauopathy associated with an A152T variation in MAPT exon 7. *Clinical neuropathology* 30, 3-10 (2011).
38. Kara, E, Ling, H, Pittman, AM, Shaw, K, de Silva, R, Simone, R, Holton, JL, Warren, JD, Rohrer, JD, Xiomerisiou, G, Lees, A, Hardy, J, Houlden, H & Revesz, T. The MAPT p.A152T variant is a risk factor associated with tauopathies with atypical clinical and neuropathological features. *Neurobiology of aging* 33, 2231 e7-2231 e14 (2012).

Chapter 5

Genome-wide association study identifies microtubule-associated protein tau (*MAPT*) and myelin-associated oligodendrocytic basic protein (*MOBP*) as shared genetic risk factors for corticobasal degeneration and progressive supranuclear palsy

5.1. Abstract

Corticobasal degeneration (CBD) is a neurodegenerative disorder that can present with several different clinical syndromes due to heterogeneous focal cortical involvement, thus resulting in <50% diagnostic accuracy. Similar to progressive supranuclear palsy (PSP) and Alzheimer's disease, CBD patients have aggregation of the tau protein in their brains, neuropathologically classifying these diseases as tauopathies. A diagnosis of CBD can only be made upon neuropathologic examination, which has until now, impeded a CBD genome-wide association study. We have conducted the first CBD genome-wide association study on 152 autopsy-proven CBD patients and 3,311 control individuals comprising the discovery series. Replication in an independent cohort was performed on 67 autopsy-proven CBD cases from the Mayo Clinic Florida Brain Bank and 439 controls. Meta-analysis identified two genome-wide significant associations with CBD at *MAPT* ($P_{\text{meta}} = 1.42 \times 10^{-12}$; OR = 3.71) and *KIF13B/DUSP4* ($P_{\text{meta}} = 3.41 \times 10^{-8}$; OR = 1.82). Testing for CBD association with the top progressive supranuclear palsy GWAS SNPs identified strong associations at *MOBP* ($P_{\text{meta}} = 2.07 \times 10^{-7}$; OR = 1.72) and *MAPT* H1c haplotype ($P_{\text{meta}} = 7.91 \times 10^{-6}$; OR = 1.57). Another novel genetic association for CBD patients was identified at *SOS1* ($P_{\text{meta}} = 1.76 \times 10^{-7}$; OR = 2.41). RNA expression quantitative trait loci analysis was performed for four of the CBD risk loci on brain samples from cerebellum ($n = 374$) and temporal cortex ($n = 399$). This resulted in SNP/transcript associations with *MAPT*/rs8070723 (cerebellum: $P = 7.02 \times 10^{-69}$; temporal cortex: $P = 8.61 \times 10^{-44}$), *MAPT*/rs242557 (cerebellum: $P = 8.80 \times 10^{-13}$; temporal cortex: $P = 1.10 \times 10^{-8}$), *MOBP*/rs1768208 (cerebellum: $P = 1.71 \times 10^{-7}$; temporal cortex: 1.57×10^{-6}), and *SOS1*/rs963731 (cerebellum: $P = 4.61 \times 10^{-4}$; temporal

cortex: $P = 2.80 \times 10^{-6}$). These findings show for the first time, that CBD and PSP share common genetic variation, other than the *MAPT* locus, at *MOBP* which confers disease risk. Together, warranting future studies to understand the mechanism by which *MOBP* contributes to the CBD and PSP disease processes.

5.2. Introduction

CBD is a neurodegenerative disorder with an age at onset typically between 50-70 years of age. First reported in 1968 by Rebeiz and colleagues, CBD was identified to be a discrete clinical and neuropathologic entity.¹ CBD is characterized as a tauopathy due to the presence of abnormal aggregates of microtubule-associated protein tau found throughout the brains of CBD patients. Neuropathologic diagnostic criteria for CBD are based on tau immunohistochemistry, requiring tau inclusions in neurons and glia, with tau astrocytic plaques, and extensive thread-like pathology in both gray matter and white matter.² There are few reported families affected with CBD or the related tauopathy, PSP, yet genetic association studies have continually shown an increased risk to develop PSP and CBD for individuals carrying the H1 haplotype at the *MAPT* locus on chromosome 17q21.³⁻⁷ Recently, the first PSP GWAS discovered three novel susceptibility loci, *STX6*, *EIF2AK3*, and *MOBP*, that increase the risk of developing disease.⁸ Until now, a GWAS for CBD has not been possible because CBD is such a rare disorder with poor clinical diagnostic accuracy.

5.3. Methods and Materials

5.3.1. Samples

The discovery stage cohort was comprised of 152 autopsy-proven CBD cases collected from multiple institutions (**Table 5.1**). These subjects were obtained through international institutions: the Mayo Clinic (n = 66), Discovery stage controls were recruited from the Children's Hospital of Philadelphia (CHOP) Health Care Network, and although these controls are not age matched to the cases, the justification for using this cohort is that they were all genotyped at the same center using the same protocol as the CBD cases. Furthermore, because CBD is such a rare disorder with an estimated prevalence of 4.9-7.3 cases per 100,000 individuals,⁹ the chance of any of the controls developing CBD is negligible.

Table 5.1 Description of samples												
Cohort	Female			Age onset/blood draw			Age at death			Disease duration		
	Total	%	<i>n</i> ^b	Mean age	Range (s.d.)	<i>n</i>	Mean age	Range (s.d.)	<i>n</i>	Mean duration ^c	Range (s.d.)	<i>n</i>
Discovery Stage^a												
CBD cases	152	50	150	64	33-80 (8.6)	103	70	44-91 (9.2)	144	6	2-14 (2.4)	103
Replication Stage												
CBD cases	67	48	67	64	40-83 (7.9)	67	70	54-96 (7.8)	67	6	2-14 (2.5)	61
Controls	457	54	457	74	24-97 (13.1)	457	---	---	---	---	---	---

^aControls (*n* = 3,311) were young healthy subjects recruited from the Children's Hospital of Philadelphia Health Care Network. ^b*n* is the number of samples with available data. Values of *n* for each type of analysis do not add up to the total samples used because of missing values. ^cDuration in years.

The replication stage samples included 67 autopsy-proven CBD cases (Mayo Clinic Florida Brain Bank) and 457 control individuals collected from Mayo Clinic Florida, all of which were diagnosed as being free of any neurological disorder. For the replication, SNPs were genotyped either using Taqman Genotyping assays (Applied Biosystems) or Sanger sequencing. The NINDS research diagnostic criteria were used for neuropathologic diagnosis.² DNA was extracted from tissue of brain donors and from blood samples of control individuals. Written informed consent was obtained from all individuals and this study was approved by the appropriate institutional review board.

The power of this study was estimated for the Discovery Stage and Replication Stage for various minor allele frequencies and odds ratios with 1000 simulations of each scenario (**Tables 5.2 and 5.3**). The power assessment assumes that genotypes frequencies are in Hardy-Weinberg equilibrium in CBD cases and control individuals separately and that association testing is performed using logistic regression under an additive model.

Table 5.2 | Discovery Stage power (%) to detect associations of SNPs and CBD status with 150 cases, 3000 controls for given odds ratios for different minor allele frequencies.

P-value	P<0.05			P<0.01			P<0.001			P<10 ⁻⁸		
	OR	1.3	1.5	2	1.3	1.5	2	1.3	1.5	2	1.5	2
Frequency of risk allele in controls												
5%	21	47	87	10	28	74	3	11	52	<1	2	24
10%	33	64	98	14	42	93	4	22	83	<1	12	65
20%	49	85	99	28	66	<99	10	40	98	1	40	94
30%	55	90	<99	32	76	<99	13	51	99	1	53	98
50%	57	91	<99	34	79	<99	13	54	99	1	40	94
70%	50	85	<99	24	65	99	6	31	92	<1	4	37
20%	35	72	99	14	44	92	3	18	69	<1	<1	1
10%	20	41	85	5	16	57	<1	2	16	<1	<1	<1
5%	12	18	48	1	3	14	<1	<1	<1	<1	<1	<1

Assumes that genotypes are distributed according to Hardy-Weinberg equilibrium in cases and controls separately and that analysis is conducted with logistic regression. The odds ratio refers to an increase of one copy of the minor allele. Power assessed with 1000 simulations of each scenario.

Table 5.3 | Replication Stage power (%) to detect associations of SNPs and CBD status with 60 cases, 700 controls for given odds ratios for different minor allele frequencies.

P-value	P<0.05				P<0.001				
	OR	1.3	1.5	2	2.5	1.3	1.5	2	1.5
Frequency of risk allele in controls									
5%	12	21	55	79	3	8	31	61	
10%	14	33	75	95	5	14	55	85	
15%	21	41	85	98	8	21	68	94	
20%	23	49	90	99	8	26	74	97	
25%	26	51	95	100	8	28	82	98	
30%	28	54	95	99	12	28	83	98	
75%	20	40	80	94	5	15	50	78	

Assumes that genotypes are distributed according to Hardy-Weinberg equilibrium in cases and controls separately and that analysis is conducted with logistic regression. The odds ratio refers to an increase of one copy of the minor allele. Power assessed with 1000 simulations of each scenario.

5.3.2. Quality control

Quality control of genotyping data was performed at the individual level and then at the SNP level. For quality control, 10 individuals were genotyped in duplicate. Exclusion criteria for individual samples included high genotype failure rate (6 individuals were removed because of a genotype failure rate >2%) and cryptic relatedness and (no individuals were removed based on an average degree of sharing or identity by state (IBS) >0.4 with other individuals in the dataset). Genetic outliers were excluded from further analyses based on IBS and distance to the nearest neighbor analysis was conducted in PLINK¹⁰ (340 individuals were removed based on Z score distributions for the first to the fifth neighbor, Z score < -2). Gender inconsistencies were assessed by chromosome X genotypes which excluded 6 individuals based on observed and expected gender. Exclusion criteria for markers included minor allele frequency (24,183 SNPs were removed because of minor allele frequency <1%), deviation from Hardy-Weinberg equilibrium in controls (1,098 SNPs gave a Hardy-Weinberg expectations test P value $\leq 10^{-7}$), and high genotype failure rates (3,199 SNPs were removed because of genotype failure rates >2%).

5.3.3. Population substructure

Multidimensional scaling was applied to a pruned dataset (~140,000 markers) using PLINK and scatter plots for the first two principle components were generated using R (**Figure 5.1a**). The first two principle components were used as covariates when testing for association using an additive model. Analysis of population stratification showed that the first principle component was sufficient to reduce the genomic inflation factor (λ) from 1.06 to 1.01, as illustrated by the quantile-quantile (QQ) plots of observed versus expected P -values (**Figure 5.2a**). Using the first two principle components resulted in $\lambda = 1.02$ (**Figure 5.2b**), thus only the first principle component was used as a covariate for all subsequent analyses.

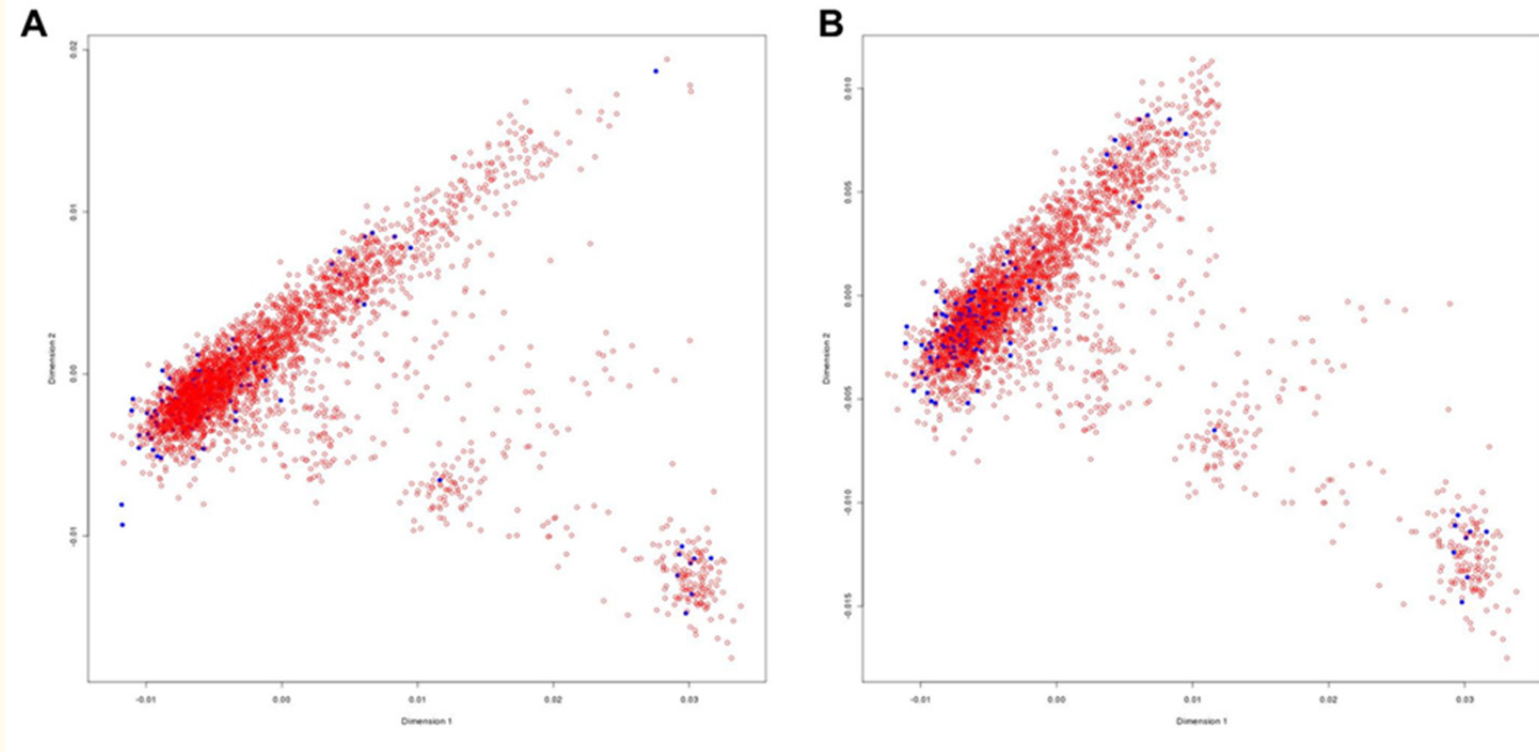


Figure 5.1 | Multidimensional scaling plots for CBD and controls

Multidimensional scaling (MDS) components were generated on a pruned dataset of ~140,000 markers using PLINK. The x-axis represents the first principle component and the y-axis is the second principle component. CBD cases (blue solid circles); CHOP controls (red open circles).

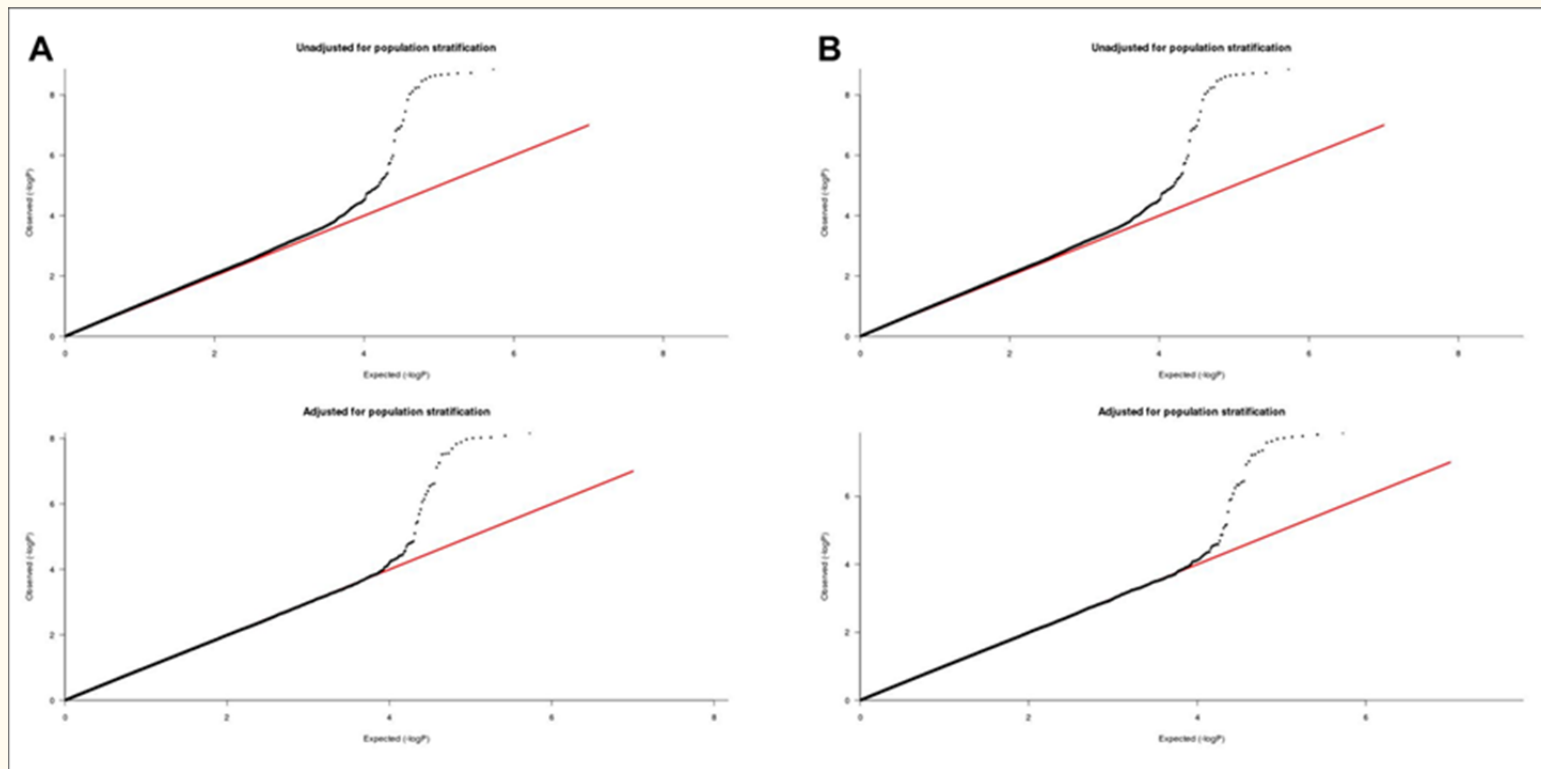


Figure 5.2 | Quantile-quantile plots in CBD genome-wide scan

Observed versus expected P values for the unadjusted logistic regression analysis (top panels) compared to an adjusted analysis using the first MDS generated component as a covariate in a logistic regression model (**A**). The components generated by MDS and the individual SNPs in the study were used to calculate the genomic inflation factor (λ). Genomic inflation factor $\lambda=1.06$ for unadjusted and $\lambda=1.01$ when adjusting for the first MDS generated component. Based on the value of λ it was determined that using only the first component from the MDS analysis in the logistic regression model was sufficient to control for population substructure. (**B**) Genomic inflation factor $\lambda=1.06$ for unadjusted and $\lambda=1.02$ when adjusting for the first and second MDS generated components.

5.3.4. Association analysis

For the discovery stage, we analyzed association between disease and 533,898 SNPs in 152 CBD cases and 3,311 control individuals by conditional logistic regression under an additive model using the first multidimensional scaling principle component as a covariate. We also tested for association from a subset of samples from stage 1 excluding outliers based on population substructure (**Figure 5.1b**), which yielded similar results.

Given the neuropathologic, clinical, and genetic similarities between CBD and PSP, we selected the top PSP GWAS SNPs at *MAPT* (H1c haplotype-tagging SNP, rs242557), *MOBP*, *EIF2AK3*, and *STX6* to test for association with CBD in the discovery stage. For the replication stage we tested the top three SNPs from the discovery stage ($P < 10^{-5}$) and two PSP GWAS SNPs which showed nominally significant association (rs1768208 and rs242557) in an independent cohort of 67 autopsy-proven CBD cases from the Mayo Clinic Florida Brain Bank and 457 control individuals again using logistic regression under an additive model, with age and sex as covariates. For rs242557, additional association testing was performed conditioning on tau haplotype (*i.e.* using 0, 1, or 2 as a covariate for the number of H1 alleles an individual had). Linkage disequilibrium (LD) values were derived from HapMap 3 release 27 (http://hapmap.ncbi.nlm.nih.gov/cgi-perl/gbrowse/hapmap27_B36/). Regional genome-wide association plots were created with LocusZoom.¹¹

5.3.5. Whole genome transcript levels – DASL

These data were generated and previously reported in a brain expression GWAS (eGWAS) by Zou and colleagues,¹² where the detailed mRNA extraction and quality assessment (Ambion RNAqueous kit and Agilent RNA 6000 Nano Chip), Whole Genome DASL assay (Illumina, San Diego, CA), and data quality control methods can be found. This DASL cohort included 374 cerebellar and 399 temporal cortex mRNA samples from the Mayo Clinic Florida Brain Bank. Neuropathologic diagnoses for the majority of the DASL cohort include Alzheimer's disease, PSP, CBD, Lewy body disease, and frontotemporal lobar degeneration (**Table 5.4**).

Table 5.4 Neuropathologic diagnoses for DASL transcriptome analysis samples				
Pathologic Diagnosis	Cerebellum		Temporal Cortex	
	N	Relative %	N	Relative %
Alzheimer's disease	197	53%	202	51%
Progressive supranuclear palsy (PSP)	98	26%	107	27%
Lewy Body Disease (LBD)	23	6%	25	6%
Corticobasal degeneration (CBD)	22	6%	22	6%
Frontotemporal lobar degeneration (FTLD)	15	4%	16	4%
Other	8	2%	10	3%
Multiple system atrophy (MSA)	7	2%	11	3%
Vascular dementia (VaD)	4	1%	6	2%

All cases were diagnosed by a single neuropathologist (Dennis W. Dickson).

The eGWAS data were queried for the top CBD GWAS SNPs (rs393152, rs963731, rs1768208, and rs242557). The GWAS dataset used for the eGWAS¹³ did not contain rs643472 (*KIF13B/DUSP4* locus) or any SNPs in LD > 0.5 with rs643472 and the call rates for two *DUSP4* probes did not pass quality control, precluding eQTL association at this locus. SNPs were tested for association with transcript levels in the eGWAS cohort by multivariable linear regression using an additive model, with the minor allele dosage (0, 1, 2) as the independent variable, and APOE ε4 dosage (0, 1, 2), age at death, gender, PCR plate, RIN, and RIN-RIN_{mean} as biological and technical covariates. The sample set was analyzed as a single cohort for maximum statistical power to detect associations. This approach is justified due to the original eGWAS study finding that neuropathologic diagnoses did not contribute significantly to eQTL associations.¹² The Bonferroni p-value threshold for SNP/transcript association significance was $P < 1.56 \times 10^{-3}$ (4 SNPs and 8 probes).

5.4. Results

5.4.1. Discovery stage

Table 5.5 displays results for discovery and replication stages, and the meta-analysis association studies for CBD cases compared to controls. The discovery stage identified a genome-wide significant association at chromosome 17q21.31 encompassing *MAPT* (rs393152, OR = 3.45, $P = 6.71 \times 10^{-9}$). We also found nominal evidence for association ($P < 10^{-5}$) at two novel CBD risk loci, rs643472 between *KIF13B* and *DUSP4* (OR = 1.88,

$P = 7.12 \times 10^{-7}$), and rs963731 intronic SNP in *SOS1* (OR = 2.46, $P = 2.04 \times 10^{-6}$) (Figure 5.3). As a candidate gene approach, association testing for the top PSP GWAS SNPs identified rs1768208, an intronic SNP in *MOBP* (myelin-associated oligodendrocytic basic protein), to be strongly associated with CBD risk (OR = 1.65, $P = 3.86 \times 10^{-5}$), as well as rs242557 (OR = 1.48, $P = 1.20 \times 10^{-3}$), tagging the H1c *MAPT* haplotype (Table 5.5). The other PSP risk SNPs at *SNTX6* and *EIF2AK3* did not show significant associations with CBD (Table 5.6). QQ plots showed that the distribution of P values was consistent with the null distribution, except for departures in the extreme tail (Figure 5.6), both including (top panel) and excluding (bottom panel) all SNPs at the *MAPT* locus. Fourteen additional SNPs tagging the H1/H2 inversion at Chr17q21 passed the threshold for genome-wide significant associations (Table 5.7).

Table 5.5 Results from discovery stage, replication stage, and meta-analysis							
SNP	Chr	Gene(s)	Stage ^a	MAF		OR (95% CI)	P
				Cases	Controls		
rs393152	17q21	<i>MAPT</i> (H1/H2)	Discovery	0.079	0.24	3.45 (2.29 - 5.34)	6.71×10^{-9}
			Replication	0.068	0.24	4.37 (2.16 - 8.83)	4.12×10^{-5}
			Meta-analysis			3.70	1.42×10^{-12}
rs643472	8p12	<i>KIF13B</i> <i>DUSP4</i>	Discovery	0.35	0.23	1.88 (1.46 - 2.40)	7.12×10^{-7}
			Replication	0.32	0.22	1.67 (1.11 - 2.52)	0.014
			Meta-analysis			1.82	3.41×10^{-8}
rs963731	2p22	<i>SOS1</i>	Discovery	0.12	0.054	2.46 (1.7 - 3.57)	2.04×10^{-6}
			Replication	0.09	0.049	2.21 (1.09 - 4.50)	0.029
			Meta-analysis			2.41	1.76×10^{-7}
rs1768208	3p22	<i>MOBP</i>	Discovery	0.39	0.29	1.65 (1.30 - 2.09)	3.86×10^{-5}
			Replication	0.39	0.25	1.89 (1.28 - 2.77)	1.3×10^{-3}
			Meta-analysis			1.71	2.07×10^{-7}
rs242557	17q21	<i>MAPT</i> (H1c)	Discovery	0.45	0.35	1.48 (1.17 - 1.88)	1.5×10^{-3}
			Replication	0.48	0.36	1.77 (1.25 - 2.52)	1.5×10^{-3}
			Meta-analysis			1.57	7.91×10^{-6}
rs1860743	7q36	<i>PRKAG2</i>	Discovery	0.20	0.11	2.05 (1.52 - 2.78)	3.46×10^{-6}
			Replication	0.09	0.13	0.71 (0.39 - 1.31)	0.27
			Meta-analysis			1.25	0.67
rs875125	21q22	<i>TSPEAR</i>	Discovery	0.17	0.10	2.02 (1.48 - 2.75)	7.92×10^{-6}
			Replication	0.05	0.08	0.65 (0.29 - 1.46)	0.29
			Meta-analysis			1.22	0.73

^aDiscovery stage (152 CBD, 3311 controls); Replication stage (67 CBD, 457 controls). The discovery and replication stages were analyzed by logistic regression under an additive model. The discovery stage analysis was adjusted for the first multidimensional scaling principle component, and the replication stage was adjusted for age and sex. Genome-wide significant is defined as variants associated with $P < 5 \times 10^{-8}$. Chr, chromosome; MAF, minor allele frequency; OR, odds ratio; CI, confidence interval.

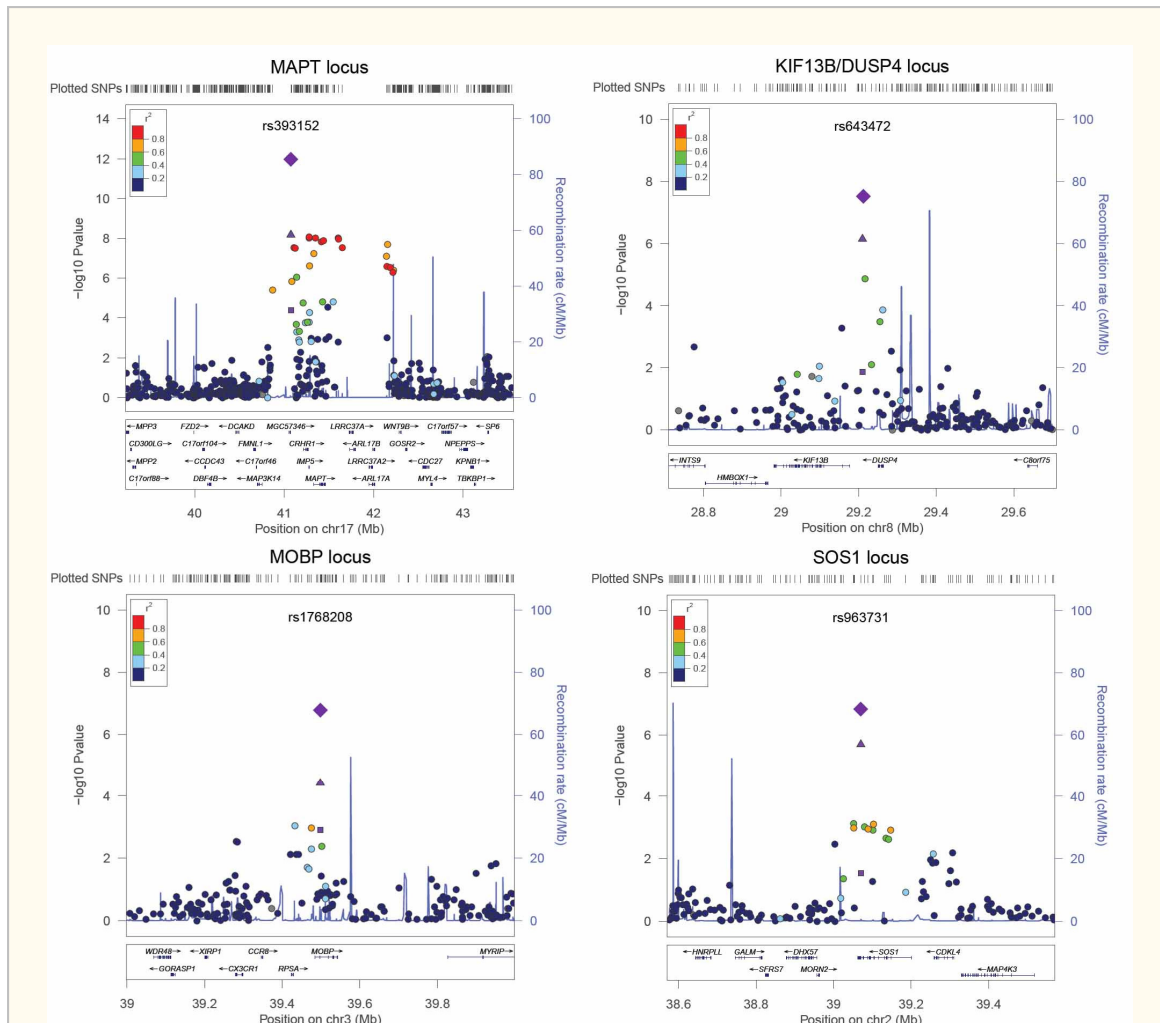


Figure 5.3 | CBD genome-wide association results

Regional associations plots made with LocusZoom. The discovery stage (▲), replication stage (■), and random effects meta-analysis (◆). Genome-wide significance threshold ($P < 5 \times 10^{-8}$).

CHR	SNP	Gene/feature	CBD MAF	Control MAF	PSP MAF	OR	L95	U95	P
17q21	rs8070723	MAPT/intron	0.08	0.24	0.05	3.34	2.21	5.07	1.30E-08
3p22	rs1768208	MOBP/intron	0.39	0.29	0.36	1.65	1.30	2.09	3.86E-05
17q21	rs242557	MAPT/intron	0.45	0.35	0.53	1.48	1.17	1.88	1.20E-03
2p11	rs7571971	EIF2AK3/intron	0.31	0.26	0.31	1.27	0.99	1.64	0.057
1q25	rs1411478	STX6/intron	0.46	0.42	0.50	1.20	0.95	1.50	0.13

The ORs are based on the minor allele (H2 tau haplotype). BP base-pair position, L95 Lower 95% confidence interval, U95 Upper 95% confidence interval

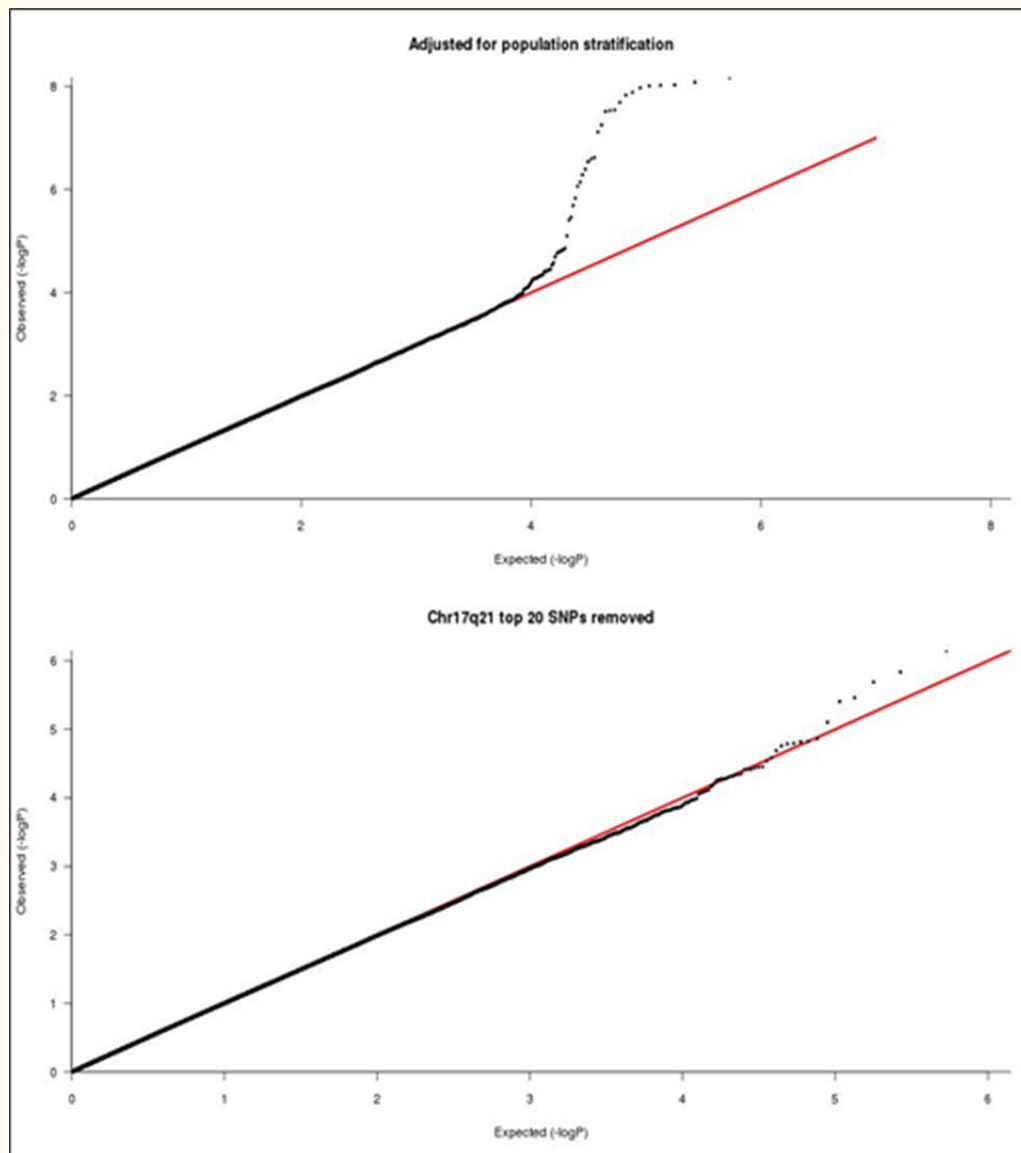


Figure 5.4 | Quantile-quantile plots in CBD genome-wide scan excluding all SNPs at 17q21.31 locus.

Departures in the extreme tail of the distribution of test statistics are due to regions with a strong signal for association. The strongest association was with rs393152 ($P = 6.7 \times 10^{-9}$) at chromosome 17q21.31 locus, and 14 additional SNPs meet the threshold for genome-wide significance ($P < 9.3 \times 10^{-8}$). Q-Q plot of the results of the trend test (top) compared to the Q-Q plot excluding all SNPs located at the chromosome 17q21.31 locus (bottom), show that departures in the extreme tail of the distribution of test statistics are due to regions with a strong signal for association.

Table 5.7 Twelve additional SNPs at Chr. 17q21 with genome-wide significant associations with CBD									
CHR	SNP	BP ^a	Gene/feature	CBD MAF	Control MAF	OR	L95	U95	P
17q21	rs393152	41074926	CRHR1/intron	0.079	0.24	0.29	0.19	0.44	6.71E-09
17q21	rs12373139	41279910	IMP5/missense	0.079	0.24	0.29	0.19	0.44	8.27E-09
17q21	rs12185268	41279463	IMP5/missense	0.079	0.24	0.29	0.19	0.44	9.28E-09
17q21	rs2532274	41602941	KANSL1/intron	0.086	0.24	0.30	0.20	0.45	9.52E-09
17q21	rs17563986	41347100	MAPT/intron	0.079	0.24	0.29	0.19	0.44	9.78E-09
17q21	rs2532269	41605885	KANSL1/intron	0.082	0.24	0.30	0.20	0.45	1.07E-08
17q21	rs8070723	41436901	MAPT/intron	0.082	0.24	0.30	0.20	0.45	1.30E-08
17q21	rs1981997	41412603	MAPT/intron	0.082	0.24	0.30	0.20	0.46	1.47E-08
17q21	rs7224296	42155230	NSF/intron	0.13	0.30	0.38	0.28	0.54	2.05E-08
17q21	rs2668692	41648797	KANSL1/intron	0.083	0.23	0.31	0.20	0.47	2.85E-08
17q21	rs1635291	41107696	CRHR1/intron	0.11	0.27	0.35	0.24	0.51	2.94E-08
17q21	rs7215239	41123556	CRHR1/intron	0.11	0.27	0.35	0.25	0.51	3.08E-08

^aAll physical positions are from the Human Reference Genome Release 36. The ORs are based on the minor allele (H2 tau haplotype). BP base-pair position, L95 Lower 95% confidence interval, U95 Upper 95% confidence interval

As previously described in the PSP GWAS, to ensure significant associations were not confounded by using young control individuals, allele frequencies for the top associated SNPs were compared and found to be similar to older controls samples (N = 5,729) from three datasets downloaded from the National Institute of Health (NIH) Database for Genotypes and Phenotypes (dbGaP) (**Table 5.8**).

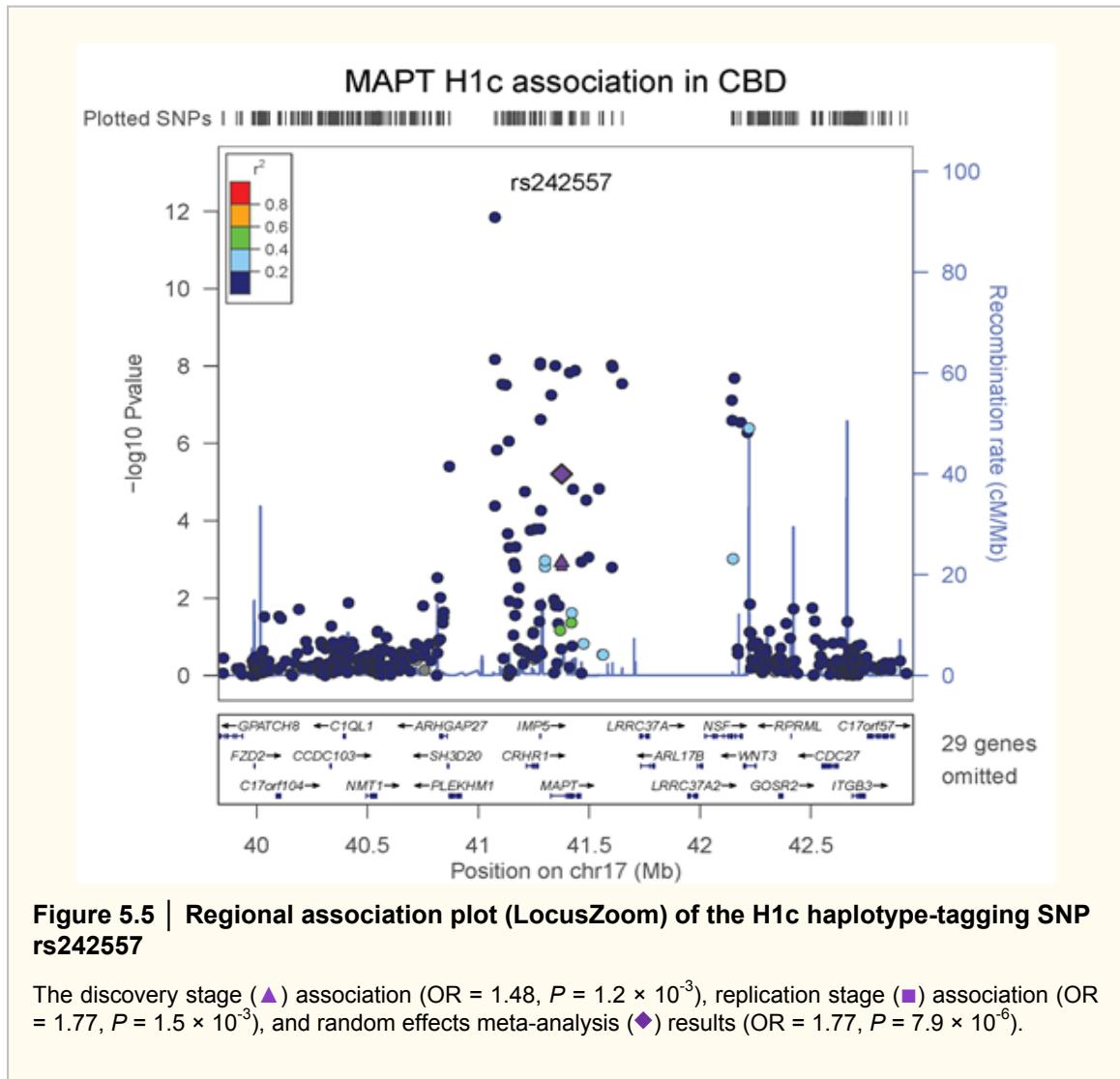
Table 5.8 | Comparison of minor allele frequencies (MAF) of SNPs with significant association with CBD based on CBD cases and controls and older controls from publicly available datasets from dbGaP.

CHR	SNP	Discovery stage		Replication stage		dbGaP datasets				
		CBD (n = 152)	Controls (n = 3311)	CBD (n = 67)	Controls (n = 457)	APDGC (n = 1986)	NGRC- PD (n = 991)	NIA- LOAD (n = 743)	Overall dbGaP (n = 3,720)	PSP Stage 1 (n = 1115)
2	rs963731	0.12	0.05	0.09	0.05	0.05	0.06	0.06	0.06	0.06
3	rs1768208	0.40	0.29	0.39	0.24	0.28 ^a	na	0.27	0.31	0.36
7	rs1860743	0.20	0.11	0.09	0.12	na	na	0.13	0.28	0.12
8	rs643472	0.35	0.23	0.32	0.21	0.23	0.24	0.26	0.25	0.23
17	rs393152	0.08	0.24	0.07	0.25	0.23 ^b	0.20 ^b	0.24	0.22	0.06
17	rs242557	0.45	0.35	0.48	0.36	0.36	0.36	0.38	0.37	0.53
21	rs875125	0.17	0.10	0.05	0.08	0.09	0.11	0.08	0.09	0.10

Datasets were obtained from Database for Genotypes and Phenotypes (dbGaP) at <http://www.ncbi.nlm.nih.gov/gap>. Autopsy-Confirmed Parkinson Disease GWAS Consortium (APDGC), (phs000394.v1.p1); NeuroGenetics Research Consortium (NGRC-PD), (phs000196.v2.p1); National Institute on Aging - Late Onset Alzheimer's Disease Family Study: Genome-Wide Association Study for Susceptibility Loci (NIA-LOAD), (phs000168.v1.p1) ^aMAF for rs545397 in LD with rs1768208 ($R^2=0.94$), ^bMAF for rs12185268 in LD with rs393152 ($R^2=1$)

5.4.2. Replication stage

The replication stage was performed in an independent cohort of 67 autopsy-proven CBD cases from the Mayo Clinic Brain Bank and 457 Mayo Clinic control individuals (**Table 5.1**). In total, five SNPs were genotyped in the replication stage, which included the three SNPs identified in the discovery stage (rs393152, rs643472, rs963731), and two of the PSP GWAS SNPs (rs1768208 and rs242557). The random effects meta-analysis (P_{meta}) combining the discovery and replication stages showed SNPs at *MAPT* (rs393152, $P_{meta} = 1.4 \times 10^{-12}$) and *KIF13B/DUSP4* (rs643472, $P_{meta} = 3.4 \times 10^{-8}$) to be highly associated with CBD and passed the genome-wide significant P -value threshold ($P < 5 \times 10^{-8}$) (**Table 5.5**). The other three SNPs at *MOBP* (rs1768208, $P_{meta} = 2.1 \times 10^{-7}$), *SOS1* (rs963731, $P_{meta} = 1.8 \times 10^{-7}$), and *MAPT* H1c haplotype (rs242557, $P_{meta} = 7.9 \times 10^{-6}$), had strong evidence for association with CBD. Upon conditioning for *MAPT* haplotype when testing for association with the H1c haplotype, the significance of the association was weakened (rs242557, OR = 1.18, $P_{meta} = 0.11$) (**Figure 5.5**). Minor allele frequencies of significant SNP associations with CBD did not differ significantly compared to older controls from three datasets (N = 3,720) available from the National Institute of Health (NIH) Database for Genotypes and Phenotypes (dbGaP) (**Table 5.8**).



5.4.3. *MOBP* locus

Upon further investigation of the *MOBP* locus, the top SNP (rs1768208) is in strong LD with two SNPs, rs631312 ($R^2 = 0.84$) and rs1768190 ($R^2 = 0.78$) (Figure 5.6) which reside in regulatory regions as predicted in Ensembl Regulation. These SNPs were genotyped in all CBD cases, 66 CBD from the discovery stage (Mayo Clinic samples) and 67 comprising the replication stage ($n = 133$), using Taqman genotyping assays or Sanger sequencing, and allele frequencies were compared to the 457 replication stage control individuals. Interestingly, the two SNPs residing in predicted regulatory regions from Ensembl Regulation, showed a stronger association with CBD (Table 5.9). The

variant rs631312 (OR = 1.89, $P = 8.77 \times 10^{-4}$) is located 346 base pairs upstream of the 5'UTR of *MOBP*, a promoter-associated region in multiple cell lines. The variant rs1768190 (OR = 1.91, $P = 7.24 \times 10^{-4}$) resides in intron 1 of *MOBP*, an enhancer/cis-regulatory element and CTCF-enriched region (**Table 5.9**).

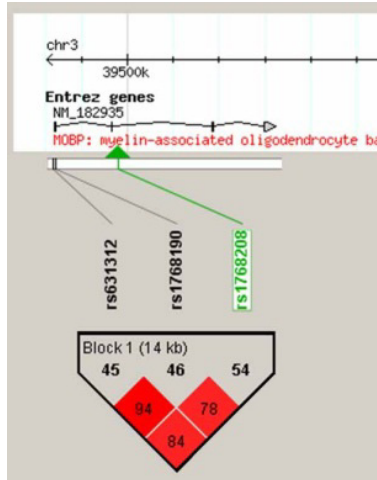


Figure 5.6 | Linkage disequilibrium structure at the *MOBP* locus

rs1768208 is the top *MOBP* CBD GWAS SNP; rs631312 ($R^2=0.84$) is located in a promoter-associated region in multiple cell lines; rs1768190 ($R^2=0.78$) is located in an enhancer/cis-regulatory element and CTCF enriched region. LD values are from HapMap 3 release 27 (CEU population).

SNP	Gene	Feature ^a	CBD MAF	Control MAF	LD R^2 rs1768208 ^b	OR (95% CI)	P
rs631312	<i>MOBP</i>	Promoter- associated in (Upstream) multiple cell lines	0.39	0.25	0.84	1.89 (1.30 - 2.75)	8.77×10^{-4}
rs1768190	<i>MOBP</i>	Enhancer/cis-regulatory (Intron 1) element and CTCF-enriched region	0.40	0.26	0.78	1.91 (1.31 - 2.77)	7.24×10^{-4}
rs1768208	<i>MOBP</i>	None (Intron 2)	0.40	0.29	---	1.89 (1.28 - 2.77)	1.27×10^{-3}

^aEnsembl Regulation¹⁴ has assembled datasets describing the mechanism of gene regulation in human cell lines. ^bLinkage disequilibrium values from HapMap release 27 with top *MOBP* SNP associated with CBD, rs1768208 (Meta analysis results, OR = 1.71, $P_{meta} = 2.07 \times 10^{-7}$).

5.4.4. Brain expression quantitative trait loci

RNA expression quantitative trait loci (eQTL) analysis was performed for each of the CBD risk loci on ~400 brain samples from both cerebellum and temporal cortex of neurodegenerative disease cases (**Table 5.4**).¹² This identified significant SNP/transcript associations with *MAPT*/rs8070723 (cerebellum: $P = 7.02 \times 10^{-69}$; temporal cortex: $P = 8.61 \times 10^{-44}$), *MOBP*/rs1768208 (cerebellum: $P = 1.71 \times 10^{-7}$;

temporal cortex: 1.57×10^{-6}), and *SOS1*/rs963731 (cerebellum: $P = 4.61 \times 10^{-4}$; temporal cortex: $P = 2.80 \times 10^{-6}$) (**Table 5.10**).

SNP	Chr	Gene	Probe	Cerebellum (<i>n</i> = 374)		Temporal cortex (<i>n</i> = 399)	
				Beta	P	Beta	P
rs963731	2	<i>SOS1</i>	ILMN_1767135		4.61×10^{-4}		2.8×10^{-6}
rs1768208	3	<i>MOBP</i>	ILMN_2298464		1.71×10^{-7}		1.57×10^{-6}
rs1768208	3	<i>MOBP</i>	ILMN_2414962		1.17×10^{-4}		1.76×10^{-5}
rs1768208	3	<i>MOBP</i>	ILMN_1768947		7.57×10^{-3}		3.03×10^{-3}
rs1768208	3	<i>MOBP</i>	ILMN_1750271		0.021		0.016
rs242557	17	<i>MAPT</i>	ILMN_1710903		8.80×10^{-13}		1.10×10^{-8}
rs242557	17	<i>MAPT</i>	ILMN_2298727		9.78×10^{-3}		0.11
rs242557	17	<i>MAPT</i>	ILMN_2310814		0.83		0.22
rs8070723	17	<i>MAPT</i>	ILMN_1710903		7.02×10^{-69}		8.61×10^{-44}
rs8070723	17	<i>MAPT</i>	ILMN_2298727		3.36×10^{-7}		9.03×10^{-4}
rs8070723	17	<i>MAPT</i>	ILMN_2310814		0.58		0.37

Top CBD GWAS SNPs were tested for transcript associations in human cerebellum and temporal cortex samples. Linear regression was employed using an additive model, with the minor allele dosage (0, 1, 2) as the independent variable, and APOE ε4 dosage (0, 1, 2), age at death, gender, PCR plate, RIN, (RIN-RINmean) as biological and technical covariates.¹²

5.5. Discussion

Here we report the results of the first CBD GWAS on 152 autopsy-proven CBD patients and 3,311 control individuals. Sample size is clearly a limitation of this study. Having been collected from multiple neuropathologists internationally, this was the largest possible cohort at the time because CBD is such a rare disorder and can only be diagnosed upon neuropathologic examination. In order to control the false-positive rate due to the small sample size of the CBD cohort, a stringent significance threshold ($P < 10^{-5}$) was applied to the Discovery Stage results in selection of SNPs to genotype in the Replication Stage. This proved to be a useful approach because the random effects meta-analysis identified two spurious associations (**Table 5.4**). The obvious disadvantage of applying these stringent criteria is the considerable, if not undeniable possibility of false-negative associations, as evidenced from the power analysis showing low power to detect genome-wide associations with variants with modest effect sizes.

The meta-analysis identified two genome-wide significant genetic loci that associate with CBD at *MAPT* ($P = 1.32 \times 10^{-12}$; OR = 3.70) and a novel association with a SNP located between *KIF13B* and *DUSP4* ($P = 2.29 \times 10^{-8}$; OR = 1.83). Another novel locus was found to be highly associated with CBD at *SOS1* ($P = 1.69 \times 10^{-7}$; OR = 2.41). Using a candidate gene approach, we selected the top PSP GWAS SNPs to check for association with CBD. Interestingly, this identified an association with rs1768208 ($P = 1.72 \times 10^{-7}$; OR = 1.72) in *MOBP* (myelin-associated oligodendrocytic basic protein), just above the Bonferroni-corrected significance threshold. In support of *MOBP* being a shared genetic risk factor between CBD and PSP, the CBD and PSP associations are going in the same direction, with CBD cases having a higher frequency of the minor allele (CBD MAF = 0.40; PSP MAF = 0.36). Testing for association in a larger CBD cohort, will allow us to compare the effect size of the genetic risk between CBD and PSP more accurately. Importantly, this is the first non-*MAPT* genetic risk factor shared between CBD and PSP.

Since the identification of *MOBP* as a new genetic risk factor for PSP, there have not been any studies to provide functional evidence that *MOBP* plays a role in PSP pathogenesis. Here we provide a brief review of the literature. Yamamoto *et al.* were the first to describe *MOBP* as one of the most abundant oligodendrocyte-expressing proteins, similar to myelin basic protein, with the main difference being that *MOBP* is only expressed in myelin of the central nervous system.¹⁵ Oligodendrocyte expression of *MOBP* occurs after MBP and other myelin proteins during development, and generates multiple transcripts which are differentially localized in the cell, with one isoform localized to myelin, and another located in distinct puncta in a perinuclear fashion.^{16,17} *MOBP* has been studied in the context of multiple sclerosis, where animal models elicit an experimental allergic encephalomyelitis,¹⁸ and *MOBP* has been shown to elicit a proliferative T-cell response in MS patients,¹⁹ reviewed by Motague *et al.*²⁰ Because oligodendrocyte pathology is common to CBD and PSP, it will be interesting to see functional studies that address the relationship between *MOBP* and tau.

This is the first study to test for association with CBD and rs242557, a SNP tagging the H1c haplotype at *MAPT*, known to be associated with PSP and located in a regulatory region influencing *MAPT* expression.¹¹ Meta-analysis for rs242557 showed a strong association with CBD ($P = 7.91 \times 10^{-6}$; OR = 1.57), but based on average allele frequencies, rs242557 appears to associate with PSP (MAF = 0.52) more than CBD (MAF = 0.47). Upon conditioning for *MAPT* haplotype, the rs242557 association with

CBD was weakened. This similarly occurred in the PSP GWAS, but because of the larger sample size, rs242557 (H1c tau haplotype) remained significantly associated with PSP risk conditioning on *MAPT* haplotype.

The *KIF13B/DUSP4* locus requires further testing for association in other CBD cohorts to determine if these findings will replicate, and if the locus can be refined to know which gene is a new genetic modifier of CBD. A limitation of our study is that we were unable to test for SNP/transcript associations at *KIF13B/DUSP4*, and therefore do not know yet whether this risk association with CBD is affecting mRNA expression levels. Kinesin family member 13B (KIF13B), or guanylate kinase associated kinesin (GAKIN), is a plus end-directed microtubule motor protein highly expressed in the brain, and is involved in synaptic vesicle trafficking along microtubules, neurite extension, and caveolin-dependent endocytosis.²¹⁻²³ Of interest, is that the new PSP risk gene *STX6*, is a SNARE-class protein that regulates vesicle membrane fusion, which suggests a dysfunction of vesicular trafficking may be a common disease mechanism shared by CBD and PSP. Dual specificity protein phosphatase 4 (*DUSP4*), or MAP kinase phosphatase-2 (MKP-2), acts through tyrosine and threonine-directed dephosphorylation.²⁴ Because tau phosphorylation state plays such a critical role in tauopathy pathogenesis, it will be interesting if *DUSP4* is responsible for the genetic association at Chr. 8p12, having the potential to affect tau phosphorylation homeostasis in CBD. Indeed, in Alzheimer's disease brain tissue there is decreased enzymatic activity of tau phosphatases such as PP-2A and PP-1,²⁵ proposing a potential role for *DUSP4* in CBD pathogenesis through aberrant tau phosphorylation. Mutations in son of sevenless homolog 1 (*SOS1*), a guanine nucleotide exchange factor for Ras,²⁶ cause Noonan syndrome 4 and hereditary gingival fibromatosis type 1.²⁷⁻²⁹ Signaling molecules such as *SOS1* control diverse biological processes, so there is not an obvious role of *SOS1* in CBD pathogenesis. On the other hand, *SOS1* activity is regulated by MAP kinase phosphorylation,^{30,31} so there may be a phosphorylation-dependent association with tau.

In conclusion, we report our findings from the first CBD GWAS, which identified *MAPT* and *MOBP* to be shared genetic risk factors between CBD and PSP. Given the significant white matter and oligodendrocyte pathology in these primary tauopathies, the genetic association with *MOBP* warrants functional characterization in order to determine its role in CBD and PSP disease processes. Additional analysis of the novel

genetic loci at *KIF13B/DUSP4* and *SOS1* has the potential to significantly advance our understanding of CBD.

5.6. References

1. Rebeiz, JJ, Kolodny, EH & Richardson, EP, Jr. Corticodentatonigral degeneration with neuronal achromasia. *Archives of Neurology* 18, 20-33 (1968).
2. Dickson, DW, Bergeron, C, Chin, SS, Duyckaerts, C, Horoupian, D, Ikeda, K, Jellinger, K, Lantos, PL, Lippa, CF, Mirra, SS, Tabaton, M, Vonsattel, JP, Wakabayashi, K & Litvan, I. Office of Rare Diseases neuropathologic criteria for corticobasal degeneration. *Journal of neuropathology and experimental neurology* 61, 935-46 (2002).
3. Baker, M, Litvan, I, Houlden, H, Adamson, J, Dickson, D, Perez-Tur, J, Hardy, J, Lynch, T, Bigio, E & Hutton, M. Association of an extended haplotype in the tau gene with progressive supranuclear palsy. *Hum Mol Genet* 8, 711-5 (1999).
4. Ezquerra, M, Pastor, P, Valldeoriola, F, Molinuevo, JL, Blesa, R, Tolosa, E & Oliva, R. Identification of a novel polymorphism in the promoter region of the tau gene highly associated to progressive supranuclear palsy in humans. *Neurosci Lett* 275, 183-6 (1999).
5. Higgins, JJ, Golbe, LI, De Biase, A, Jankovic, J, Factor, SA & Adler, RL. An extended 5'-tau susceptibility haplotype in progressive supranuclear palsy. *Neurology* 55, 1364-7 (2000).
6. Hoenicka, J, Perez, M, Perez-Tur, J, Barabash, A, Godoy, M, Vidal, L, Astarloa, R, Avila, J, Nygaard, T & de Yébenes, JG. The tau gene A0 allele and progressive supranuclear palsy. *Neurology* 53, 1219-25 (1999).
7. Houlden, H, Baker, M, Morris, HR, MacDonald, N, Pickering-Brown, S, Adamson, J, Lees, AJ, Rossor, MN, Quinn, NP, Kertesz, A, Khan, MN, Hardy, J, Lantos, PL, St George-Hyslop, P, Munoz, DG, Mann, D, Lang, AE, Bergeron, C, Bigio, EH, Litvan, I, Bhatia, KP, Dickson, D, Wood, NW & Hutton, M. Corticobasal degeneration and progressive supranuclear palsy share a common tau haplotype. *Neurology* 56, 1702-6 (2001).
8. Hoglinger, GU, Melhem, NM, Dickson, DW, Sleiman, PM, Wang, LS, Klei, L, Rademakers, R, de Silva, R, Litvan, I, Riley, DE, van Swieten, JC, Heutink, P, Wszolek, ZK, Uitti, RJ, Vandrovicova, J, Hurtig, HI, Gross, RG, Maetzler, W, Goldwurm, S, Tolosa, E, Borroni, B, Pastor, P, Cantwell, LB, Han, MR, Dillman, A, van der Brug, MP, Gibbs, JR, Cookson, MR, Hernandez, DG, Singleton, AB, Farrer, MJ, Yu, CE, Golbe, LI, Revesz, T, Hardy, J, Lees, AJ, Devlin, B, Hakonarson, H, Muller, U & Schellenberg, GD. Identification of common variants influencing risk of the tauopathy progressive supranuclear palsy. *Nature genetics* 43, 699-705 (2011).
9. Togasaki, DM & Tanner, CM. Epidemiologic aspects. in *Corticobasal degeneration* (eds. Litvan, I., Goetz, C.G. & Lang, A.E.) 53-59 (Lippincott, Williams & Wilkins, Philadelphia, 2000).
10. Purcell, S, Neale, B, Todd-Brown, K, Thomas, L, Ferreira, MA, Bender, D, Maller, J, Sklar, P, de Bakker, PI, Daly, MJ & Sham, PC. PLINK: a tool set for whole-genome association and population-based linkage analyses. *American journal of human genetics* 81, 559-75 (2007).
11. Pruim, RJ, Welch, RP, Sanna, S, Teslovich, TM, Chines, PS, Gliedt, TP, Boehnke, M, Abecasis, GR & Willer, CJ. LocusZoom: regional visualization of genome-wide association scan results. *Bioinformatics* 26, 2336-7 (2010).
12. Zou, F, Chai, HS, Younkin, CS, Allen, M, Crook, J, Pankratz, VS, Carrasquillo, MM, Rowley, CN, Nair, AA, Middha, S, Maharjan, S, Nguyen, T, Ma, L, Malphrus, KG, Palusak, R, Lincoln, S, Bisceglia, G, Georgescu, C, Kouri, N, Kolbert, CP, Jen, J, Haines, JL, Mayeux, R, Pericak-Vance, MA, Farrer, LA, Schellenberg, GD, Petersen, RC, Graff-Radford, NR, Dickson, DW, Younkin, SG & Ertekin-Taner, N. Brain expression genome-

wide association study (eGWAS) identifies human disease-associated variants. *PLoS genetics* 8, e1002707 (2012).

13. Carrasquillo, MM, Zou, F, Pankratz, VS, Wilcox, SL, Ma, L, Walker, LP, Younkin, SG, Younkin, CS, Younkin, LH, Bisceglia, GD, Ertekin-Taner, N, Crook, JE, Dickson, DW, Petersen, RC & Graff-Radford, NR. Genetic variation in PCDH11X is associated with susceptibility to late-onset Alzheimer's disease. *Nature genetics* 41, 192-8 (2009).
14. Flicek, P, Amode, MR, Barrell, D, Beal, K, Billis, K, Brent, S, Carvalho-Silva, D, Clapham, P, Coates, G, Fitzgerald, S, Gil, L, Giron, CG, Gordon, L, Hourlier, T, Hunt, S, Johnson, N, Juettemann, T, Kahari, AK, Keenan, S, Kulesha, E, Martin, FJ, Maurel, T, McLaren, WM, Murphy, DN, Nag, R, Overduin, B, Pignatelli, M, Pritchard, B, Pritchard, E, Riat, HS, Ruffier, M, Sheppard, D, Taylor, K, Thormann, A, Trevanion, SJ, Vullo, A, Wilder, SP, Wilson, M, Zadissa, A, Aken, BL, Birney, E, Cunningham, F, Harrow, J, Herrero, J, Hubbard, TJ, Kinsella, R, Muffato, M, Parker, A, Spudich, G, Yates, A, Zerbino, DR & Searle, SM. Ensembl 2014. *Nucleic acids research* 42, D749-55 (2014).
15. Yamamoto, Y, Mizuno, R, Nishimura, T, Ogawa, Y, Yoshikawa, H, Fujimura, H, Adachi, E, Kishimoto, T, Yanagihara, T & Sakoda, S. Cloning and expression of myelin-associated oligodendrocytic basic protein. A novel basic protein constituting the central nervous system myelin. *The Journal of biological chemistry* 269, 31725-30 (1994).
16. Holz, A, Schaeren-Wiemers, N, Schaefer, C, Pott, U, Colello, RJ & Schwab, ME. Molecular and developmental characterization of novel cDNAs of the myelin-associated/oligodendrocytic basic protein. *The Journal of neuroscience : the official journal of the Society for Neuroscience* 16, 467-77 (1996).
17. Gould, RM, Freund, CM & Barbarese, E. Myelin-associated oligodendrocytic basic protein mRNAs reside at different subcellular locations. *Journal of neurochemistry* 73, 1913-24 (1999).
18. Holz, A, Bielekova, B, Martin, R & Oldstone, MB. Myelin-associated oligodendrocytic basic protein: identification of an encephalitogenic epitope and association with multiple sclerosis. *Journal of immunology* 164, 1103-9 (2000).
19. Arbour, N, Holz, A, Sipe, JC, Naniche, D, Romine, JS, Zyroff, J & Oldstone, MB. A new approach for evaluating antigen-specific T cell responses to myelin antigens during the course of multiple sclerosis. *Journal of neuroimmunology* 137, 197-209 (2003).
20. Montague, P, McCallion, AS, Davies, RW & Griffiths, IR. Myelin-associated oligodendrocytic basic protein: a family of abundant CNS myelin proteins in search of a function. *Developmental neuroscience* 28, 479-87 (2006).
21. Hanada, T, Lin, L, Tibaldi, EV, Reinherz, EL & Chishti, AH. GAKIN, a novel kinesin-like protein associates with the human homologue of the *Drosophila* discs large tumor suppressor in T lymphocytes. *The Journal of biological chemistry* 275, 28774-84 (2000).
22. Horiguchi, K, Hanada, T, Fukui, Y & Chishti, AH. Transport of PIP3 by GAKIN, a kinesin-3 family protein, regulates neuronal cell polarity. *The Journal of cell biology* 174, 425-36 (2006).
23. Kanai, Y, Wang, D & Hirokawa, N. KIF13B enhances the endocytosis of LRP1 by recruiting LRP1 to caveolae. *The Journal of cell biology* 204, 395-408 (2014).
24. Misra-Press, A, Rim, CS, Yao, H, Roberson, MS & Stork, PJ. A novel mitogen-activated protein kinase phosphatase. Structure, expression, and regulation. *The Journal of biological chemistry* 270, 14587-96 (1995).
25. Gong, CX, Singh, TJ, Grundke-Iqbal, I & Iqbal, K. Phosphoprotein phosphatase activities in Alzheimer disease brain. *Journal of neurochemistry* 61, 921-7 (1993).

26. Chardin, P, Camonis, JH, Gale, NW, van Aelst, L, Schlessinger, J, Wigler, MH & Bar-Sagi, D. Human Sos1: a guanine nucleotide exchange factor for Ras that binds to GRB2. *Science* 260, 1338-43 (1993).
27. Hart, TC, Zhang, Y, Gorry, MC, Hart, PS, Cooper, M, Marazita, ML, Marks, JM, Cortelli, JR & Pallos, D. A mutation in the SOS1 gene causes hereditary gingival fibromatosis type 1. *American journal of human genetics* 70, 943-54 (2002).
28. Roberts, AE, Araki, T, Swanson, KD, Montgomery, KT, Schiripo, TA, Joshi, VA, Li, L, Yassin, Y, Tamburino, AM, Neel, BG & Kucherlapati, RS. Germline gain-of-function mutations in SOS1 cause Noonan syndrome. *Nature genetics* 39, 70-4 (2007).
29. Tartaglia, M, Pennacchio, LA, Zhao, C, Yadav, KK, Fodale, V, Sarkozy, A, Pandit, B, Oishi, K, Martinelli, S, Schackwitz, W, Ustaszewska, A, Martin, J, Bristow, J, Carta, C, Lepri, F, Neri, C, Vasta, I, Gibson, K, Curry, CJ, Sigüero, JP, Digilio, MC, Zampino, G, Dallapiccola, B, Bar-Sagi, D & Gelb, BD. Gain-of-function SOS1 mutations cause a distinctive form of Noonan syndrome. *Nature genetics* 39, 75-9 (2007).
30. Waters, SB, Yamauchi, K & Pessin, JE. Insulin-stimulated disassociation of the SOS-Grb2 complex. *Molecular and cellular biology* 15, 2791-9 (1995).
31. Bernards, A & Settleman, J. GEFs in growth factor signaling. *Growth factors* 25, 355-61 (2007).

Chapter 6

Conclusions

This is a dissertation on the neurodegenerative tauopathy CBD. Because CBD is a rare disorder and has <50% antemortem diagnostic accuracy, we sought to learn as much as possible from our invaluable resource, having the largest, single neuropathologically-confirmed CBD cohort in the world. This is a culmination of several different projects, all focused on neuropathologic, genetic, and clinical features of CBD, with the overall intent being to help patients who will suffer from this devastating disorder. Each study/chapter had a specific hypothesis, aimed to elucidate various unanswered questions about CBD. The approach we have used to further our understanding of CBD is to use patient tissue and DNA samples who have donated their brains to research.

With respect to neurodegenerative diseases, identifying biomarkers, or quantifiable features, that can reliably predict the underlying pathology, is a top research priority. This has of course been known for years, but as more and more clinicopathologic studies are performed, and the fact that pharmaceutical companies' primary strategy is to develop therapeutics targeting disease-specific proteins, biomarker discovery is fundamental to helping people who are otherwise going to die, undeniably, if afflicted with a neurodegenerative disease. For these reasons, using patient biospecimens, whether it be brain tissue, DNA, or molecular imaging, to name a few, may be the most effective approach to identify measurable disease characteristics that can tell us a patient's underlying pathology.

6.1. Richardson syndrome is a common clinical presentation of CBD

We hypothesized that there are neuropathologic differences in CBD patients presenting with corticobasal syndrome (CBD-CBS) versus Richardson syndrome (CBD-RS). Broadly speaking, we predicted CBD-CBS to have greater cortical tau pathology and that CBD-RS would have greater hindbrain tau pathology, and utilized digital microscopy and image analysis to test this hypothesis. We performed retrospective clinical-pathologic analysis to determine whether there are clinical features that differentiate

CBD-RS from PSP-RS, in hopes to improve CBD clinical diagnostic accuracy. Finally, pathologic tau protein was extracted from the brains of the three study groups, CBD-CBS, CBD-RS, and PSP-RS, and examined by immunoblot to compare disease-specific tau protein species, which are known to biochemically differentiate CBD from PSP.

We found that CBD-CBS had greater tau pathology in the primary motor and somatosensory cortices and putamen, whereas those presenting with Richardson syndrome had greater tau pathology in limbic and hindbrain structures, with relative sparing of the peri-Rolandic cortex. Neuronal loss assessment in the substantia nigra, identified patterns of neuronal loss unique to CBD-RS cases. CBD-RS, those CBD patients misdiagnosed as having PSP, had marked neuronal loss in the medial limbic portion of the substantia nigra (ventral tegmental area, A10), which may have contributed to their severe cognitive and behavioral dysfunction.

By measuring and comparing the thickness of the corpus callosum, we found that CBD pathology, irrespective of clinical presentation had significantly greater callosal atrophy than PSP cases. Future imaging studies will determine whether this can be reliably used to improve antemortem diagnostic accuracy of CBD. Retrospective analysis of medical records identified two clinical features that were present more often in CBD-RS compared to PSP-RS. Richardson syndrome with significant frontal-behavioral changes and urinary incontinence most often had underlying CBD rather than PSP pathology. These results will also need to be validated to determine whether these clinical features consistently are able to differentiate CBD from PSP pathology.

Importantly, analysis of protein extracted from patient brain tissue showed that CBD-RS cases had the same insoluble tau protein species as CBD-CBS, substantiating the idea that when we observe CBD pathology microscopically, then we can make the assumption that regardless of clinical presentation, we are studying a distinct disease process occurring in these patients.

In chapter three, we reported a new pathologic variant of CBD, CBD with olivopontocerebellar atrophy (CBD-OPCA), a pathology that is associated with multiple system atrophy (MSA), an α -synucleinopathy. Two of these patients presented with Richardson syndrome and the other patient had cerebellar ataxia and was thought to have idiopathic OPCA based on MRI findings. This is the first study to describe this unusual neuropathologic entity. Neuropathologic features including tau pathology severity and neuronal loss in the OPC system were compared among CBD-OPCA, MSA, CBD, and PSP. Interestingly, CBD-OPCA had neuropathologic commonalities

with all three, MSA, PSP, and typical CBD. An unexpected finding was that these CBD-OPCA cases had significant TDP-43 pathology, with the burden being greatest in hindbrain structures, where the highest burden of tau pathology was observed. The identification of a relationship between pathology and clinical presentation is not novel by any means, but there are specific conclusions that our studies support. In addition to greater hindbrain tau pathology, CBD-RS had greater tau pathology in limbic structures, with relative sparing of the peri-Rolandic cortex compared to CBD-CBS. Taken together, we can attribute the Richardson syndrome presentation to hindbrain tau pathology, but the cognitive and behavioral changes that were more frequent in CBD-RS compared to PSP-RS, are as evidenced from our studies, most likely due to greater tau pathology in limbic structures. An additional neuropathologic finding was the relative sparing of pre- and post-central gyri in CBD-RS, which can explain the lack of focal cortical signs and symptoms exhibited by CBD-CBS patients.

Regarding TDP-43 pathology in CBD, our findings that ~30% of CBD cases have TDP-43 pathology is twice the frequency previously reported by Uryu et al.¹ On immunohistochemical analysis, our results were not consistent with this study in that the distribution of TDP-43 pathology in CBD was greatest in the basal ganglia, and not a single case had TDP-43 pathology in the dentate fascia of the hippocampus as one would find in FTLD. It is not yet clear what the basis for these discrepancies are, but it posits an interesting possibility, that TDP-43 pathology may be a secondary consequence to tau pathology in CBD, as has been postulated for its role in Alzheimer's disease. Of importance, and something that remains to be determined, is the connection between argyrophilic grain disease (AGD, a 4R tauopathy affecting medial temporal structures) and TDP-43 pathology. In the Mayo Clinic Florida Brain Bank, AGD is twice as frequent in CBD cases positive for TDP-43 pathology. What makes this finding especially unusual is that the AGD 4R tau pathology is not located in the same regions as the TDP-43 pathology in CBD, again finding the greatest amount of TDP-43 inclusions in the basal ganglia. In a current study, we have not been able to identify a single neuropathologic, clinical, or genetic difference between CBD with or without TDP-43 pathology. These findings, along with other studies of TDP-43 concomitant with AD pathology, suggest that TDP-43 pathology may be secondary to tau pathology with unknown consequence. In support of TDP-43 being a secondary pathology in tauopathies, the CBD-OPCA cases described in Chapter 3 had marked TDP-43 pathology that correlated with the most affected brain regions with tau pathology.

6.2. *MAPT* mutation identified in a CBD case

The feasibility of genetic studies on CBD has been limited due to the rare nature of the disorder in combination with the required neuropathologic diagnosis. Furthermore, there are no families reported to have multiple autopsy-confirmed CBD cases, precluding genetic linkage studies. The only genetic risk factor for CBD has been the H1 haplotype at the Chr17q21 inversion encompassing *MAPT*. Since this is not sufficient to cause disease, we hypothesized that there is an unknown genetic component to CBD and we aimed to identify this by performing a systematic sequence analysis of *MAPT* in the Mayo Clinic Florida CBD cohort.

Sequence analysis of all central nervous system-expressed *MAPT* exons and the entire 3' untranslated region (3'UTR), identified a novel *MAPT* mutation, p.N410H, in a CBD case that is neuropathologically indistinguishable from sporadic CBD. Because we were unable to test additional family members, we excluded the p.N410H mutation in over 1200 controls and 560 PSP cases, and this mutation is not present in any genome databases. To provide further evidence that the mutation disrupts normal tau function, in vitro assays were performed and showed a decreased ability of the mutant tau to promote microtubule assembly and a marked increase in tau filament formation. These findings suggest that there is a toxic gain of function with the p.N410H mutation.

It is difficult applying the word “causal” to genetics as it is to apply the word “truth” to reality. I refer the reader to a review on causal inference by Vansteelandt and Lange, because they address the cause and effect paradigm with respect to genetic association studies and highlight inherent biases in genetic effect estimates.² In the case of the p.N410H *MAPT* mutation, it is equally logical to reason that it is a mutation that caused CBD as it is to reason that it is a rare polymorphism. We do provide evidence in Chapter 4 that shows p.N410H causes a biological change in the the tau protein. Whether or not p.N410H caused CBD in this patient, the mutation only lead to tau dysfunction not directly related to CBD, or had no effect on any of the above, are a few examples of the difficulty when making a statement of “causal” in genetics, or “truth” in reality.

Neurologically normal individuals can carry an autosomal dominant mutation that “causes” frontotemporal dementia. This phenomenon is called incomplete penetrance, because the patient has the disease-causing mutation, yet they do not develop the disease. In this situation, we can attribute lack of disease to the patient having another, yet to be discovered genetic variant that protects against disease. Conversely, it is equally logical to suggest that none of the family members developed disease because

of this mutation. Rather it must have been an environmental exposure since all mutation carriers did not develop disease. Interestingly, there are also patients that have mutations in two frontotemporal lobar degeneration-causing genes, or double mutants. On neuropathologic examination, a patient harboring both a *GRN* mutation and *C9ORF72* expansion actually had mixed neuropathology associated with the two mutations.³ Although one cannot make a definitive statement as to the pathogenicity or “causal” nature of these mutations, the study does show that there is a pathologic consequence associated with certain genetic mutations. The likelihood of a patient with two mutations showing features of both pathologies, supports that the mutations are disease-causing, or at least pathology-causing.

A more recent hypothesis has been proposed in the complex genetics field that genome-wide association signals are tagging a haplotype harboring multiple rare variants, as opposed to solely identifying common variation which associates with disease. Based on this hypothesis, we sought to determine whether there was genetic variation in the regulatory 3'UTR of *MAPT*, especially since alterations in tau expression are observed in neurodegenerative tauopathies. We identified two rare *MAPT* 3'UTR variants that are 5 times more frequent in CBD compared to controls. Interestingly, one of these variants replicated in PSP, although did not show as strong of an association as CBD. In summary, although these studies used a more traditional sequencing approach i.e. Sanger sequencing, we were able to identify genetic variability in CBD at the *MAPT* locus. Future deep resequencing and whole-exome/genome studies will be able to teach us more about the *MAPT* locus once the bioinformatics and computational methods become well established.

6.3. CBD and PSP have shared and unique genetic risk factors

The last study of this dissertation, are the results of the first CBD genome-wide association study (GWAS), which resulted in some very interesting findings. Again, genetic studies on CBD have been limited due to CBD being such a rare disorder which can only be diagnosed upon neuropathologic examination due to a <50% clinical diagnostic accuracy. In other words, if you gathered a clinical cohort of patients diagnosed with CBS, more than 50% of the patients would have pathology other than CBD. As discussed in Chapter 5, this GWAS is statistically underpowered to identify moderate genetic associations, yet power analysis shows sufficient power to detect associations with large effect sizes.

The *MAPT* H1 haplotype was identified as a genetic risk factor for CBD back in 2001 by Houlden and colleagues.⁴ Now with the results from the PSP GWAS and our findings for the CBD GWAS, while not a novel association, we now have a clear picture of the magnitude of the H1 haplotype genetic association, PSP (OR = 5.5, $P = 1.5 \times 10^{-116}$) and CBD (OR = 3.7, $P = 1.4 \times 10^{-12}$).⁵ We can assume that with a larger sample size, the H1 association would be stronger for CBD.

The Discovery Stage also identified four novel genetic loci showing strong association ($P < 10^{-5}$) with CBD at *KIF13B/DUSP4*, *SOS1*, *PRKAG2*, and *TSPEAR*. As a candidate gene approach, we also selected the top PSP GWAS SNPs to test for association with CBD in the discovery stage. Surprisingly, this showed a nominally significant association with rs1768202 ($P = 3.86 \times 10^{-5}$), an intronic SNP in myelin-associated oligodendrocytic basic protein (*MOBP*). Additionally, there was a moderate association with the H1c haplotype-tagging SNP, rs242557 ($P = 1.50 \times 10^{-3}$), but we did not identify an association with the other new PSP risk loci at *STX6* and *EIF2AK3*. Based on these findings, we designed a replication stage SNP set including the top CBD GWAS SNPs and *MOBP* and H1c SNPs ($n = 7$).

The replication stage was performed in independent cohorts of 67 pathologically-confirmed CBD and ~450 control individuals. The meta-analysis resulted in genome-wide significant associations at *MAPT* and an intragenic SNP between *KIF13B* (a member of the kinesin family) and *DUSP4* (a protein phosphatase). Importantly, we identified the first non-*MAPT* genetic risk factor shared by PSP and CBD at the *MOBP* locus, and although this association did not meet genome-wide significance, the association is reasonably strong and the risk is in the same direction as observed in PSP. Since both CBD and PSP have significant white matter pathology and tau inclusions in oligodendrocytes, we expect *MOBP* to play a significant role in CBD and PSP pathogenesis. The SNPs at *PRKAG2* and *TSPEAR* did not show significant association in the replication stage, thus we assume these were spurious associations.

Altogether, CBD and PSP share genetic risk factors at *MAPT* and *MOBP*, with moderate association with CBD at the H1c haplotype. Yet CBD has unique genetic associations with *KIF13B/DUSP4* and *SOS1*, as does PSP at *STX6* and *EIF2AK3*. We look forward to functional studies to elucidate the relationship between tau and *MOBP*, which could lead to significant advances in our current understanding of CBD and PSP, with the potential of identifying novel therapeutic targets for these patients.

6.4. Future directions

6.4.1. Mechanism of p.N410H *MAPT* mutation

What we still do not understand is how a mutation located in exon 13, outside of the microtubule-binding domain of tau, causes the 4R tauopathy CBD. This mutation causes an asparagine to histidine change. Arginine is a polar uncharged amino acid and histidine has a basic polar, positively charged side chain, suggesting that this mutation exerts its pathogenicity at the protein level. On the other hand, tau mRNA expression studies provide evidence that the dysfunction is at the RNA level. Quantification of 3R and 4R tau mRNA transcript levels showed an increase in the 4R:3R ratio in the p.N410H carrier, yet this mutation is not located in exon 10 or in regions known to regulate exon 10 splicing (Athena Andreadis, personal communication). There is evidence that another exon 13 *MAPT* mutation, p.R406W, causes microtubule network dysfunction when expressed in a 3R construct, yet 4R tau with the p.R406W mutation displayed normal microtubule network morphology.⁶ Another possibility is that there could be differential degradation of mutant 3R versus mutant 4R tau, and this is why we are seeing 4R tau only on immunohistochemistry. Our in vitro studies were performed in the 4R0N isoform of tau, thus there is much to be learned by introducing p.N410H to 3R tau.

Possibly related to these different effects of 3R versus 4R tau with exon 13 mutations, is our findings that there was a marked increase in the 4R:3R tau mRNA expression ratio. The p.N410H carrier in fact had reduced 3R tau mRNA, but similar 4R tau levels compared to controls, AD, sporadic CBD, and p.N279K mutation carrier. It is interesting to postulate that because the mutation is more pathogenic in 3R tau versus 4R tau, there is a disruption in normal tau isoform homeostasis, and as a result there could be some compensatory mechanism altering tau mRNA expression.

What will be interesting and greatly increase our understanding of CBD, is to understand how p.N410H has decreased 3R tau mRNA, has strictly 4R tau immunoreactivity on neuropathologic examination, and yet on immunoblot, p.N410H has the same insoluble tau cleavage fragments as observed in sporadic CBD. There are currently studies underway to generate a mouse model with the p.N410H mutation, which has the potential to become the first animal model of CBD. This will be a significant advancement in understanding the CBD disease process, because with a successful animal model, it will be possible to test for therapeutic intervention.

6.4.2. Complex genetics of CBD

A top priority moving forward from the CBD GWAS, it to elucidate the role of the genetic variation at *MOBP* associating with CBD and PSP. Future studies will be performed on several levels. We will determine whether there is differential mRNA and protein expression in the brains of these patients, and test to see if these changes are genotype-dependent. Another future study will be to create a luciferase construct with the different genotypes at the two regulatory SNPs in LD with rs1768208, rs631312 and rs1768190, to determine whether these directly alter *MOBP* expression levels. Followed by in vitro studies to determine the effect of *MOBP* overexpression and knockdown on tau and oligodendrocytes.

Regarding the other two novel CBD risk loci at *KIF13B/DUSP4* and *SOS1*, fine-mapping studies may refine the genetic association, but before doing this, we will evaluate genotype-phenotype correlations with mRNA and protein expression in patient tissue samples. Another interesting approach to further understand the role of these genes in CBD pathogenesis is to perform gene-environment interactions, as has been done in Parkinson's disease.⁷ This would require clinical data such as environmental exposure or head injury to be collected for the CBD cohort. Current studies are underway to create a CBD clinical rating scale, which would also be very useful for testing for genetic association with clinical progression or clinical phenotype (i.e. are there genetic variants that associate with the various clinical presentations of CBD, or are the already identified genetic associations dependent on these environmental or clinical factors).

Although we only selected very few SNPs to genotype in the replication stage, future studies could include more SNPs with a less-stringent significance threshold. This has the potential to identify even more genetic associations, that we undoubtedly have missed using a more stringent threshold in the CBD GWAS. Our justification for using a more stringent threshold to design the replication stage was simply based on sample size and thus a direct reflection on the power to detect genetic associations. As we gather additional CBD cases, these future genetic association studies will become more feasible. Now that we have GWAS data on CBD cases, clearly the next step is to move forward along with advances in whole-exome and whole-genome sequencing. We have begun a collaborative effort, the CBD Genetics Consortium, in order to gather CBD cases from national and international collaborators to make these studies possible.

The studies herein have contributed to efforts to define/refine clinical diagnostic criteria for CBD. Moving forward, with CBD research, our studies will be focused on using neuropathology as quantitative traits to identify genetic loci which associate with differential distribution and severity of tau pathology. These studies have the potential of identifying novel CBD genetic associations as compared to the case-control paradigm. Complementary to these neuropathology-genetic studies, will be the generation of the whole-exome and whole-genome data, which we will also use to determine if there are genetic loci that associate with CBD quantitative features. CBD is a rare disorder, but it is a tauopathy, opening up the possibility that these studies may contribute to our understanding of other tauopathies including PSP and Alzheimer's disease. Furthermore, the H1 *MAPT* haplotype association extends to Parkinson's disease,⁸ thus the more information we obtain can better our chances of understanding the effect of this intriguing genetic locus at chromosome 17q21 on neurodegenerative disorders.

6.5. References

1. Uryu K, Nakashima-Yasuda H, Forman MS, Kwong LK, Clark CM, Grossman M, Miller BL, Kretschmar HA, Lee VM, Trojanowski JQ, Neumann M. Concomitant TAR-DNA-binding protein 43 pathology is present in Alzheimer disease and corticobasal degeneration but not in other tauopathies. *J Neuropathol Exp Neurol.* 2008; 67(6): 555-64.
2. Vansteelandt, S & Lange, C. Causation and causal inference for genetic effects. *Human genetics* 131, 1665-76 (2012).
3. van Blitterswijk, M, Baker, MC, DeJesus-Hernandez, M, Ghidoni, R, Benussi, L, Finger, E, Hsiung, GY, Kelley, BJ, Murray, ME, Rutherford, NJ, Brown, PE, Ravenscroft, T, Mullen, B, Ash, PE, Bieniek, KF, Hatanpaa, KJ, Karydas, A, Wood, EM, Coppola, G, Bigio, EH, Lippa, C, Strong, MJ, Beach, TG, Knopman, DS, Huey, ED, Mesulam, M, Bird, T, White, CL, 3rd, Kertesz, A, Geschwind, DH, Van Deerlin, VM, Petersen, RC, Binetti, G, Miller, BL, Petrucelli, L, Wszolek, ZK, Boylan, KB, Graff-Radford, NR, Mackenzie, IR, Boeve, BF, Dickson, DW & Rademakers, R. C9ORF72 repeat expansions in cases with previously identified pathogenic mutations. *Neurology* 81, 1332-41 (2013).
4. Houlden H, Baker M, Morris HR, MacDonald N, Pickering-Brown S, Adamson J, Lees AJ, Rossor MN, Quinn NP, Kertesz A, Khan MN, Hardy J, Lantos PL, St George-Hyslop P, Munoz DG, Mann D, Lang AE, Bergeron C, Bigio EH, Litvan I, Bhatia KP, Dickson D, Wood NW, Hutton M. Corticobasal degeneration and progressive supranuclear palsy share a common tau haplotype. *Neurology.* 2001; 56(12): 1702-6.
5. Hoglinger GU, Melhem NM, Dickson DW, Sleiman PM, Wang LS, Klei L, Rademakers R, de Silva R, Litvan I, Riley DE, van Swieten JC, Heutink P, Wszolek ZK, Uitti RJ, Vandrovicova J, Hurtig HI, Gross RG, Maetzler W, Goldwurm S, Tolosa E, Borroni B, Pastor P, Cantwell LB, Han MR, Dillman A, van der Brug MP, Gibbs JR, Cookson MR, Hernandez DG, Singleton AB, Farrer MJ, Yu CE, Golbe LI, Revesz T, Hardy J, Lees AJ, Devlin B, Hakonarson H, Muller U, Schellenberg GD. Identification of common variants influencing risk of the tauopathy progressive supranuclear palsy. *Nat Genet.* 2011; 43(7): 699-705.
6. Sahara N, Tomiyama T, Mori H. Missense point mutations of tau to segregate with FTDP-17 exhibit site-specific effects on microtubule structure in COS cells: a novel action of R406W mutation. *J Neurosci Res.* 2000; 60(3): 380-7.
7. McCulloch CC, Kay DM, Factor SA, Samii A, Nutt JG, Higgins DS, Griffith A, Roberts JW, Leis BC, Montimurro JS, Zabetian CP, Payami H. Exploring gene-environment interactions in Parkinson's disease. *Hum Genet.* 2008; 123(3): 257-65.
8. Nalls, MA, Plagnol, V, Hernandez, DG, Sharma, M, Sheerin, UM, Saad, M, Simon-Sanchez, J, Schulte, C, Lesage, S, Sveinbjornsdottir, S, Stefansson, K, Martinez, M, Hardy, J, Heutink, P, Brice, A, Gasser, T, Singleton, AB & Wood, NW. Imputation of sequence variants for identification of genetic risks for Parkinson's disease: a meta-analysis of genome-wide association studies. *Lancet* 377, 641-9 (2011).